Investigation into the Cohesin Loading Complex of *Caenorhabditis elegans*

Andrew Peter Banks

A Thesis Submitted for the Degree of Doctor of Philosophy at the University of Newcastle

2007

Institute of Human Genetics

International Centre for Life

University of Newcastle

Investigation into the Cohesin Loading Complex of *Caenorhabditis elegans*

Andrew Peter Banks

A Thesis Submitted for the Degree of Doctor of Philosophy at the University of Newcastle

2007

Institute of Human Genetics

International Centre for Life

University of Newcastle

Declaration

This is to certify that this thesis titled "Investigation into the Cohesin Loading Complex of *Caenorhabditis elegans*" presented for the Degree of Doctor of Philosophy at the University of Newcastle, is my own work except where stated, and has not been presented at any other University.

Andrew Peter Banks

October 2007

Acknowledgments

I would like to thank my supervisors Professor Tom Strachan and Dr Sarah Newbury for their time and patience and for allowing me to conduct my PhD within their laboratories. I would like to express my gratitude towards Dr Emma Tonkin, Dr Alison Trainer, Dr Elizabeth Veal and Dr Steve Laval whose valuable experience set me in the correct road on many occasions. I would also like to thank the many laboratory members with whom I have shared a great deal of time and of particular note is Vlad (with whom I have spent many an evening proving that neither of us can play tennis), Nazia, Steve, Nancy, Mel and last but not least Helen. I also greatly acknowledge the support given to me throughout the duration of my PhD by the Medical Research Council and the Graduate School at the University of Newcastle. Finally I would like to thank my wife Caley for tolerating my mostly unreasonable nature displayed whilst writing this thesis and would also like to thank my parents for giving me the opportunities to have achieved this goal.

Abstract

Sister chromatid cohesion is important to ensure faithful chromosome segregation occurs during mitosis and is mediated by the multisubunit cohesin complex. In *Saccharomyces cerevisiae* the cohesin complex is loaded onto chromosomes by a protein complex composed of Scc2 and Scc4. *Caenorhabditis elegans* PQN-85 is readily identified as the orthologue of Scc2 and the sequence similarity between PQN-85 and its orthologues from all organisms suggests that their function in cohesin loading is conserved throughout evolution. Data presented in this thesis shows that in accordance with its suspected role in cohesin loading RNA interference against *pqn-85* results in chromosome segregation defects in *C. elegans* embryos similar to those observed when the cohesin subunit *scc-3* is depleted. Although it has been problematic to identify homologues of Scc4 in metazoans, it has recently been proven that *C. elegans* MAU-2 is distantly related to Scc4. Co-depleting *scc-3* with either *pqn-85* or *mau-2* result in exacerbation of the chromosome segregation defects with very similar phenotypes suggesting that *mau-2* as well as *pqn-85* functions in chromosome segregation. Data is also presented demonstrating that MAU-2 physically interacts with the N-terminus of the PQN-85 protein in a directed yeast two-hybrid assay consistent with the idea that PQN-85 and MAU-2 form a complex. Microscopic examination of *mau-2::GFP* embryos in this thesis demonstrates that MAU-2::GFP localises to the nucleus in accordance with a role in cohesin loading, whilst depletion of *pqn-85* by RNAi in *mau-2::GFP* embryos resulted in the reduction of MAU-2 ::GFP within the nucleus and concurrent accumulation within the cytoplasm. Together these results suggest that the cohesin loading complex is conserved in *C. elegans* whilst the extensive homology between PQN-85, MAU-2 and their metazoan orthologues suggests that it is also likely that the cohesin complex is conserved amongst all metazoans.

Contents

List of Tables

CHAPTER 1

CHAPTER 2

CHAPTER 3

CHAPTER 4

CHAPTER 5

List of Figures

CHAPTER 1

CHAPTER 3

CHAPTER 4

CHAPTER 5

CHAPTER 6

Chapter 1

Introduction

1.1 The Molecular Mechanism of Sister Chromatid Cohesion

In this introduction I will discuss the eukaryotic cohesin complex and its function in maintaining sister chromatid cohesion. I will then introduce the role of the *S. cerevisiae* cohesin loading complex in depositing cohesin onto chromosomes and discuss the identification of the cohesin loading complex in metazoans. I shall also summarise other factors required for the establishment and maintenance of sister chromatid cohesion and introduce the currently held models for sister chromatid cohesion. Finally I will discuss the increasing evidence of the role that the genes in involved in sister chromatid cohesion play in metazoan development and in the pathogenesis of complex human diseases.

1.1.1 Eukaryotic Cell Division and Sister Chromatid Cohesion

The eukaryotic genome is organised into a series of individual units called chromosomes which are replicated prior to the onset of mitotic cell division producing two identical sister chromatids. As cells undergo division they must ensure that the sister chromatids are segregated equally between two daughter cells. When the cells enter mitosis the chromosomes undergo well characterised movements and dramatic changes in structure which culminates in the faithful distribution of sister chromatids to daughter cells (Summarised in Table 1.1). The changes in chromosome dynamics during the mitotic cell cycle must be tightly controlled; failure to do so can result in aneuploidy or polyploidy which have well documented roles in cancer and birth defects. It has become clear that a key mechanism to ensure that sister chromatids are segregated efficiently, is to tether them together after DNA replication during S-phase but before the timely separation of sister chromatids in the anaphase stage of mitosis. The mechanism by which sister chromatids are bound together after S-phase is called sister chromatid cohesion.

1.1.2 Cohesin as the Molecular Basis for Sister Chromatid Cohesion

In all eukaryotes studied it has been shown that sister chromatid cohesion requires the function of four evolutionarily conserved proteins; Smc1, Smc3, Scc1 and Scc3 [Table 1.2 (Guacci et al., 1997, Michaelis et al., 1997, Toth et al., 1999, Darwiche et al., 1999, Losada et al., 1998, Sonoda et al., 2001, Tomonaga et al., 2000, Warren et al., 2000)]. The four proteins

can be readily coimmunoprecipitated together in all organisms studied (Chan et al., 2003, Michaelis et al., 1997, Sumara et al., 2000, Tomonaga et al., 2000, Toth et al., 1999, Vass et al., 2003, Losada et al., 1998, Darwiche et al., 1999) and the complex they form has been termed cohesin. Two key observations link the cohesin complex to sister chromatid cohesion. First, the cohesin complex is bound to chromosomes at times when sister chromatid cohesion exists and second, when the function of any of the members of the cohesin complex is abrogated sister chromatids separate in mitosis before the onset of anaphase (which has been called premature sister chromatid separation) (Chan et al., 2003, Losada et al., 1998, Michaelis et al., 1997, Mito et al., 2003, Pasierbek et al., 2003, Sonoda et al., 2001, Tomonaga et al., 2000, Toth et al., 1999).

Table 1.1 Summary of Mitotic Cell Division [adapted from (Hagstrom and Meyer, 2003)]

DNA replication and cohesion establishment	Chromosomes are replicated during S-phase of the cell cycle to produce identical sister chromatids, the chromosomes at this stage are not condensed and appear as a mass of disorganised DNA
Prophase	Chromosomes begin to condense from the amorphous mass of DNA that is found during DNA replication and continue to condense until chromosomes reach the characteristic shape associated with metaphase chromosomes
Prometaphase	The nuclear envelope breaks down and the centromere of each sister chromatid assembles a kinetochore – a proteinaceous structure required for the attachment of the mitotic spindle apparatus. At this point sister chromatids are arranged such that the kinetochore associated with each sister chromatid attaches to microtubules from only one pole in a process called bi-orientation
Metaphase	The chromosomes are fully condensed in metaphase and the chromosomes align in the middle of the cell along the metaphase plate, the force generated by the microtubules attached at kinetochores is opposed by a process called sister chromatid cohesion.
Anaphase	Sister chromatid cohesion is dissolved and the sister chromatids are pulled apart by the force generated from the microtubules and segregate from the metaphase plate to opposite poles of the cell
Telophase	The segregated chromosomes decondense into the mass of DNA observed during DNA replication

Table 1.2 Nomenclature of Cohesin Orthologues

The names within brackets represent alternative protein names in the literature

S. cerevisiae	*S. pombe*	*Drosophila*	*C. elegans*	Human
Scc1 (Mcd1)	Rad21	Rad21	SCC1	hRAD21 (hSCC1)
Smc1	Psm1	Smc1	SMC1	hSMC1
Smc3	Psm3	Smc3	SMC3	hSMC3
Scc3	Psc3	Stromalin (SA)	SCC3	hSA1 hSA2

1.1.3 Structure of the Cohesin Complex

Smc1 and Smc3 belong to an evolutionarily conserved family of proteins and interact to form a distinctive structure. Members of the structural maintenance of chromosome (SMC) family of proteins to which Smc1 and Smc3 belong contain globular N-terminal and C-terminal domains separated by antiparallel coiled coil domains and a hinge domain (Melby et al., 1998) (Figure 1.1A). In yeast the Smc1 and Scm3 proteins fold back on themselves via the hinge region allowing the globular N-terminal and C-terminal domains of the proteins to interact (Haering et al., 2002) (Figure 1.1B). Smc1 and Smc3 interact via their respective hinge regions to form a V shaped heterodimer (Haering et al., 2002).

Although the globular head domains of Smc1 and Smc3 can interact with one another (Weitzer et al., 2003), Scc1 forms a bridge between them. The N terminus of Scc1 binds to the globular head of Smc3 and the C-terminus of Scc1 binds to the globular head of Smc1 to form a large ring with an internal diameter of 35nm (Haering et al., 2002). Electron microscopic studies of the structure of the cohesin complex have clearly shown this ring structure (Anderson et al., 2002, Haering et al., 2002). The globular head domains of Smc1 and Smc3 are putative ATPases which are predicted to bind and hydrolyse ATP. Mutations that are proposed to abolish the ATP binding ability of the globular head domains of Smc1 and Smc3 inhibit the ability of Scc1 to bind to Smc1 and Smc3 so that tripartite cohesin rings are not formed (Arumugam et al., 2003). The final component of the yeast cohesin complex is Scc3 which binds directly to Scc1. However, whilst Scc3 is considered vital component of the cohesin complex it is not thought to constitute a key component of the ring structure (Figure 1.1C).

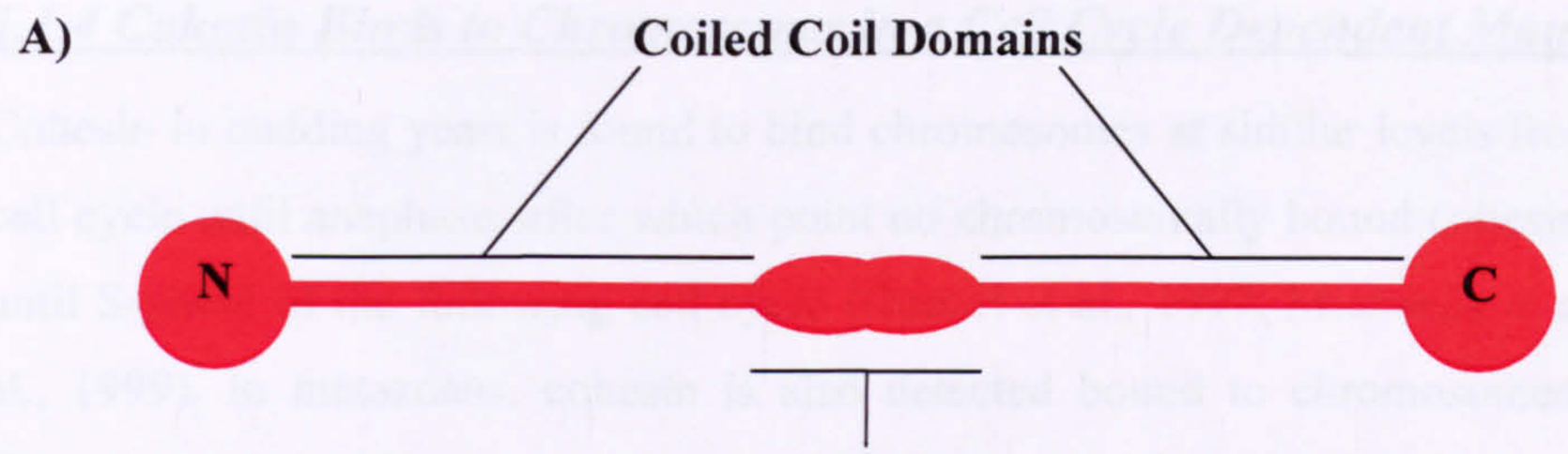

Figure 1.1 Structure of SMC Proteins and the Cohesin Complex

A) The SMC family of protein contain globular head domains at their N-terminal and C-terminal ends which are separated by two antiparallel coiled coil domains and a hinge domain. **B)** In *S. cerevisiae* Smc1 and Smc3 fold at their hinge domain so that the N-terminal and C-terminal globular heads interact. **C)** The Smc1 and Smc3 subunit of cohesin interact via their respective hinge domains whilst the Scc1 protein bridges the gap between the globular head domain of Smc1 and Smc3 to form a tripartite ring structure. The Scc3 subunit of cohesin binds Scc1 but it not thought to be an integral part of the tripartite ring hence is shown bound only to Scc1.

1.1.4 Cohesin Binds to Chromosomes in a Cell Cycle Dependent Manner

Cohesin in budding yeast is found to bind chromosomes at similar levels from S-phase of the cell cycle until anaphase, after which point no chromosomally bound cohesin can be detected until S-phase of the following cell cycle (Guacci et al., 1997, Michaelis et al., 1997, Toth et al., 1999). In metazoans, cohesin is also detected bound to chromosomes during S-phase (Darwiche et al., 1999, Losada et al., 1998, Sumara et al., 2000, Mito et al., 2003, Losada et al., 2000). However, cohesin also localises to chromosomes during telophase in mouse fibroblasts, *Xenopus* cell-free extracts [in which DNA replication can be reproduced by in vivo replication of sperm DNA (Walter et al., 1998)] and HeLa cells and remains bound until the following cell cycle (Sumara et al., 2000, Losada et al., 2000). This is consistent with the role of the cohesin complex in ensuring replicated sister chromatids remain bound from S-phase to anaphase and the observation that sister chromatid cohesion is established during S-phase.

In HeLa cell, *Xenopus* cell-free extracts and *C. elegans* the majority of cohesin is observed to dissociate from chromosome arms by the prophase stage of mitosis when replicated chromosomes are condensing (Losada et al., 1998, Losada et al., 2000, Mito et al., 2003, Sumara et al., 2000, Wazenegger et al., 2000). Despite this loss of cohesin during prophase, sister chromatids do not segregate: a small amount of cohesin (~10% of the total cohesin loaded onto chromosomes) is found to persist at centromeric regions in humans, *Xenopus* and *Drosophila* which is sufficient to maintain sister chromatid cohesion. This residual amount of cohesin dissociates at anaphase (Losada et al., 2000, Wazenegger et al., 2000, Warren et al., 2000). This suggests that only a small amount of cohesin is required for sister chromatid cohesion in metazoans.

1.1.5 Subchromosomal Localisation of Cohesin

The cohesin complex localises non-randomly to specific regions on chromosomes. Immunofluorescent data has shown that cohesin complexes are enriched at centromeric regions in many organisms (Losada et al., 2000, Warren et al., 2000, Wazenegger et al., 2000). Using chromatin immunoprecipitation studies the localisation and enrichment of cohesin on the centromeres of yeast chromosomes has also been extensively confirmed (Laloraya et al., 2000, Megee and Koshland, 1999, Nonaka et al., 2002, Tanaka et al., 1999, Tomonaga et al., 2000, Glynn et al., 2004, Lengronne et al., 2004). Genome wide analysis of cohesin localisation on yeast chromosomes has shown that the amount of cohesin bound to

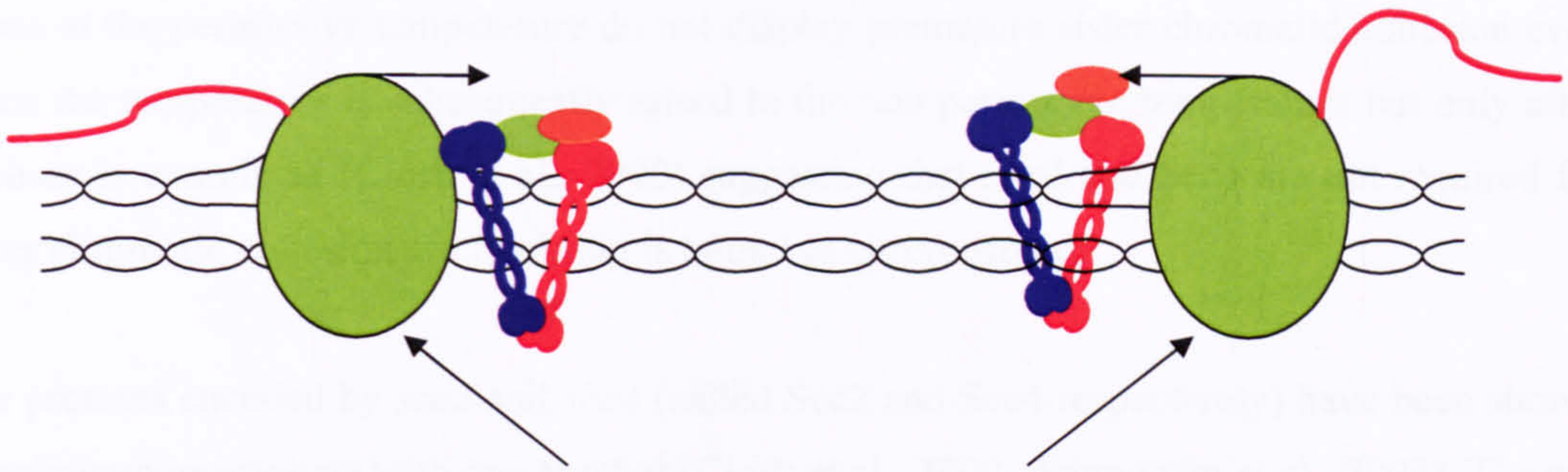

Figure 1.2 the Transcription Machinery may Actively Move Cohesin along Chromosomes

The cohesin complex is thought to be pushed along chromosomes by the transcription machinery which is too large to pass through the cohesin ring. As a result cohesin accumulates at regions of convergent transcription.

chromosomes correlates with the size of the chromosome and binding occurs on average once every 11Kb (Glynn et al., 2004). Specific regions of chromosomes however have consistently been associated with cohesin, in several independent chromatin immunoprecipitation studies (Blat and Kleckner, 1999, Glynn et al., 2004, Laloraya et al., 2000) and these sites have been called cohesin associated regions. The cohesin associated regions have specific characteristics and are mostly but not exclusively AT rich regions of the genome (Blat and Kleckner, 1999, Laloraya et al., 2000, Glynn et al., 2004). Cohesin is often localised to areas of convergent transcription between genes transcribed in opposite directions and as such it has been suggested that the transcription machinery may actively push the cohesin complex along chromosomes which ultimately convene in regions where two genes are transcribed in opposing directions (Figure 1.2) (Glynn et al., 2004, Lengronne et al., 2004).

1.1.6 Loading of the Cohesin Complex onto Chromosomes

The loading of the cohesin complex in *S. cerevisiae* requires a specialist loading complex (Ciosk et al., 2000). Budding yeast with temperature sensitive mutations in the *scc2* and *scc4* genes (called the *scc2-4* and *scc4-4* mutant strains) display premature sister chromatid cohesion at the non permissive temperature (Ciosk et al., 2000). Further analysis demonstrated that whilst all subunits of the cohesin complex can be coimmunoprecipitated with each other at the non permissive temperature in the *scc2-4* and *scc4-4* strains, a marked defect in the binding of cohesin to chromatin during S-phase is observed (Ciosk et al., 2000, Toth et al., 1999, Lengronne et al., 2004). Further, *scc2-4* or *scc4-4* cells that complete S-

phase at the permissive temperature do not display premature sister chromatid cohesion even when the temperature is subsequently raised to the non permissive temperature but only after S-phase is completed (Ciosk et al., 2000) suggesting that Scc2 and Scc4 are not required for sister chromatid cohesion after cohesin is bound to chromosomes.

The proteins encoded by *scc2* and *scc4* (called Scc2 and Scc4 respectively) have been shown to coimmunoprecipitate with one another (Ciosk et al., 2000, Arumugam et al., 2003). The co-localisation of Scc2 and Scc4 on chromosomes has been confirmed using immunofluorescence on chromatin spreads (Ciosk et al., 2000) and in chromatin immunoprecipitation studies (Lengronne et al., 2004) suggesting that this interaction is likely biologically relevant. Consistent with the role of the Scc2 and Scc4 complex in the loading of cohesin, chromatin immunoprecipitation studies have also showed that cohesin initially co-localises with the cohesin loading complex of Scc2 and Scc4 on chromosomes before moving to cohesin associated regions shortly after (Lengronne et al., 2004). This suggests that the Scc2 and Scc4 proteins are not key structural components of the cohesin complex but are required for cohesin loading in S-phase before the onset of mitosis.

It is currently unclear how the cohesin loading complex functions in the loading of the cohesin complex. Cohesin has been shown to bind the cohesin loading complex as would be expected (Ciosk et al., 2000). However, it has been postulated that the cohesin loading complex facilitates the binding of cohesin to DNA by promoting ATP hydrolysis (Arumugam et al., 2003). Mutations that are proposed to abolish the ability of the globular head domains of Smc1 and Smc3 to hydrolyse ATP can still form cohesin rings but cannot bind chromosomes (Arumugam et al., 2003). This phenotype is identical to that seen in *S. cerevisiae scc2-4* and *scc4-4* strains (Ciosk et al., 2000) suggesting that the deposition of cohesin on to chromosomes by the cohesin loading complex may be ATP dependent.

1.1.7 Scc2 Orthologues are Highly Conserved

Orthologues of the *S. cerevisiae* Scc2 protein that have been identified in other organisms are well conserved and are collectively named adherins (see Table 1.3 for a list of Scc2 orthologues). Standard BLAST analyses can readily identify sequence homologues of the Scc2 protein in humans, *C. elegans* , *Drosophila*, *Xenopus*, mouse, rat and zebra fish (Tonkin et al., 2004). Mammalian adherins demonstrate a high degree of conservation with human, rat and mouse sequences sharing ~90% identity (Krantz et al., 2004, Tonkin et al., 2004). Whilst

yeast Scc2 shares ~20% identity with the *C. elegans*, *Drosophila* and human orthologues respectively.

Table 1.3 Adherin Nomenclature

The *gene*/protein name of adherin orthologues

S. cerevisiae	*S. pombe*	*C. elegans*	*Drosophila*	*Xenopus*	*H. sapiens*
scc2/Scc2	*mis4*/Mis4	*pqn-85*/ PQN-85	*Nipped-B*/ Nipped-B	*xscc2*/ XScc2	*NIPBL*/ delangin

Sequence conservation amongst the adherins is confined to particular regions of the proteins with a 1500 amino acid C-terminal region of the adherin proteins displaying extensive conservation [Figure 1.3 and (Tonkin et al., 2004, Strachan, 2005)]. Further analysis of the C-terminal region of the human delangin protein sequence using the Rep programme (http://www.embl-heidelberg.de/%7Eandrade/papers/rep/search.html) detects five HEAT repeats (Strachan, 2005). HEAT repeats are tandemly arranged bihelical structures that act as scaffolds for the binding of other molecules and are found in other chromosomally associated proteins (Neuwald and Hirano, 2000). Although the same programme cannot detect HEAT repeats within the PQN-85 protein sequence a ClustalW (http://www.ebi.ac.uk/Tools/clustalw/index.html) alignment of the delangin and PQN-85 protein sequences suggests that the HEAT repeats detected within delangin are well conserved within PQN-85 (Figure 1.4). The extensive conservation of the C-terminus of the adherins throughout evolution would suggest that this region is likely to be vital for a function shared by all orthologues.

The N-terminal region of the adherins has extended in size though evolution (Figure 1.3) and is not so well conserved. A repetitive sequence that appears to be relatively well conserved amongst vertebrates (Strachan, 2005) is not found in the *Drosophila* or *C. elegans* sequences whilst the first ~200 amino acids of *C. elegans* PQN-85 contains extensive runs of glutamine residues (henceforth called the polyglutamine region) which is not found in any other adherin sequence. The delangin protein also contains a bipartite nuclear localisation signal (NLS) and analysis of the PQN-85 protein sequence using the NLS prediction programme NLSdb (http://cubic.bioc.columbia.edu/cgi/var/nair/resonline.pl) demonstrates that this bipartite NLS

appears to be conserved and also detects several other simple NLS (see Figure 1.5 for summary of PQN-85 protein domains).

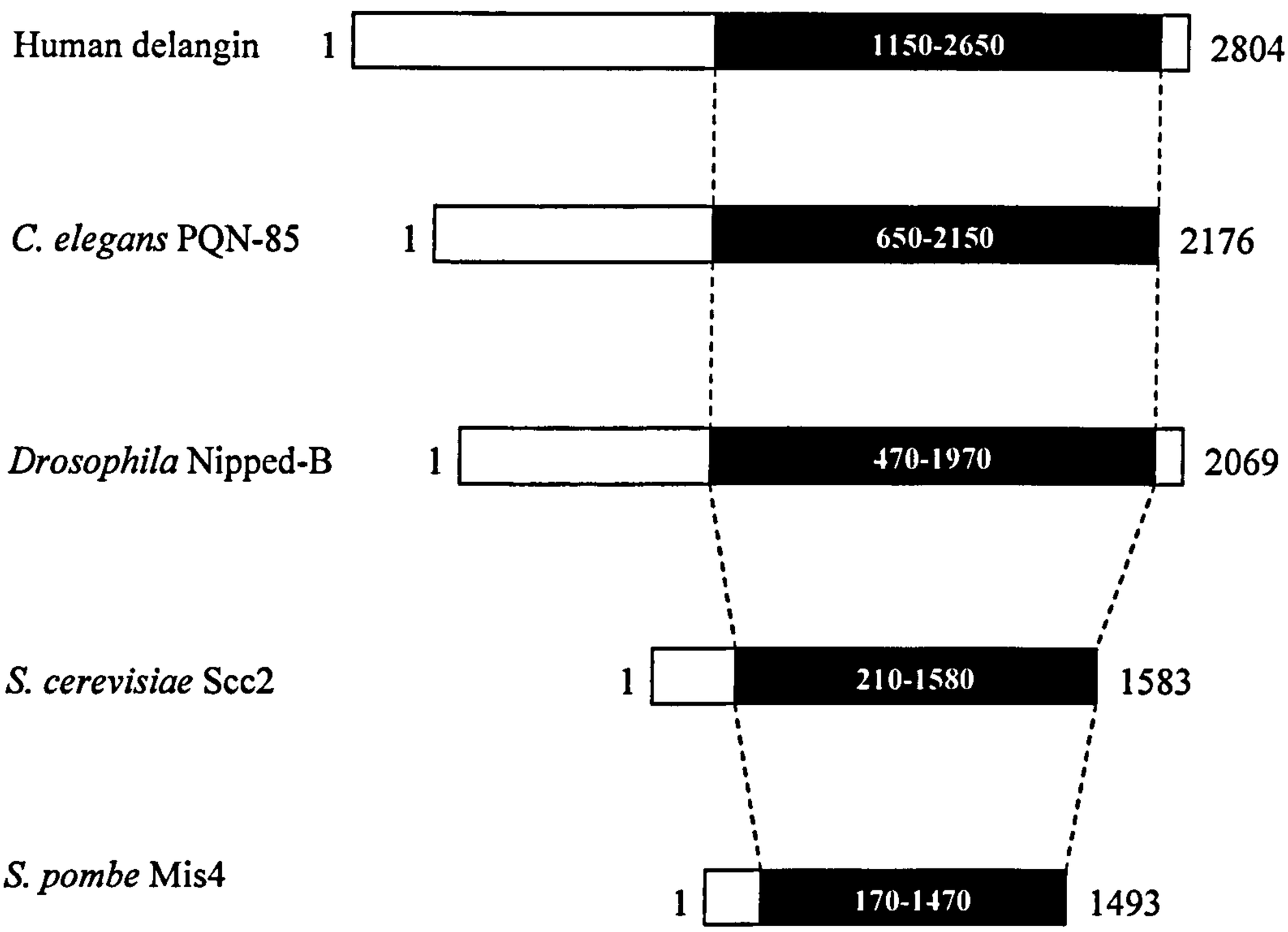

Figure 1.3 Conservation of Adherins throughout Evolution

A ClustalW alignment of human, *C. elegans*, *Drosophila S. pombe* and *S. cerevisiae* adherin sequences is summarised above and demonstrates that a large region of the C-terminus is conserved in sequence through evolution (highlighted in blue). In metazoans the size of the conserved region is also maintained at around 1500 amino acids however this region is slightly smaller in yeast. Adherins in metazoans display an extended N-terminus which is poorly conserved relative to the C-terminal region.

```
delangin        EIETTGQIMHRAENRKKFLRSIIKTTPSQFSTLKMNSDTVDYDDACLIVRYLASMRPFAQ 1768
PQN-85          AERKYEKIQYRGAEMKVFLSKILDKKEIKRRLEKSNKVKMLDSDAFWAVKFLAQSREFTH 1277
                  ..  :* :*. : * ** .*:...  :    * *. .:  .**   *::**. * *::

delangin        SFDIYLTQILRVLG-ENAIAVRTKAMKCLSEVVAVDPSILARLDMQRGVHGRLMDNSTSV 1827
PQN-85          SFDTYLKHIVFGAGSETIVALRSKALKCLSSIIEADSSVLILEDVQQAVHTRMVDSHAQV 1337
                *** **.:*:   * *. :*:*:**:****.:: .*.*:*   *:*:.** *::*. :.*

delangin        REAAVELLGRFVLCRPQLAEQYYDMLIERILDTGISVRKRVIKILRDICIEQPTFPKITE 1887
PQN-85          RESAVELIGRFVLYDEEYVRKYYSQIAERILDTGVAVRKRVIRIMREICEKFPTFEMIPD 1397
                **:****:*****   : ..:**. : *******:******:*:*:** : ***  *.:

delangin        MCVKMIRRVNDEEGIKKLVNETFQKLWFTPTPHNDKE-AMTRKILNITDVVAACR-DTGY 1945
PQN-85          MLARMIRRVTDEEGVKKLVFETFTTLWFQPVDTRIYTNAVATKVTTMCSVAQHCIKDAMS 1457
                * .:*****.****:**** *** .*** *.  .    *:: *: .: .*.  *  *:

delangin        DWFEQLLQNLLKSEEDSSYKPVKKACTQLVDNLVEHILKYEESLADSDNKGVNSGR---- 2001
PQN-85          DYLEQLILHIVKNGQEG--SGMSVAVKQIIDSLVDHILNLEQHKSSENVSEVELMRRKEQ 1515
                *::***: :::*. ::.  . :. * .*::*.**:***: *:  :..: . *:  *

delangin        ELLMYFTKHSDEEVQTKAIIGLGFAFIQHPSLMFEQEVKNLYNNILSDKNSSVN--LKIQ 2232
PQN-85          ITLEFFSRYHKGGLRQKALTAMGHFCAQHSTYLTKRQLTNTYLEILNAANSPQQQQQRIL 1755
                  * :*::: .  :: **: .:*.   **.: : ::::.* * :**.  **. :   :*

delangin        VLKNLQTYLQEEDTRMQQADRDWKKVAKQEDLKEMGDVSSGMSSSIMQLYLKQVLEAFFH 2292
PQN-85          VLQNLEMFLQCEEQKLAASHDKWDENKEAQNLKEMELSGSGLGSSVIQKYWKAVLESYVD 1815
                **:**: :** *: ::  :. .*.:  : ::****   .**:.**::* * * ***::..

delangin        TQSSVRHFALNVIALTLNQGLIHPVQCVPYLIAMGTDPEPAMRNKADQQLVEIDKKYAGF 2352
PQN-85          ADIQLRRAAVQVVWLTLNQGLVTPGASIPTLIAMTTDPVDVIRNRIDILLKEIDSKYSGM 1875
                ..  .*. *..*. ******* *   .* **** ***  .**. *  * *** **.*.
```

Figure 1.4 HEAT Repeats Identified within delangin are Conserved within PQN-85

ClustalW (http://www.ebi.ac.uk/Tools/clustalw/index.html) alignment of the five HEAT repeats that can be identified in the delangin protein using the rep programme (http://www.embl-heidelberg.de/%7Eandrade/papers/rep/search.html) against the PQN-85 protein sequence demonstrated that the HEAT repeats appear to be well conserved. The HEAT repeats are highlighted in yellow.

* denotes that the residues in that column are identical in both sequences in the alignment

: denotes conserved amino acid substitutions residues in both sequences in the alignment

. denotes semi-conserved amino acid substitutions are observed in both sequences in the alignment

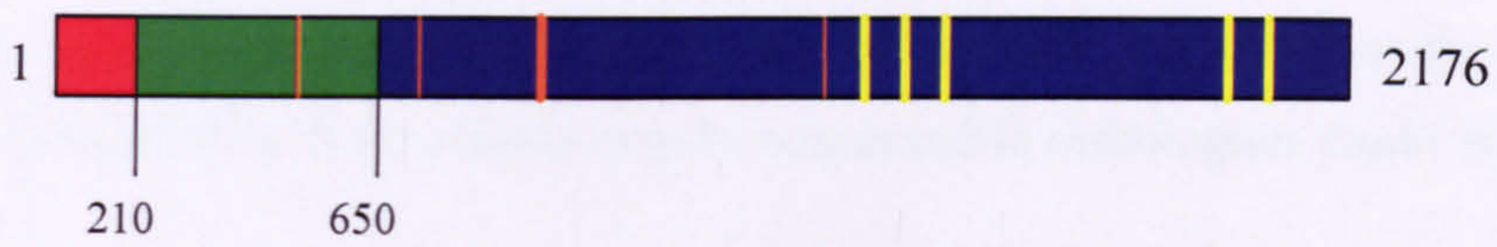

Figure 1.5 Summary of PQN-85 Protein Domains

The PQN-85 protein sequence contains five predicted HEAT repeats within the conserved region (between the residues 1270 and 1880) and four NLS sequences, three simple (at positions 591, 677 and 1241) characterised by four basic amino acids (K-lysine or R-arginine) or three basic amino acids (K or R) and either H-histidine or P-proline. Also identified is one bipartite NLS (at position 846) characterised by 2 basic residues, 10 residue spacer, and another basic region consisting of at least 3 basic residues out of 5 residues (Robbins et al., 1991). In PQN-85 the sequence is KKKDRAPEEARRRKK and is represented by the thicker orange line above. Extensive runs of glutamine residues are found at the extreme N-terminal end of the sequence; of the 164 glutamine residues found in the PQN-85 protein 67 of them are found in the first 210 amino acids representing over 40%of the total.

1.1.8 Metazoan Adherins Function in Chromosome Segregation

The majority of adherins studied to date function in sister chromatid cohesion possibly in loading cohesin. *Drosophila* that contain mutations in the *Nipped-B* gene shows evidence of premature sister chromatid separation (Rollins et al., 2004). Immunodepletion of XScc2 from *Xenopus* cell-free extracts also results in sister chromatid cohesion defects. However the authors go further and show that this causes a cohesin loading defect (Gillespie and Hirano, 2004, Takahashi et al., 2004). Recently mutations in *NIPBL* have been shown to cause the severe developmental disease Cornelia de Lange Syndrome (CdLS; OMIM 122470) (Krantz et al., 2004, Tonkin et al., 2004, Gillis et al., 2004). Analysis of whole blood metaphase spreads from patients with CdLS were reported to display premature sister chromatid separation (Kaur et al., 2005); however, it should be noted that other reports have not

observed any evidence of this (Tonkin et al., 2004). This suggests that the cohesin loading function of Scc2 from *S. cerevisiae* may be conserved in orthologues found in all organisms.

1.1.9 Identification of scc4 Orthologues

Standard BLASTP searches cannot identify proteins with homology to Scc4 outside of organisms closely related to *S. cerevisiae*. However, recently more sensitive approaches have yielded new information. The position specific iterative BLAST (PSI-BLAST) programme uses a position specific scoring matrix to identify conserved residues within proteins. By running the result of the previous PSI-BLAST search through several iterations distantly related proteins can be identified (Altschul et al., 1997). The BLAST-PSI programme has been used to show that Scc4 is distantly related in sequence to the product of the *C. elegans mau-2* gene, the Drosophila *CG4203* gene and the human gene *KIAA0892* (GenBank ID: NM_015329.3) (Tom Strachan, personal communication).

The proteins encoded by *KIAA0892* and its orthologues are extremely well conserved at the sequence level in mammals (99% identity), vertebrates (95% identity) and *C. elegans* (25% identity) (Benard et al., 2004) although apparently not in *S. cerevisiae*. Further evidence that these genes may represent orthologues of *S. cerevisiae* Scc4 in higher eukaryotes is that the protein encoded by the Drosophila gene *CG4203* interacts with *Drosophila* adherin Nipped-B in a yeast two hybrid assay (Giot et al., 2003) suggesting that the *S. cerevisiae* cohesin loading complex of Scc2 and Scc4 may be conserved in metazoans.

.

1.1.10 Establishment of Sister Chromatid Cohesion Requires an Establishment Factor

The binding of cohesin to chromosomes is not sufficient for the establishment of sister chromatid cohesion (Toth et al., 1999). The *eco1* gene of *S. cerevisiae* was identified in temperature sensitive mutants displaying a high rate of chromosome loss at the non permissive temperature (Toth et al., 1999). Further analysis of *eco1* mutants showed that these cells displayed premature sister chromatid separation (Skibbens et al., 1999, Toth et al., 1999). Despite the defects in sister chromatid cohesion observed in *eco1* mutants, no defect in the binding of cohesin to chromosomes is observed (Toth et al., 1999). Therefore the function of *eco1* is distinct from that of *scc2* and *scc4* which as previously mentioned are required for cohesin binding to chromosomes.

The role of *eco1* in sister chromatid cohesion is confined to S-phase of the cell cycle and appears to be linked to DNA replication. Budding yeast carrying a temperature sensitive *eco1* mutation which complete S-phase at the permissive temperature, establish sister chromatid cohesion and can maintain this sister chromatid cohesion when the cells are subsequently incubated at the non-permissive temperature after completion of S-phase (Toth et al., 1999, Skibbens et al., 1999). This suggests that *eco1* is required for the establishment of cohesion but not for its maintenance to anaphase. The link between the establishment of sister chromatid cohesion and DNA replication is provided by the genetic interaction of *eco1* with the proliferating cell nuclear antigen (PCNA). In *S. cerevisiae* the PCNA protein is encoded by the *POL30* gene (Bauer and Burgers, 1990) and it has a proven function in increasing the processivity of DNA polymerases (Burgers, 1988). Over-expression of the *POL30* gene in *S. cerevisiae* reduces the level of chromosome loss observed in *eco1* mutant cells (Skibbens et al., 1999).

Orthologues of the protein encoded by *S. cerevisiae eco1* have been identified in *S. pombe*, *Drosophila*, mice and humans [Table 1.4 and (Toth et al., 1999, Bellows et al., 2002, Hou and Zou, 2005, Williams et al., 2003)]. Fission yeast Eso1 is also required for S-phase establishment of sister chromatid cohesion (Tanaka et al., 2000a) and both human orthologues of Eco1 have been shown to function in sister chromatid cohesion (Bellows et al., 2002, Hou and Zou, 2005). Consistent with this Eco1 and its human orthologues are found to bind chromosomes (Hou and Zou, 2005, Toth et al., 1999). Interestingly the two human orthologues are not functionally redundant and cannot substitute for one another in sister chromatid cohesion when the function of either is disrupted (Hou and Zou, 2005). *ESCO2* is mutated in the developmental diseases Roberts syndrome (RBS; OMIM 268300) and SC phocomelia (SC; OMIM 269000) (Schule et al., 2005, Vega et al., 2005) and a particular characteristic of RBS and SC is premature (pre-anaphase) centromere separation observed in metaphase spreads of DNA patients (Vandenberg and Francke, 1993).

It is not clear how Eco1 and its orthologues function in establishing sister chromatid cohesion. All orthologues of Eco1 contain a highly conserved C-terminal acetyl transferase domain whose function in acetylating proteins has been demonstrated (Hou and Zou, 2005, Ivanov et al., 2002). Evidence from studies in *S. cerevisiae* has also demonstrated that the target of acetylation is the cohesin complex (Ivanov et al., 2002), although the significance of this reaction is yet to be elucidated. Whilst the C-terminal domain of Eco1 is conserved the N-

terminal domain is not and fission yeast, *Drosophila* and human orthologues display an extended N-terminal sequence relative to Eco1 (Bellows et al., 2002, Hou and Zou, 2005). It is the N-terminal region, however, that appears to mediate the binding of ESCO1 and ESCO2 to chromosomes in human cells (Hou and Zou, 2005) suggesting that the function of the N-terminal region is likely important in cohesion establishment.

Table 1.4 Nomenclature of *S. cerevisiae* Eco1 Orthologues

The *gene*/protein name of *S. cerevisiae* Eco1 orthologues

S. cerevisiae	***S. pombe***	***Drosophila***	***H. sapiens***
eco1/Eco1	*eso1*/Eso1	*Deco*/Deco	*ESCO1*/ESCO1 *ESCO2*/ESCO2

1.1.11 Establishment of Sister Chromatid Cohesion at Double Strand DNA Breaks

Cohesin mediated sister chromatid cohesion can be established outside of S-phase by double stranded DNA break repair mechanisms. Cohesin localises to a region of chromatin ~50kb either side of a dsDNA break site in *S. cerevisiae* (Unal et al., 2002, Strom et al., 2003). Temperature sensitive *S. cerevisiae smc1* mutants which establish sister chromatid cohesion at the permissive temperature during S-phase show premature sister chromatid cohesion if the temperature is raised to the non-permissive temperature before anaphase begins (Michaelis et al., 1997). This premature sister chromatid cohesion can not be rescued by the addition of wild type Smc1 after S-phase has been completed unless the cell has been subjected to DNA damaging agents that cause double stand breaks (Strom et al., 2003). The binding of cohesin around sites of double strand break repair is perturbed in *scc2-4* and *scc4-4* temperature sensitive mutant strains at the non permissive temperature (Strom et al., 2003, Unal et al., 2004) suggesting that the mechanism by which cohesin is loaded either during S-phase or at sites of DNA damage utilises the same mechanism. Consequently temperature sensitive mutants in *scc2* or *scc4* are defective in dsDNA break repair at the non-permissive temperature (Strom et al., 2003). This suggests that wild type cohesin recruited to double strand breaks outside of S-phase can establish sister chromatid cohesion in a manner dependent on the cohesin loading complex.

The repair of dsDNA breaks requires a complex series of protein interactions at the DNA break site (summarised in Figure 1.6). Once recruited to the site of dsDNA damage budding yeast Tel1/Mec1 phosphorylate histone variant H2AX in a 50 kb domain either side of the damage site (Unal et al., 2002). The phosphorylation of H2AX appears to be important for the localisation of cohesin to chromosome breaks as the binding pattern of cohesin at dsDNA breaks is disrupted when the H2AX phosphorylation event is inhibited (Unal et al., 2002). Independent of the phosphorylation of H2AX the localisation of cohesin to dsDNA breaks is also found to be dependant on the Mre11 component of the MRX complex (Unal et al., 2002). It seems likely that cohesin mediated sister chromatid cohesion establishment is conserved in metazoans as cohesin is recruited to sites of laser induced dsDNA breaks (Kim et al., 2002). Consistently cohesin localisation is also disrupted in human ATLD2 cell lines, which have mutations in the Mre11 subunit of the MRX (Kim et al., 2002). The role of the cohesin complex in dsDNA break repair is presumably to ensure that the sister chromatid is placed such that homologous recombination can occur.

Figure 1.6 Mechanism of double strand break repair [reviewed in (Garber et al., 2005)]

Two conserved mechanisms exist to repair double strand breaks, non-homologous enjoining (NHEJ) whereby two ends of broken DNA are ligated together and homologous recombination (HR). In *S. cerevisiae* a complex of proteins collectively known as the MRX and comprising the proteins Mre11, Rad50 and Xrs1 localises to the break site. The human homologues of these proteins are called Mre11, Rad50 and Nbs1 respectively and are collectively known as the MRN complex. The MRX complex recruits the phosphatidyl inositol 3-kinase (PI3K) – related protein kinase Tel1 to the site of DNA damage. Subsequently repair of the double strand break by NHEJ or HR occurs in a cell cycle dependant manner. In G1 prior to S-phase there is prevalence of the NHEJ pathway where NBX in combination with Ku70/Ku80 ligates the two ends of broken DNA molecules together in a DNA ligase IV mediated manner. In G2 phase when cells are preparing for mitosis the HR pathway is preferred. In the HR dsDNA repair pathway, 5'-3' DNA degradation results in the production of ssDNA – a process called resection and the MRX complex and Tel1 are displaced by Sae2. In their place a heterotrimeric ssDNA binding replication protein A (RPA) and a replication factor C variant (RFCv) in combination with Rad24 bind to the single stranded DNA. RPA and RFCv-Rad24 recruit a second phosphotidylinositol 3-kinase like protein Mec1 (known as ATR in humans) in combination with Ddc2 (ATRIP in humans) and the PCNA-like 9-1-1 complex (comprised of the proteins Ddc1, Mec3 and Rad17) respectively. The recombinases Rad51 and Rad52 displace the RPA and promote strand invasion for HR.

Figure 1.6 Mechanism of double strand break repair - See page 15 for figure legend

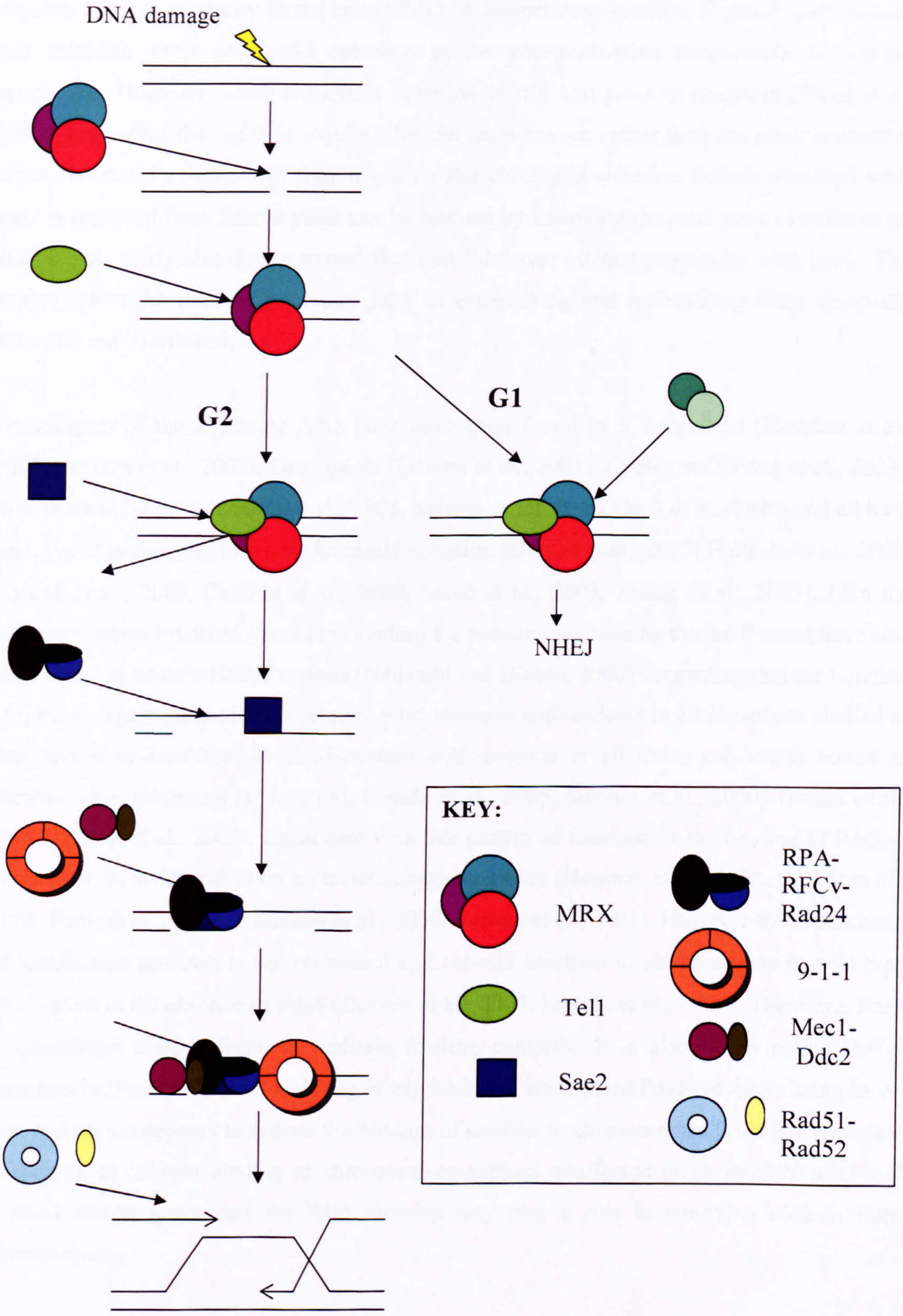

1.1.12 Maintenance of Sister Chromatid Cohesion

To maintain its function in sister chromatid cohesion after establishment the cohesin complex requires another accessory factor called Pds5. A temperature sensitive *S. pombe pds5* mutant can establish sister chromatid cohesion at the non-permissive temperature as S-phase progresses. However, sister chromatid cohesion is still lost prior to anaphase (Stead et al., 2003) suggesting that *pds5* is required for the maintenance rather than the establishment of sister chromatid cohesion. In fission yeast sister chromatid cohesion defects observed when *eso1* is removed from fission yeast can be rescued by removing the *pds5* gene (Tanaka et al., 2001). This study also demonstrated that that Pds5 can interact physically with Eso1. This suggests that the roles of *eso1* and *pds5* in establishing and maintaining sister chromatid cohesion are interlinked.

Orthologues of the *S. pombe pds5* gene have been found in *S. cerevisiae* (Hartman et al., 2000, Panizza et al., 2000), *Drosophila* (Dorsett et al., 2005), *C. elegans* (Wang et al., 2003), *Xenopus* and humans (Losada et al., 2005, Sumara et al., 2000, Geck et al., 1999) and all have been found to function in sister chromatid cohesion (Dorsett et al., 2005, Hartman et al., 2000, Losada et al., 2005, Panizza et al., 2000, Stead et al., 2003, Zhang et al., 2005). Like the adherin proteins involved in cohesin loading the proteins encoded by the *pds5* genes have also been found to contain HEAT repeats (Neuwald and Hirano, 2000) suggesting that the function of these two protein families is related. Pds5 interacts with cohesin in all organisms studied to date and it co-localises on chromosomes with cohesin at all times cohesin is bound to chromosomes (Hartman et al., 2000, Losada et al., 2005, Sumara et al., 2000, Tanaka et al., 2001, Dorsett et al., 2005). Consistent with this pattern of localisation the binding of Pds5 to chromosomes is dependent on an intact cohesin complex (Hartman et al., 2000, Losada et al., 2005, Panizza et al., 2000, Sumara et al., 2000, Tanaka et al., 2001). However the dependence of localisation however is not reciprocal and cohesin localises to chromosomes in wild type levels even in the absence of Pds5 (Dorsett et al., 2005, Losada et al., 2005). Therefore, Pds5 is considered distinct from the cohesin loading complex. It is also worth noting that a mutation in *Drosophila pds5* resulting in expression of a truncated Pds5 protein missing its N-terminal region appears to reduce the binding of cohesin to chromosomes. This is a dominant phenotype as cohesin binding to chromosomes appears unaffected in *Drosophila pds5* null mutants and suggests that the Pds5 proteins may play a role in removing cohesin from chromosomes.

1.1.13 Removal of cohesin from chromosomes

The dissociation of cohesin from chromosomes in anaphase and sister chromatid segregation is dependent on the conserved protein separase. The yeast strain *esp1-1* contains a temperature sensitive mutation in the *esp1* gene. Cohesin does not dissociate from anaphase chromosomes at the non permissive temperature in *esp1-1* mutants and subsequently chromosomes do not segregate at anaphase (Ciosk et al., 1998, Uhlmann et al., 2000) suggesting that *esp1* is required for the timely dissolution of sister chromatid cohesion. Orthologues of *esp1* have also been found in humans (Wazenegger et al., 2000), *C. elegans* (Siomos et al., 2001) and *S. pombe* (Funabiki et al., 1996). The *esp1* gene and its orthologues in other organism encode the protein separase and all contain a separin domain characteristic of certain proteases (Uhlmann et al., 2000), this suggests that separase dependent proteolysis is required for cohesin removal from chromosomes in most if not all eukaryotic organisms.

Removal of cohesin from chromosomes and dissolution of sister chromatid cohesion in anaphase is ultimately regulated by separase dependent proteolysis of the cohesin subunit Scc1. Over expression of the *esp1* gene in budding yeast results in accumulation of Scc1in two smaller cleavage products (an Scc1 N-terminal cleavage product and an Scc1 C-terminal cleavage product) (Uhlmann et al., 1999) and separase has also been shown to cleave purified Scc1 in vitro (Uhlmann et al., 2000). In vivo studies have shown that accumulation of Scc1 cleavage products occurs simultaneously with cohesin dissociation from yeast and sister chromatid separation (Uhlmann et al., 1999) suggesting that the cleavage of Scc1 is the mechanism by which cohesin is removed from chromosomes in anaphase. Consistent with this budding yeast expressing a non cleavable form of Scc1 cannot segregate their chromosomes (Uhlmann et al., 1999) mimicking the phenotype of *esp1-1* cells incubated at the non permissive temperature.

The cleavage of Scc1 is a non reversible reaction which ensures that cohesin cannot bind until the next cell cycle. Following cleavage of Scc1 the N-terminal and C-terminal cleavage products remain bound to the globular heads of Smc3 and Smc1 respectively (Haering et al., 2002). The binding of the Scc1 C-terminal cleavage product appears to be important for ensuring that the globular head domain of Smc1 and Smc3 do not interact (Weitzer et al., 2003) and as such may inhibit the further interaction of cohesin with chromosomes and thus the separation of chromosomes. This C-terminal cleavage fragment undergoes proteolysis before the onset of the next cell cycle (Rao et al., 2001) to ensure that functional cohesin is available when it is next required. The level of *scc1* mRNA increases to its maximum level

during S-phase in *S. cerevisiae* suggesting that newly manufactured Scc1 is used in the next cell cycle.

In metazoans the dynamics of cohesin dissociation is more complex; cohesin largely dissociates from chromosome arms in prophase and sister chromatid cohesion is maintained after prophase and before anaphase by a small population of cohesin at centromeric regions. The removal of large amounts of cohesin during prophase is dependent on phosphorylation of the Scc3 subunit of cohesin (Hauf et al., 2005). HeLa cells containing a non-phosphorylatable form of Scc3 incorporated into the cohesin complex displayed similar levels of level of cohesin binding across chromosomes in prometaphase and metaphase suggesting that the prophase dissociation of cohesin did not occur (Hauf et al., 2005).

Interestingly the cohesin complexes that are removed in prophase do regulate sister chromatid cohesion. Microtubule poisons such as colcemid and nocodazole inhibit the progression of the cell cycle and cells accumulate in metaphase (Rieder and Palazzo, 1992). Whilst sister chromatid cohesion is maintained in HeLa cells treated with nocodazole, the delay in the cell cycle results in loss of arm cohesion which is in accordance with a loss of cohesin binding (Gimenez-Abian et al., 2004). The chromosomes from HeLa cell arrested in metaphase in the presence nocodazole containing a non-phosphorylatable form of Scc3 incorporated into the cohesin complex do not lose arm cohesion (Hauf et al., 2005) suggesting that the cohesion complexes dissociating from chromosomes do function in sister chromatid cohesion.

Despite the removal of the majority of cohesin from chromosome well before anaphase, sister chromatid separation is still dependent on Scc1 cleavage in *C. elegans* (Siomos et al., 2001), humans and *Xenopus* (Wazenegger et al., 2000). The cleavage of Scc1 in anaphase and subsequent separation of sister chromatids is also unaffected in HeLa cells expressing a non-phosphorylatable form of Scc3 which inhibits a dissociation of cohesin in prophase. This suggests that cohesin dissociation in prophase by a mechanism dependent on Scc3 phosphorylation is not essential for sister chromatid separation anaphase to occur.

1.1.14 The Mechanism of Sister Chromatid Cohesion

The popular prevailing model proposes an elegant mechanism for sister chromatid cohesion. It is thought that the cohesin complex encircles both sister chromatids within one cohesin ring topologically trapping the sister chromatids together (Figure 1.7A) (Haering et al., 2002). The

cohesin ring is large enough to encircle two condensed sister chromatids (Haering and Nasmyth, 2003) and cohesin binding to DNA is highly salt resistant (Ciosk et al., 2000) suggesting that the interaction is very stable. The finding that Scc1 is actively cleaved to ensure cohesin irreversibly dissociates from chromosomes is also consistent with a ring encircling sister chromatids. Further, cohesin complexes bound to chromatin can be easily removed by synthetic cleavage of either Scc1 or Smc3 (Gruber et al., 2003) whilst intact cohesin can also be removed from circular minichromosomes by restriction digestion of the minichromosome (Ivanov and Nasmyth, 2005) suggesting that DNA is not physically bound to cohesin. This model suggests that cohesin can actively slide along DNA once bound without becoming dislodged whilst the transcription machinery - which is too large to pass through the cohesin ring - is thought to push the cohesin complex to areas of convergent transcription (Nasmyth, 2005). Consistent with this is the finding that cohesin translocates from its point of loading to the cohesin associated regions (Lengronne et al., 2004).

The model for sister chromatid cohesion whereby cohesin entraps both sister chromatids within one cohesin ring has led to a novel mechanism for the establishment, maintenance and dissolution of sister chromatid cohesion (Nasmyth and Haering, 2005). At the onset of DNA replication the cohesin loading complex recruits the cohesin complex to chromosomes (Figure 1.8A). Once bound the cohesin complex recruits Pds5 and Eco1 (Figure 1.8B), the Eco1 protein enables establishment of sister chromatid cohesion in a manner linked to DNA replication. Pds5 ensures that sister chromatid cohesion is maintained until anaphase at which time cohesin is removed and sister chromatids move apart. In this model the cleavage of the Scc1 subunit of cohesin is sufficient for removal of the cohesin complex from chromosomes (Figure1.9A) during anaphase allowing sister chromatids to separate (Figure 1.9B).

Other models have been put forward to explain the mechanism by which cohesin generates sister chromatid cohesion. One such model suggests that two cohesin rings encircling separate sister chromatids interlock with each other or that the Scc1 subunit mediates a bridge between two cohesin rings to generate sister chromatid cohesin [Figure 1.7B and (Nasmyth and Haering, 2005)]. This model is consistent with the data previously mentioned in that cleavage of the cohesin ring would allow its removal from chromosomes however no evidence currently exists demonstrating that there is an interaction between two separate cohesin rings (Haering et al., 2002, Weitzer et al., 2003). Another model suggests that two cohesin rings actively bound to sister chromatids can interact with one another (Milutinovich and Koshland, 2003). As well as lacking evidence that two cohesin rings can interact, no defined DNA

binding domain for cohesin has ever been identified and cohesin association with DNA appears to be dynamic such that cohesin can actively move along chromosomes.

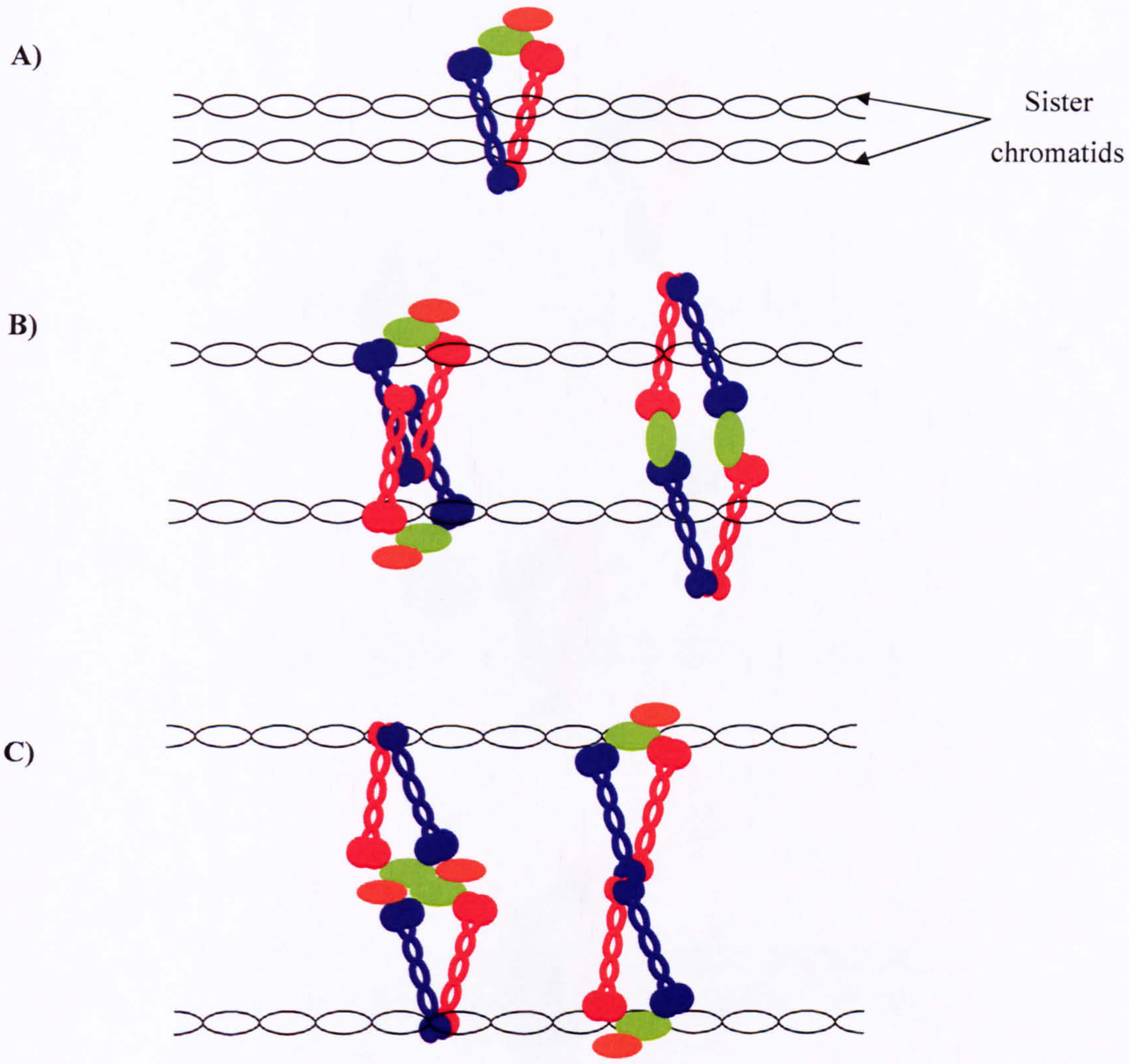

Figure 1.7 Proposed Models for the Mechanism of Sister Chromatid Cohesion

A) The cohesin complex (Figure 1.1 demonstrates a schematic of cohesin complex structure) is thought to encircle both sister chromatids thus ensuring sister chromatid cohesion is maintained. **B)** Two cohesin complexes bound separately to each sister chromatid could either interlock or Scc1 could mediate the interaction between two separate cohesin rings to generate sister chromatid cohesion. **C)** Two cohesin complexes bound separately to each sister chromatid could bind to one another to generate sister chromatid cohesion

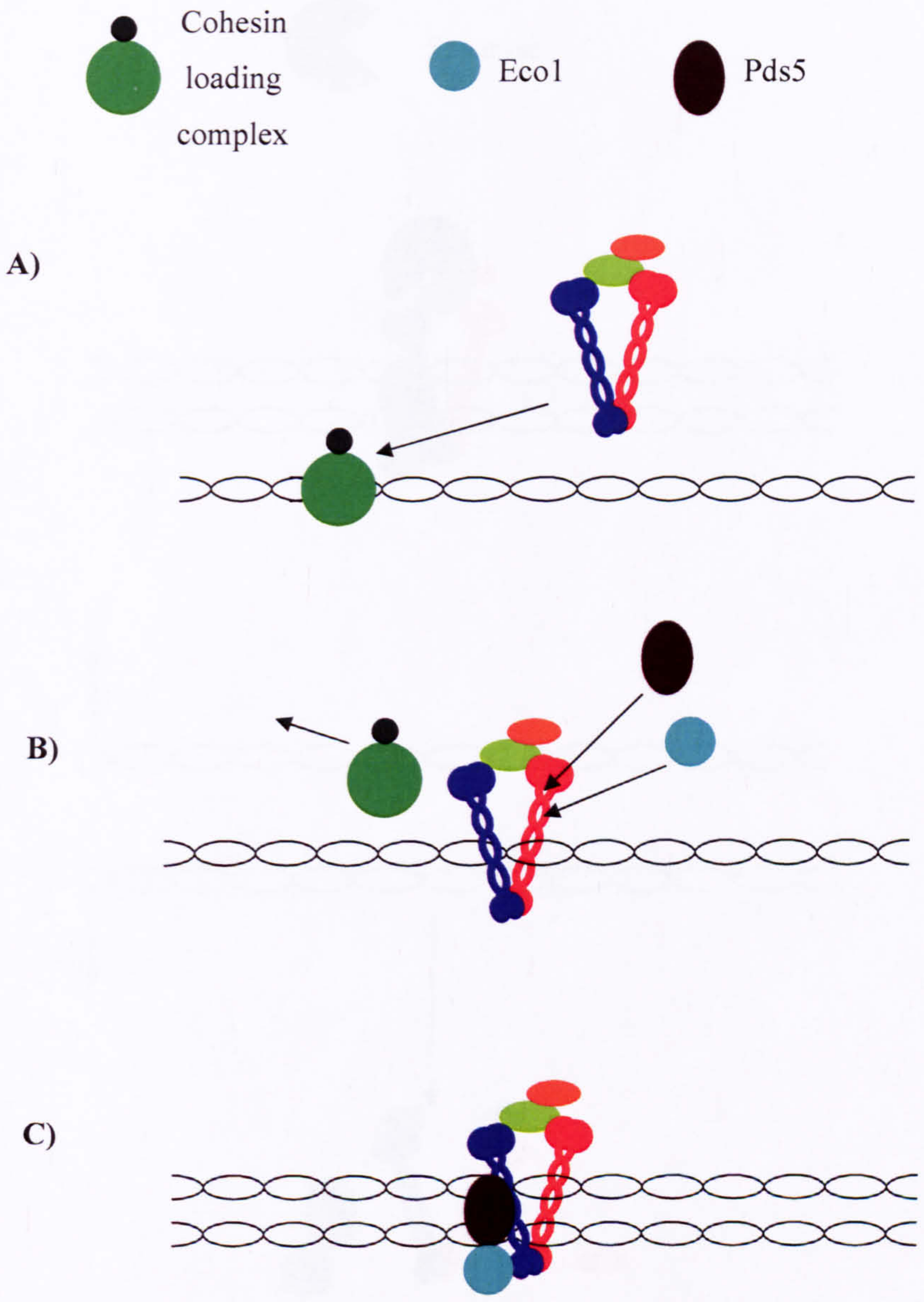

Figure 1.8 The establishment of sister chromatid cohesion [adapted from (Nasmyth and Haering, 2005)]

A) The cohesin loading complex binds to DNA and recruits the cohesin complex. **B)** Once bound the cohesin complex recruits Pds5 and Eco1 which are required for the establishment and maintenance of sister chromatid cohesion during DNA replication and onwards to anaphase. **C)** Sister chromatids are trapped together within the cohesin ring.

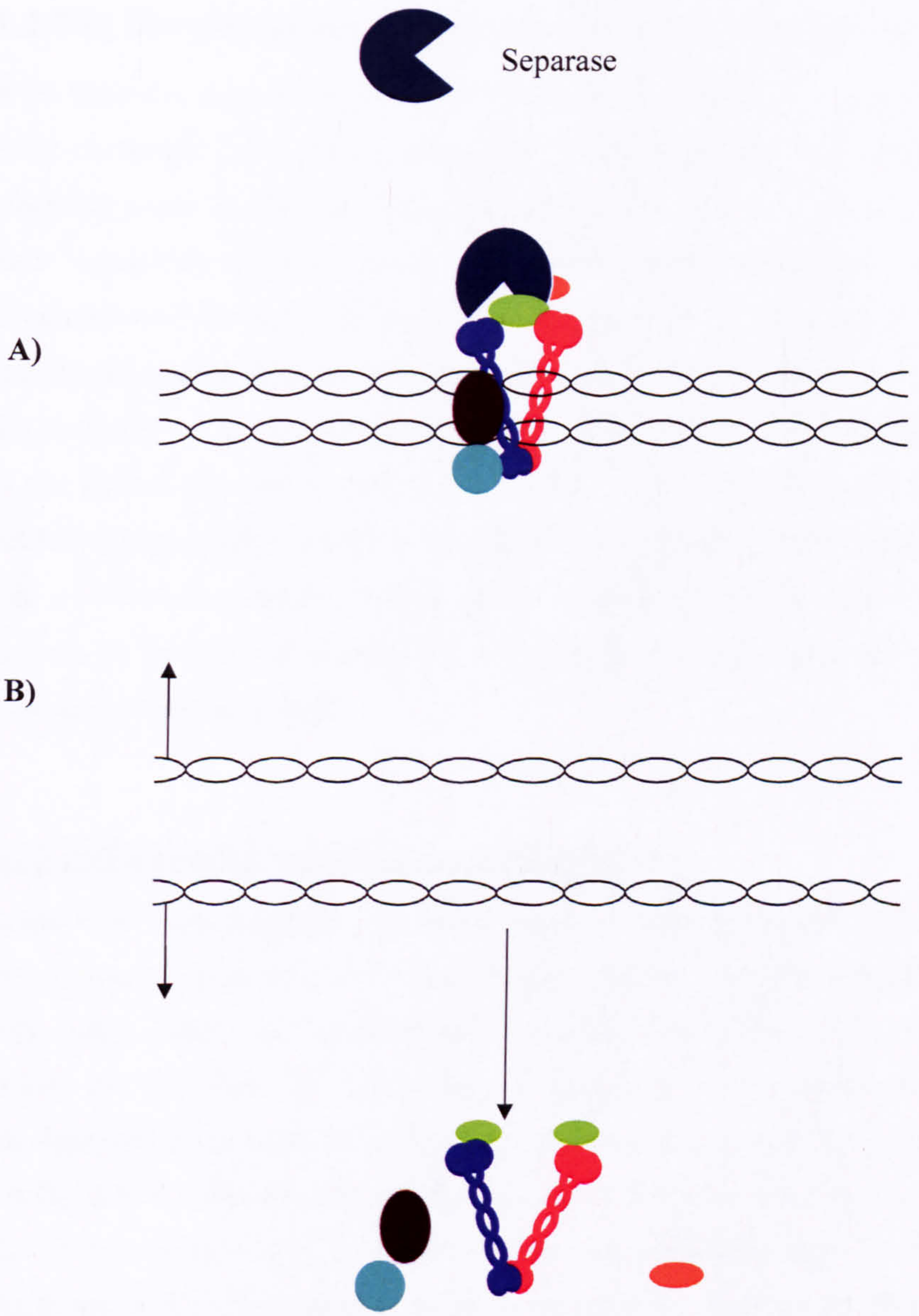

Figure 1.9 Removal of cohesin and sister chromatid separation [adapted from (Nasmyth and Haering, 2005)]

A) At anaphase the protease separase cleaves the Scc1 subunit of cohesin and the cohesin complex dissociates from chromosomes which are released from sister chromatid separation and can segregate **B)**.

1.2 The Developmental Significance of Sister Chromatid Cohesion Genes

With their key role in regulating chromosome segregation it is clear that genes involved in sister chromatid cohesion are important for the development of metazoans. It is becoming clear that genes involved in sister chromatid cohesion may be involved in functions outside of their canonical roles in sister chromatid cohesion that have implications in severe developmental diseases. Discussed here is the role of mutations in the *NIPBL* gene (that encodes the human adherin delangin) in causing of Cornelia de Lange Syndrome (CdLS) and the similarity of CdLS to Roberts syndrome and SC phocomelia which is caused by mutation in the cohesion establishment factor *ECSO2*. I shall introduce the role of the *Drosophila* cohesin complex and the adherin Nipped-B in long range gene regulation and shall discuss the role of sister chromatid cohesion genes in the development of *C. elegans*. Finally I shall summarise the role of the newly identified Scc4 orthologue MAU-2 in the development of the *C. elegans* nervous system

1.2.1 NIPBL and Cornelia de Lange Syndrome

Cornelia de Lange Syndrome is characterised by a distinctive set of physical defects including limb reduction (primarily in the upper limbs), growth, distinctive facial features (occasionally with a cleft palate) and hirsutism (Ireland et al., 1993, Kline et al., 1993). A range of other defects are prevalent in CdLS patients including mental retardation and defects in the development of the heart, kidneys, ocular, hearing and genitoutinary systems. Analysis of rare familial CdLS cases has demonstrated that it is a dominantly inherited condition (Russell et al., 2001) and the level to which patients are affected varies considerably, patients are diagnosed with either classical or mild forms with classical patients being more severely affected.

Several independent mutation screens on CdLS patients have identified *NIPBL* mutations in only ~30-50% of CDLS patients (Tonkin et al., 2004, Krantz et al., 2004, Borck et al., 2004, Gillis et al., 2004). The majority of *NIPBL* mutations are expected to cause premature stop codons within the delangin protein encoded by *NIPBL* (Strachan, 2005). Interestingly *NIPBL* mutations identified that affect only a single amino acid change in delangin map to the C-terminal region of the protein that is conserved through to *S. cerevisiae* (Strachan, 2005) suggesting that inhibiting the function of this region of the protein is key in the pathogenesis of the disease.

It is currently unclear whether mutations in *NIPBL* cause premature sister chromatid cohesion in CdLS patients and conflicting reports exist arguing that they do and do not (Kaur et al., 2005, Tonkin et al., 2004). Given the dominant nature of *NIPBL* mutations at least one copy of the *NIPBL* gene is unaffected; therefore, functional delangin protein may still be produced. Interestingly Roberts syndrome and SC phocomelia (which is a less severe form of Roberts syndrome) patients display phenotypes such as physical and mental growth retardation, limb defects (affecting all four limbs), distinctive facial features and cleft palate. As previously mentioned Roberts syndrome is caused by recessive mutations in *ESCO2* (Schule et al., 2005, Vega et al., 2005) which is involved in the establishment of sister chromatid cohesion (Hou and Zou, 2005). The recessive nature of *ESCO2* mutations means that all ESCO2 protein in patients with Roberts syndrome and SC phocomelia will be affected and consequently premature sister centromere separation is observed in these patients. This suggests that aberrant cell division in these patients as a result of a defect in sister chromatid cohesion could lead to the phenotypes observed in Roberts syndrome and SC phocomelia patients. The similarity of phenotypes shared by CdLS and Roberts syndrome/SC phocomelia patients suggests that the pathogenesis of the diseases is similar.

1.2.2 C. elegans Developmental Defects Caused by Aberrant Cell Division

The effect of cohesin related defects in cell division on the development of *C. elegans* has been shown to lead to abnormal development. *C. elegans* depleted of the cohesin complex members Scc1 or Scc3 display defect in cell division and consequent embryonic lethality with 99% - 100% penetrance depending upon which report is considered (Mito et al., 2003, Pasierbek et al., 2003). However, depletion of Scc1 or Scc3 during larval stages of worm development results in worms displaying an uncoordinated phenotype in which the worm cannot move backwards and worms displaying a protruding vulval phenotype in which the vulva of the worm is everted outside of the body (Mito et al., 2003, Pasierbek et al., 2003). The cell types affected in these worms namely the ventral nerve cord and vulva are known to divide postembryonically (Sulston and Horvitz, 1977) and the uncoordinated and vulval phenotype have been previously attributed to defects in cell division (Albertson et al., 1978, Sulston and Horvitz, 1981).

Analysis of the *C. elegans* adherin (PQN-85) function has been restricted to genome wide RNA interference (RNAi) screens. In *C. elegans* RNAi is an effective tool to inactivate gene function by introducing double stranded RNA sharing specific sequence with the targeted

gene (Fire et al., 1998). Global RNAi screens which successively target each individual *C. elegans* gene by RNAi have shown that depleting *pqn-85* results in embryonic lethality, a clear phenotype indicative of osmoregulation defects, body morphology defects (which are not described in the report) and uncoordination (Kamath et al., 2003). The significant phenotypic overlap observed between *pqn-85* depleted worms and those depleted of cohesin subunits including uncoordination and embryonic lethality suggests that the cohesin loading role of PQN-85 may well be conserved.

1.2.3 Nipped-B Functions in Long Range Gene Regulation

It is currently unclear how mutations in *NIPBL* cause CdLS but studies of its orthologue in *Drosophila* (called *Nipped-B*) suggest that aberrant gene regulation may play a role. In wild type *Drosophila*, expression of the *cut* gene is increased by a remote enhancer sequence 85Kb upstream of the *cut* promoter (Jack et al., 1991). Introduction of a *gypsy* transposon sequence between the remote enhancer and the *cut* gene reduces expression of the *cut* gene by binding of the Su(Hw) insulator protein to the gypsy insulator sequence (Dorsett, 1990, Dorsett, 1993). The reduction of *cut* expression by Su(Hw) binding manifests in flies as a series of small nicks along the edge of the wing. Mutations in the *Nipped-B* gene were found to increase the level of wing nicks in flies with the gypsy transposon inserted between the *cut* gene and its enhancer (Rollins et al., 1999) thus reducing *cut* expression.

The effect of *Nipped-B* on the *cut* gene is confined to overcoming the insulating effects of the *gypsy* transposon. Flies which contain a reduced dosage of the *cut* enhancer display wing nicks even in the absence of a gypsy insertion (Rollins et al., 1999), presumably as a result of a reduction in *cut* gene activation due to a reduction in the function of the enhancer. Mutations in *Nipped-B* do not exacerbate the wing nicking phenotype of these flies (Rollins et al., 1999) as they do when the gypsy insulator is present. This suggests that *Nipped-B* does not act directly on the enhancer sequence but rather on overcoming the effects of the gypsy insertion.

1.2.4 Cohesin opposes the effect of Nipped-B on long range gene regulation

Flies containing the gypsy insertion between the *cut* gene and its enhancer were depleted of either Nipped-B or Scc-3 by RNAi (Rollins et al., 2004). Interestingly whilst depletion of Nipped-B resulted in an increase in the number of wing nicks (as was expected from the mutational data previously mentioned), depletion of Scc3 resulted in a decrease in the number

of wing nicks (Rollins et al., 2004) suggesting that *cut* gene expression is increased. The authors suggested that cohesin binding to specific regions between the *cut* gene and its enhancer inhibits the ability of the enhancer to increase expression of the *cut* gene. Consistent with this hypothesis, chromatin immunoprecipitation studies showed that Scc3 and Smc1 localise to four specific regions between the *cut* gene and its enhancer (Dorsett et al., 2005). This however appears to be contradictory to the suspected role of Nipped-B in loading cohesin. Loss of Nipped-B function would presumably reduce the level of chromosomally bound cohesin and would mimic the phenotype of flies depleted of Scc3 or Smc3, but is not the case as demonstrated by these results. The authors speculated that Nipped-B may also be required to remove cohesin thereby establishing an equilibrium of cohesin bound to chromosomes, and that when Nipped-B function is perturbed the equilibrium takes longer to be established thereby altering gene expression (Rollins et al., 2004).

1.2.5 Delangin and Cohesin Bind to Mediators of Chromatin Structure

An HP1 binding motif in the N-terminal region of delangin has been mapped and the specific motif required for HP1 binding is well defined (Murzina et al., 1999, Lechner et al., 2005). The human HP1 family consists of three proteins - HP1a, which localises to centromeres, HP1ß, which is distributed widely on chromosome arms and HP1?, which localises to euchromatin (Minc et al., 2000, Minc et al., 1999). Of the HP1 family members delangin has been shown to bind HP1a and HP1? (Lechner et al., 2005). HP1 is also linked to cohesin function, the *S. pombe* Smc3 subunit of cohesin (called Psc3) binds the *S. pombe* HP1 homologue Swi6 (Nonaka et al., 2002). Centromeric association of the Smc3 subunit of cohesin and presumably the whole cohesin complex is reduced in *S. pombe* lacking *swi6* (Nonaka et al., 2002). Consistent with this result, *Drosophila* with mutations in *HP1* display chromosome segregation defects (Kellum and Alberts, 1995) suggesting that cohesin localisation may also be perturbed in these mutants. The finding that delangin binds to and loads proteins with links to gene silencing suggests that aberrant gene transcription caused by mutations in *NIPBL* may result in some of the phenotype observed in CdLS patients.

1.2.6 The mau-2 Gene is Developmentally Significant

The *mau-2* gene which has been identified as a potential orthologue of *scc4* is important in the development of *C. elegans*. All strains of *C. elegans* with mutations in the *mau-2* gene (summarised in Table 1.5) present identical phenotypes (Benard et al., 2004, Takagi et al.,

1997). The frequency with which *mau-2* mutant worms lay dead eggs is no greater than that observed in wild type *C. elegans* (Benard et al., 2004, Takagi et al., 1997) suggesting that the *mau-2* gene is not essential for oogenesis or embryogenesis. Approximately half of the mutant worms develop into adults where upon they display a variety of defects. The defects include those in egg laying, a living death (LID) phenotype in which the worm becomes fluid filled (indicative of osmoregulation defects) and uncoordinated movement in which the worms are capable of forward movement (albeit sluggish) but are incapable of backwards movement, (Benard et al., 2004). Whilst none of the mutant strains have the *mau-2* gene completely removed, it is considered that they are null mutants. A construct expressing the first 84 amino acids of the MAU-2 protein does not rescue any of the *mau-2* mutant strains suggesting that they all represent null alleles.

Table 1.5 Summary of *mau-2* Mutant Strain Genotypes

Mutant strain	Details of mutation
qm4	Missense that causes a glycine to an arginine substitution at residue 53
qm5	Nonsense mutation in codon 20
qm40	Nonsense mutation in codon 279
qm160	Codon 66 is joined to the last 54bp of intron 5 which introduced two stop codons. Any translated product would be 68 amino acids long

It is likely that all of the phenotypes associated with *mau-2* mutants are due to defects in the nervous system. Ectopic expression of *mau-2* exclusively within the nervous system rescues all *mau-2* mutant phenotypes (Benard et al., 2004). Similarly a *mau-2::GFP* construct can rescue all mutant phenotypes observed in the in the *qm160* strain (Benard et al., 2004) and whilst the MAU-2::GFP protein is ubiquitously expressed from midembryogenesis it becomes restricted to the cytoplasm of the nervous system in adult *C. elegans* (Benard et al., 2004). Closer study of *qm4* LID mutants showed that cells undergoing long range migrations such as neurones are frequently misplaced [(Takagi et al., 1997) and summarised in Table 1.6]. Takagi et al (1997) also report that non-LID *qm4* mutants also display neuronal migration defects but not to such a severe degree as those observed in LID *qm4* mutant.

It is currently unclear how the MAU-2 protein that is encoded by the *mau-2* gene functions in neuron and axon migration. Ectopic expression of *mau-2* in the AVM in a *mau-2* mutant background can rescue the axon migration defect of that specific neuron (Benard et al., 2004). It has also been shown that *mau-2* functions independently of other genes controlling the migration of the AVM axon such as *unc-6* and *slit* (which encode guidance cues) and *unc-40* and *sax-3* (which respectively encode receptors for the *unc-6* and *slit* guidance cues) (Benard et al., 2004). The data summarised in Table 1.6 show that neurons do migrate in *mau-2* mutants but either not far enough and sometimes in the wrong direction, this suggests that *mau-2* functions in the guidance of neuronal migration and not on the physical of movement of neurons. This suggests that *mau-2* may be part of a novel mechanism to control neuronal guidance within *C. elegans*.

Table 1.6 Summary of Neuron Migration Defects Associated with *qm4* LID Mutants

Name of Neuron	Migratory pattern	Placement affected in *qm4* strain	Axon Affected
Hermaphrodite specific neuron (HSN)	Born posterior to the anus and migrates anteriorly to slightly posterior to the vulva	Yes – excessively posteriorly, anteriorly and dorsally placed	Not reported
BDU	Non-migratory anteriorly placed cells	No	Not reported
Anterior Lateral Microtubule cells (ALM)	Sister cells of the BDU which migrate posteriorly from the position of the BDU	Yes – excessively anteriorly placed and rarely too ventrally placed	No
Sub-dorsal, Right Neuroblast Descendent (SDQR)	Migrates dorsally and anteriorly	Yes – excessively posteriorly, anteriorly and ventrally placed	Not reported
Anterior Ventral Microtubule cell (AVM)	Sister of SDQR migrates ventrally and anteriorly	Yes – excessively posteriorly, anteriorly and dorsally placed	Yes – axons are normally directed ventrally then anteriorly but run on the lateral body side and are directed both anteriorly and posteriorly
Canal Associated neuron (CAN)	Born in the head and migrates posteriorly	No	Yes – axons migrated ventrally and dorsally instead of anteriorly and posteriorly

1.3 Aims of Thesis

The principal aim of this study was to explore links between the *C. elegans pqn-85* and *mau-2* genes and to determine their role in the regulation of chromosome segregation. As previously mentioned orthologues of the *C. elegans pqn-85* gene include the human *NIPBL* gene, mutations in which have been implicated in the cause of the severe developmental disease CdLS, and the *scc2* gene of *S. cerevisiae* which has a well characterised role in sister chromatid cohesion. The protein encoded by *mau-2* functions in the guidance of long range migratory cells and axons and is well conserved amongst higher eukaryotes. However, a potential orthologue of *mau-2* in *S. cerevisiae* has only recently been identified as the *scc4* gene of *S. cerevisiae*. The products of the budding yeast *scc2* and *scc4* genes form a complex that has a well characterised role in loading cohesin onto chromosomes during cell division.

To further study whether the cohesin loading complex is conserved in metazoans the *pqn-85* and *mau-2* genes will be studied in *C. elegans. C. elegans* was first used a model organism by Brenner (1970) and constitutes an excellent model system for a number of reasons. Although male *C. elegans* exist, hermaphrodite *C. elegans* are capable of self fertilisation in the absence of males producing several hundred progeny in just a few days. *C. elegans* are transparent at all stages of the cell cycle and as such their development has been well recorded and is found to be invariant from animal to animal (Sulston and Horvitz, 1977, Sulston et al., 1983). The discovery of RNA interference (RNAi) as an efficient method of targeting gene expression has greatly benefited research into *C. elegans*. The expression of specific genes can be silenced by introduction of exogenous double stranded RNA (dsRNA) sequences sharing homology to the gene into *C. elegans* (Fire et al., 1998). The effect of RNAi is not confined to the worm into which the dsRNA is introduced and the corresponding genes in the progeny resulting from the worm are also silenced (Fire et al., 1998). Introduction of dsRNA into only a few hermaphrodite *C. elegans* allows functional analysis of specific genes within several hundred progeny at one time.

The identification of a conserved complex in organisms other than *S. cerevisiae* with functions in chromosome segregation potentially has wider implications in understanding the pathogenesis of a complex human disease.

Chapter 2

Materials and Methods

Media agar and solutions were sterilised by autoclaving at 121°C for 30minutess unless otherwise stated.

2.1 Media, Agar Plates and Solutions

2.1.1 LB Broth - 1 litre

10g Bacto-tryptone

5g Yeast extract

10g NaCl

Make up to 1L with dh_20

2.1.2 SOC - 1 litre

20g Bacto-Tyrptone

5g Yeast Extract

10ml 1M NaCl

2.5ml1M KCl

10ml 1M $MgCl_2$

10ml 1M $MgSO_4$

10ml 2M Glucose

Make up to 1 litre with dH_2O

2.1.3 YPDA - 1 litre

20g Difco peptone

10g Yeast extract

15ml of 0.2% Adenine Hemisulphate

Make up to 950mls with dH_2O

After autoclaving add 50mls of sterile 40% dextrose

2.1.4 Agar Plates

LB and YPDA Agar plates were made by the addition of 15g/L of agar to media detailed in sections 2.1.1 and 2.1.3 respectively prior to autoclaving.

2.1.5 Selective Media and Plates

Selective media and plates were made by the addition of filter sterilised antibiotics to sterile media or sterile molten agar. Ampicillin was used at a final concentration of 100µg/ml in dH_2O, Kanamycin was used at a final concentration of 50µg/ml in dH_2O and Tetracyclin was used at a final concentration of 30µg/ml in ethanol.

2.1.6 SD Base and SD Agar Base

SD Base (product number: 630411) and SD Agar Base (product number: 630412) were bought as a pre-prepared powder (Clontech) and were rehydrated with 950mls of dH_2O and autoclaved as per manufacturers instructions. To make media and agar lacking specific amino acids 50mls of the appropriate sterile 10 X dropout supplement (Section 2.1.7) was added whilst the agar/medium was hand hot.

2.1.7 10 X Dropout Supplements

The appropriate amount of dropout supplement was added to 100mls dH_2O and was sterilised.

-Trp dropout supplement (Clontech catalogue number 630413)

-Leu dropout supplement (Clontech catalogue number 630414)

-Trp/-Leu/-Ade/-His dropout supplement (Clontech catalogue number 630428)

2.1.8 NTE buffer

0.1M NaCl

10mMTris HCl pH8

1mM EDTA

2.1.9 10X TE Buffer

100mM Tris HCl pH8

10mM EDTA

Dilute 1:10 in sterile dH_2O for 1X TE

2.1.10 Extraction Buffer

450µl NTE buffer (Section 2.1.8)

50µl 10% SDS

500µl Phenol

Solution was not autoclaved

2.1.11 M9 Buffer - 1 litre

3 g KH_2PO_4

6 g Na_2HPO_4

5g NaCl, 1 ml 1M $MgSO_4$

Make up to 1L with dH_2O

2.1.12 1 X TAE

40mM Tris base

20mM Actetae

2mM EDTA

Make up to correct volume with dH_2O

2.1.13 Gel Loading Buffer

0.25% Bromophenol blue

0.25% Xylene Cyanol FF

15% Ficoll

Make up to correct volume with sterile dH_2O

Solution was not autoclaved

2.1.14 Proteinase K Solution

500µg/ml Proteinase K (sigma P6556)

1% SDS

Make up to correct volume with NTE (Section 2.1.8)

Solution was not autoclaved

2.1.15 Stop Solution

1M Sodium Acetate

10mM EDTA

0.2% (W/V) SDS

Make up to correct volume with sterile DNAse and RNase free dH_2O (Sigma Catalogue number W4502)

Solution was not autoclaved

2.1.16 Z buffer - 1 litre

16.1g $Na_2HPO_4.7H_2O$

5.5g $Na_2PO_4.H_2O$

0.75g KCl

0.246g $MgSO_4.7H_2O$

Make up to 1L with dH_2O

2.1.17 X-gal Stock Solution

20mg/ml 5-bromo-4-chloro-3-indolyl-ß-D-galactopyranoside (X-Gal - Sigma Catalogue number B4252)

N,N-dimethylformamide (DMF- Sigma Catalogue number D4551)

Solution was not autoclaved but stored in dark at -20°C

2.1.18 Zbuffer/X-gal Solution

100ml Z buffer (see Section 2.1.16)

0.27ml ß-mercaptoethanol (Sigma Cat No. M-6250)

1.67ml X-gal stock solution (see Section 2.1.18)

Solution was not autoclaved

2.1.19 50% Polyethylene Glycol (PEG) - 1 litre

50% w/v of PEG 3350 (Sigma Cat No. P3640)

Make up to 1 litre with dH_2O

2.1.20 10X Lithium Acetate (LiAc)

1M LiAc (Sigma Cat No. 517992)

Make up to 1 litre with dH_2O

2.1.21 1 litre 1X TE/1X LiAc

5% 10X TE (see Section 2.1.9)

5% 10X LiAc (see Section 2.1.20)

Make up to 1 litre with sterile dH_2O

Solution was not autoclaved

2.1.22 PEG/LiAc

8ml 50% PEG (see Section 2.1.19)

1ml 10X LiAc (see Section 2.1.20)

1ml 10X TE (see Section 2.1.9)

2.2 General Molecular Biological Techniques

2.2.1 C. elegans Total RNA Extraction

1 ml of extraction buffer (Section 2.1.10) was heated to single phase at 85°C, 100µl of packed adult N2 *C. elegans* was added and the tube was inverted briefly and centrifuged at 14000rpm for 15 minutes at 4°C. The aqueous layer was removed to a fresh eppendorf tube and 500µl of Phenol:Chloroform (1:1 volume to volume) was added, mixed and the tube was centrifuged at 14000rpm for 15mins at 4°C. This was repeated once more with Phenol:Chloroform and then twice with Chloroform. The RNA was precipitated by adding 500µl of isopropanol and. The pellet was washed by adding 1ml of 100% ethanol, spun at 14000rpm for 15 mins at 4°C followed by 70% ethanol. The pellet was air dried and resuspended in 20µl of RNase free TE.

2.2.2 First Strand Synthesis of cDNA

First-strand cDNA was made from total RNA using Invitrogen Superscript III kit. 10pg-5µg of total RNA (Section 2.2.1) was added to an RNase free eppendorf with 1µl of oligo$(dT)_{20}$ (50µM), 1µl dNTP (10 mM) and sterile dH_20 to a maximum volume of 13µl. The mixture was heated to 65°C for 5 minutes and incubated on ice for at least 1 minute. The contents of the tube were collected by centrifugation 4µl of 5X first strand buffer, 1µl DTT (0.1M), 1µl RNAsin (Promega) and 1µL Superscript III enzyme was added. The reaction was mixed by gentle pipetting and was incubated at 50°C for 1 hr followed by 15mins at 70°C.

2.2.3 Polymerase Chain Reaction

All polymerase chain reactions (PCR) were carried out using Phusion (Finnzyme catalogue number FS530S), Pfx DNA polymerase (Invitrogen catalogue number 11708013) or Taq DNA polymerase (Promega catalogue number M2661) and were carried out as per manufacturer's instruction unless otherwise stated. The DNA template and the cycling conditions for the PCR varied depending on the experiment and this is specifically detailed in each individual chapter. The dNTPs used in all PCRs were obtained from Invitrogen (catalogue number 18427-013) and were used at a final concentration of 2mM. PCR Primers were designed using the web based Primer-3 design program and the sequences for each individual experiment are detailed within the chapters, all primers were ordered form Invitrogen and were used at a final concentration of 10µM. Unless otherwise stated all PCR were carried out using a DYAD thermal cycler PCR machine with a heated lid.

2.2.4 Agarose Gel Electrophoresis

A 100ml solution of 1X TAE buffer (Section 2.1.12) containing 1% agarose was briefly heated in microwave until the agarose had fully melted. Once the agarose solution had cooled enough to be held comfortably in the hand 2µl of 10mg/ml ethidium bromide solution (Sigma) was added to enable visualisation of DNA and RNA. The agarose solution was poured into a sealed gel tray and once set was transferred into a gel running tank containing 1X TAE buffer (Section 2.1.12). The correct amount of 6X DNA loading solution (Sigma) was added to each Nucleic acid sample such that the final concentration of dye was 1X. The samples were loaded alongside an adequate molecular weight marker. The tank was

connected to a BioRad Power Pac 300 set at 100mV until the blue dye was close to the bottom of the gel. DNA bands within the gel were visualised on a UV transilluminator.

2.2.5 Purification of DNA from Agarose Gels

DNA samples were size fractionated by agarose gel electrophoresis (Section 2.2.4) and bands corresponding to the DNA were extracted from the gel using a fresh scalpel and placed in a fresh microcentrifuge tube. The excised bands were placed into a sterile microcentrifuge tube and the DNA was purified from agarose gels using QIAquick gel extraction kit as per manufacturers' instructions.

2.2.6 Making Chemically Competent E. coli

A fresh colony of the *Escherichia coli* (*E. coli*) strain DH5a was used to inoculate 10ml LB broth (Section 2.1.1) and was grown overnight with shaking. 1ml of the starter culture was added to 100ml LB broth (Section 2.1.1) and the culture was incubated at 37°C until reaching log phase (the OD of the culture is 0.2 @ 600nm). The culture was incubated on ice for 10 minutes and then centrifuged at 4000rpm for 5 minutes at 4°C. The supernatant was discarded and the pellet was resuspended in 25mls of $CaCl_2$ (chilled on ice). The suspension was incubated on ice for 60mins before centrifugation at 6000rpm for 10mins at 4°C. The supernatant was discarded and the pellet was resuspended in 5mls of 100mM chilled $CaCl_2$. The suspension was incubated on ice for 1hr before addition of 1ml of 100% glycerol. The suspension was dispensed in 100µl aliquots into eppendorf tubes and snap frozen in liquid nitrogen. The frozen aliquots were stored at -80°C.

2.2.7 Transformation of Chemically Competent E. coli

A 2µl solution of the plasmid or ligation to be transformed was added to a 100µl aliquot of chemically competent cells (Section 2.2.6), gently mixed and was incubated on ice for 30 minutes. The cells were heat shocked at 42°C for 45 seconds and were recovered on ice for 5 minutes. The cells were incubated for 1 hr at 37°C in 1ml of SOC (Section 2.1.2) before being plated onto LB agar (Section 2.1.4) containing the appropriate antibiotic selection (Section 2.1.5) and grown overnight at 37°C.

2.2.8 Plasmid Purification from E.coli

E. coli carrying the plasmid to be purified were cultured overnight in 5ml of LB broth (Section 2.1.1) with appropriate selection (Section 2.1.5) at 37°C. After 16 hours the culture was centrifuged at 3000rpm for 10 mins at room temperature and the supernatant was discarded. A mini preparation of plasmid DNA was carried out on the pelleted cells using the QIAprep Spin Miniprep kit (QIAGEN) as per manufacturers' instructions.

2.2.9 Restriction Digestion

Restriction enzyme digests were performed according to the manufacturers' instructions. A single digest was composed of the DNA sample, 1 X concentration of the appropriate restriction enzyme buffer (supplied with enzyme), 0.1mg/ml BSA (supplied with enzyme) 1µl restriction enzyme and sterile dH_2O to a final volume of 20µl. If more than one enzyme was required in the digest 1µl of dH_2O was replaced with 1µl of the appropriate enzyme. The digest was incubated at the appropriate temperature for 1-4 hours after which time the digested DNA was analysed by agarose gel electrophoresis (Section 2.2.4).

2.2.10 DNA Sequencing

Plasmid DNA to be sequenced was purified (Section 2.2.8) and 5µl was placed at 37°C until sample had completely dried. The sample was sent to MWG (http://www.mwg-biotech.com/html/all/index.php) to be sequenced with appropriate primers.

2.3 Cloning and Subcloning of DNA

2.3.1 Cloning of PCR Products from Taq Polymerase Reactions

The pGEM-T easy system (Promega) was used to clone PCR products into the pGEM-T easy vector. The pGEM-T easy vector supplied with the kit is a linear DNA molecule with 3' thymidine overhangs. PCR products amplified with Taq polymerase have a 5' adenosine overhang thus providing compatible ends allowing the PCR product to ligate into the pGEM-T easy vector. To ligate the PCR product into pGEM-T easy a 3:1 ratio of vector:insert was combined in an eppendorf tube with 1µl T4 DNA ligase (Promega), 2µl 10 X T4 DNA ligase buffer (Promega) and dH_2O to 20µl final reaction volume. The reaction was gently mixed and was incubated at 4°C for at least 16hrs. 2µl of the ligation reaction was used to transform

chemically competent DH5a (Section 2.2.7). The transformed bacteria were grown on LB agar containing 100µg/ml ampicillin, 0.1mM IPTG and 40µg/ml X-Gal.

A blue/white colour screen was used to identify colonies that contained the PCR product inserted in the plasmid. The pGEM-t easy vector contains an IPTG inducible *lacZ* gene encoding B-galactosidase, an enzyme that can cleave the chemical X-gal yielding galactose and 5-bromo-4-chloro-3-hydroxyindole. The 5-bromo-4-chloro-3-hydroxyindole oxidizes into 5,5'-dibromo-4,4'-dichloro-indigo, an insoluble blue product. A PCR product ligated into pGEM-t easy disrupts the *lacZ* gene and results in bacteria producing white colonies when grown in the presence of IPTG and X-gal. Bacteria containing pGEM-T easy with no PCR product inserted have a functional *lacZ* gene and result in blue colonies when grown in the presence of IPTG and X-gal. Plasmid DNA was extracted from white colonies and was analysed for the correct insert by restriction digestion (Section 2.2.9) using appropriate restriction enzymes followed by agarose gel electrophoresis (Section 2.2.4).

2.3.2 Cloning of PCR Products from Pfx Platinum and Phusion Polymerases

The Pfx platinum (Invitrogen) and Phusion (Finzzymes) polymerases have a proofreading function that removes the adenosine residue at the 5' end of the PCR product. Therefore before ligation of the PCR product into pGEM-T easy (Promega and Section 2.3.1) the adenosine residue was reattached to the PCR product using an A-tail reaction. The PCR product was incubated with 0.2mM dATP (Invitrogen catalogue number 18427-013), 1 X Taq buffer containing 1.5mM $MgCl_2$ (Promega), 0.5µl of Taq DNA polymerase (Promega) and dH_2O to 15µl at 72°C.

2.3.3 Subcloning of Inserts into New Vectors

The plasmid containing the gene of interest and the plasmid that the insert was to be cloned into were purified and digested with the appropriate restriction enzymes. The products of the digestion were visualised by agarose gel electrophoresis (Section 2.2.4) and bands of the appropriate size were excised from the gel and purified (Section 2.2.5). To ligate the gene of interest into the new vector a 3:1 ratio of vector:insert was combined in an eppendorf tube with 1µl T4 DNA ligase (Promega), 2µl 10 X T4 DNA ligase buffer (Promega) and dH_2O to 20µl final reaction volume. The reaction was gently mixed and was incubated at 4°C for at least 16hrs. 2µl of the ligation reaction was used to transform chemically competent cells

(Section 2.2.7). The transformed bacteria were grown on LB agar (Section 2.1.4) containing the appropriate selection antibiotic (Section 2.1.5). Plasmid DNA was extracted from the resultant colonies (Section 2.2.8) and was analysed for the presence of the insert by restriction digest (Section 2.2.9) using appropriate restriction enzymes followed by agarose gel electrophoresis (Section 2.2.4).

2.4 General *C. elegans* Techniques

2.4.1 C. elegans strains

N2 (Bristol isolate)	Wild type (Brenner, 1974)
histone::GFP	F54E12.4::GFP = H2B::GFP (Strome et al., 2001)
a tubulin::GFP	OD3: Itls24[pAZ132;pie-1/GFP::tba-2 + unc-119(+)]

2.4.2 E. coli strain

OP50 Uracil auxotroph E. coli B

2.4.3 Nematode Growth Media (NGM) Plates

3g NaCl, 2.5g Bacto-peptone (BD Biosciences Catalogue number 211820)

17g Bacto-agar (BD Biosciences Catalogue number 214030)

Make up to 975mls with dH_2O.

After autoclaving the following is added –

1ml cholesterol (5mg/ml in ethanol)

1ml 1M $CaCl_2$ (sterilised by autoclaving),

1ml 1M $MgSO_4$ (sterilised by autoclaving) and

25ml 1M potassium phosphate buffer pH 6.0 (sterilised by autoclaving) (Brenner, 1974).

After addition of the supplements the media was poured into 50mm plates (Barloworld Sterilin item number 124), allowed to set at room temperature and then kept at 4°C until required.

2.4.4 Fresh NGM Plates

The *E. coli* OP50 strain (Section 2.4.2) was used to inoculate 5mls of LB broth (Section 2.1.1) without selection and was incubated overnight to stationary phase at 37°C with shaking. The OP50 culture was streaked onto NGM plates allowed to dry and the plates were incubated at 37°C overnight to produce a bacterial lawn. The plates were stored at 4°C until required.

2.4.5 Maintenance of C. elegans Strains

C. elegans strains were maintained at 15°C as previously described (Brenner, 1974), all experiments were carried out at 20°C unless otherwise stated.

2.4.6 C. elegans Genomic DNA Extraction

100µl of packed worms were collected by centrifugation in a microcentrifuge tube and were washed twice in 1ml of M9 Buffer (Section 2.1.11) and once in 1ml NTE (Section 2.1.8). The supernatant was removed and the pellet was frozen in liquid nitrogen. The washed worms were incubated in 1ml of Proteinase K solution (Section 2.1.14) at 65 °C for 1 hour during which time the solution becomes viscous. 1ml of buffered phenol (Sigma) was added and the tube was gently inverted and centrifuged at 14000rpm for 5 minutes at room temperature. The upper aqueous phase was removed to a fresh microcentrifuge tube and the phenol extraction was repeated two more times. The aqueous phase was removed to a fresh 15ml falcon tube and 2.5ml ice cold ethanol was added. The nucleic acid which should be visible at this stage was removed by spooling it around a sealed glass pipette and resuspended in 100µl dH_2O in a microcentrifuge tube.

2.4.7 Double Stranded RNA Production for RNA Interference

A small segment of the *scc-3*, *mau-2* and *pqn-85* genes were amplified by PCR (Section 2.2.3) from *C. elegans* genomic DNA using Taq DNA polymerase (Promega) as per the manufacturer's instructions. The PCR primers used were Scc-3 froward with Scc-3 reverse for *scc-3*, Pqn-85 forward with Pqn-85 reverse for *pqn-85* and Mau-2 forward with Mau-2 reverse for *mau-2* and the sequences are detailed in table 2.1. the primer were designed such that the PCR product is flanked by a T7 and T3 promoter. The forward primers contain the 19bp T3 promoter sequence (Italicised in bold in table 2.1) and the reverse primers contain the 19bp T7 promoter (italicised in bold in table 2.1). The PCR reaction was carried out using

the conditions detailed in table 2.2. The PCR products were size fractionated using agarose gel electrophoresis (Section 2.2.4) and a specific band of the correct size was excised from the gel (Section 2.2.5). The purified DNA (4µl) was transferred to a fresh microcentrifuge tube with 4µl of 5X transcription buffer (Promega), 4µl 5X rNTPs (2.5mM stock concentration) (Promega), 1µl RNasin RNase inhibitor (Promega), 2µl DTT (Promega - 100mM stock concentration) and 4µl sterile RNAse free dH_2O (Sigma). The solution was thoroughly mixed and 9.5µl was removed to a fresh microcentrifuge tube to which 1µl of T3 polymerase was added, 1µl of T7 polymerase was added to the remaining mix. The T3 reaction was incubated at 25°C for 1.5hr and the T7 reaction was incubated at 37°C for 1.5hr. In a fresh microcentrifuge tube 9.5µl of each reaction was combined (the remaining 1ul of the T3 and T7 reaction was placed at -20°c for subsequent agarose gel analysis) and 380µl stop solution with 0.3µl glycogen was added. 200µl of phenol/choroform/isoamyl alcohol (25:24:1) was added, the tube was vortexed briefly and centrifuged for a few seconds to resolve the phases. The upper aqueous phase was transferred to a fresh microcentrifue tube to which 200µl chloroform was added, the tube was vortexed briefly and centrifuged for a few seconds to resolve the phases. The upper aqueous phase was again removed to a fresh microcentrifuge tube and the sample was incubated at 68°C for 10mins to relax the secondary structure of the single stranded RNA. The sample was then incubated at 37°C for 30 minutes to anneal the two strands of RNA. The RNA was precipitated by vigorous vortexing with 1ml 100% ethanol followed by centrifugation at 14000rpm for 10mins. The supernatant was removed and the pellet was washed in 1ml of 70% ethanol followed by centrifugation at 14000rpm for 10mins. The supernatant was removed and the sample was air dried for several minutes before the pellet was resuspended in 10 µl of RNase free sterile dH_2O. To check the quality of the RNA and to confirm that all single stranded RNA reactions worked, 1µl of the double stranded RNA sample was run on a gel alongside against the T3 and T7 single stranded RNA samples with a suitable size marker.

Table 2.1 Sequence of PCR primers used to generate the DNA template for dsRNA production

The T7 and T3 promoter sequence within the primers are represented by the italicised sequence and the gene specific sequence is represented by the bold sequence. The *mau-2* genomic sequence used for reference was the CO9H6 cosmid with GenBank accession number Z81466.1. The *pqn-85* genomic sequence used for reference was the Y43H11AL cosmid (Genbank accession number AC024781.2). The *scc-3* genomic sequence used for reference was the F18E2 cosmid (Genbank accession number Z75537.1).

Primer name	Sequence (5'-3')	Position of 5' base within Gene Sequence
Scc-3 forward	*AATTAACCCTCACTAAAGG***ACAGCGACTTTTTGCGCTAT**	11143
Scc-3 reverse	*TAATACGACTCACTATAGG***TCGATGAAGAACGTCGTGAG**	11885
Mau-2 forward	*AATTAACCCTCACTAAAGG***AGCGCCTTTCAAAAATCAAA**	28712
Mau-2 reverse	*TAATACGACTCACTATAGG***CGCCAAAAATGTGAAAACTG**	29647
Pqn-85 forward	*AATTAACCCTCACTAAAGG***CCGCCAATAATTCAAGCAGT**	30534
Pqn-85 reverse	*TAATACGACTCACTATAGG***TGTGACCCAAAGAAATGCTG**	29850

Table 2.2 PCR cycling conditions for PCR reactions using primers in Table 2.1

Step	Temperature	Time	Number of Cycles
Initial Denaturation	95	2 minutes	1
Denaturation Annealing Extension	95 55 72	30 seconds 30 seconds 1 minute	40
Final Extension	72	10 minutes	1

2.4.8 Fabrication of Microinjection Needles

Microinjection needles were pulled from borosilicate glass capillaries tubes (Harvard apparatus Ltd - part number 30-0051) using a Flaming Brown micropipette puller model P-97 following the instruction provided by the manufacturer. Good needles required a fine point to minimise damage during injection whilst being stiff enough to break the cuticle of the worm.

2.4.9 Loading of Samples into Microinjection Needles

The sample to be loaded was centrifuged at 14000rpm for 1 minute to remove debris and prevent blockage of the needle. 0.5µl of the sample was pipetted onto the open end of the microinjection needle and the solution travelled to the closed end of the needle by capillary action.

2.4.10 Fabrication of Dried Agarose Pads for Microinjection

A 2% solution of agarose (Sigma) in dH_2O was gently melted in a glass test tube over a Bunsen burner. The molten solution was dropped onto a new coverslip using a Pasteur pipette and another new coverslip was immediately place on top of the molten agarose such that the agarose spread into a thin pad. The pad was allowed to cool for 30 seconds and the coverslips were carefully slid apart. The coverslip with the agarose pad was placed pad side up at room temperature and covered gently with foil, the pad was allowed to dry for 24 hrs before use.

2.4.11 Microinjection of C. elegans

Young adult *C. elegans* were placed into M9 buffer (Section 2.1.11) to remove the majority of bacteria transferred from growth plates. The washed worms were mounted on dried agarose pads (Section 2.4.10) under heavy liquid paraffin and were stroked flat such that the worm became glued from head to tail to the agarose pad and was unable to move. The pad was placed onto the gliding stage of Zeiss Axiovert over an A plan 10X objective and the worm was manipulated into the centre of the field of vision. The needle was loaded with the appropriate solution (Section 2.4.9) and was placed in an Eppendorf Transjector 5246 attached to a Micromanipulator 5171. The end of the needle was brought into view and moved close to the gonad of the worm. To give a better feel of depth the worm and needle were viewed under a Plan Neofluar 40X DIC objective. The needle was manipulated such that the tip broke the surface of the gonad and the end was clearly visible inside the worm. The

solution was injected such that the syncital nuclei surrounding the end of the needle could be seen to swell slightly and return to their original position. The needle was removed and the pad was removed form the injection apparatus. The worm was lifted from the agarose pad using a drop of M9 (Section 2.1.11) and placed on a fresh NGM plate under 5µl of M9 to recover (the M9 helps to rehydrate the worm after being attached to the dried agarose pad).

2.4.12 Fabrication of Fresh Agarose Pads for Microscopic Examination of C. elegans Embryos

A 2% solution of agarose (Sigma) in dH_2O was gently melted in a glass test tube over a Bunsen burner and the test tube was placed in a hot block at 80°C to keep the solution molten. Using a Pasteur pipette a drop of agarose was placed onto a clean microscope slide that was sat between two other microscope slides with sellotape placed along their length. A fourth slide was placed across all three slides such that the fourth slide spread the agarose but sat on the sellotape of the two outer slides. This gives a pad that is well spread but not too thin. The pad was used immediately.

2.4.13 Extraction of C. elegans Embryos from Adult Hermaphrodites by Dissection

Adult *C. elegans* were picked and placed into 10µl of sterile dH_2O in a round bottomed embryo dish. The worm was held at one end using fine tweezers and was dissected in half along the centre point using a scalpel. The embryos were stroked from either half of the worm by holding the head/tail and stroking the worm with the scalpel from the head/tail to the open end of the worm.

2.4.14 Fabrication of Mouth Pipettes

Narrow-bore mouth pipettes were made by rolling and heating glass Pasteur pipettes in a Bunsen burner until the glass became noticeably soft. The pipettes were then removed from the flame and either end was pulled apart by hand, this resulted in a long, narrow shaft which gradually changed in diameter over the pulled length of the pipette.

2.4.15 Mounting of C. elegans Embryos for Microscopic Analysis

Embryos dissected from adult *C. elegans* (Section 2.4.13) were transferred onto a fresh agarose pad (Section 2.4.12) using a mouth pipette (Section 2.4.14) in dH_2O, excess dH_2O was removed and a coverslip was placed over the sample.

2.4.16 Microscopic Analysis of C. elegans Embryos

C. elegans embryos were mounted (Section 2.4.11) visualised on a Zeiss Axiophot using a Plan Apochromat 63X objective. Microscopic images were taken in black and white using a Zeiss MRc camera and were managed and manipulated using Zeiss Axiovision version 4.6.

Chapter 3

Investigation into the role of *pqn-85* and *mau-2* in Mitotic Chromosome Segregation.

3.1 Introduction

The *scc2* and *scc4* genes from *S. cerevisiae* encode proteins (called Scc2 and Scc4 respectively) whose function in loading the cohesin complex during mitotic chromosome segregation has long been recognised (Ciosk et al., 2000). Whilst orthologues of Scc2 (called adherins) in other organisms are readily identifiable by BLASTP searches, Scc4 orthologues have remained elusive. Adherin proteins from almost all organisms have been shown to function in sister chromatid cohesion (Ciosk et al., 2000, Cummings et al., 2002, Furuya et al., 1998, Kaur et al., 2005, Rollins et al., 2004) however *Xenopus* is the only metazoan in which the cohesin loading function of these proteins has been proven (Gillespie and Hirano, 2004, Takahashi et al., 2004). The *C. elegans* adherin (called PQN-85) is encoded by the gene *pqn-85* gene and has only been studied using genome wide RNAi although its role in chromosome segregation has never been examined. Potential orthologues of Scc4 outside organisms closely related to *S. cerevisiae* have only recently been identified using PSI-BLAST searches and include the MAU-2 protein (Tom Strachan personal communication) which is encoded by the *C. elegans mau-2* gene. Analysis of worms with mutations in *mau-2* has shown that it functions in the development of the *C. elegans* nervous system (Benard et al., 2004, Hekimi et al., 1995, Takagi et al., 1997) however from these experiments it is unclear whether *mau-2* plays a role in sister chromatid cohesion or in cohesin loading.

The movement of chromosomes throughout the first mitotic cell division can be followed using a strain of *C. elegans* which express histone H2B fused to GFP (henceforth called the *histone::GFP* strain) (Strome et al., 2001). Mito and colleagues previously used a similar strain of *C. elegans* to track the movement of chromosomes in embryos depleted of the cohesin subunits *smc-1*, *smc*-3, *scc-1* and *scc-3* by RNAi (Mito et al., 2003). In this study the authors were able to show that depletion of any of the cohesin subunits in the *histone::GFP* strain resulted in aberrant chromosome segregation with lagging chromosomes at anaphase

(Mito et al., 2003). To determine whether *pqn-85* and *mau-2* function in the first mitotic chromosome segregation of *C. elegans,* RNA interference was carried out to deplete the expression of the *scc-3*, *pqn-85* and *mau-2* genes in *histone::GFP C. elegans.*

3.2 Methods

3.2.1 Analysis of Embryonic Lethality

To obtain embryos depleted for *pqn-85*, *mau-2* and *scc-3* double stranded RNA for microinjection was produced as per Section 2.4.7. Young adult hermaphrodite *C. elegans* were microinjected (Section 2.4.11) with specific dsRNA. To analyse the effect of microinjection on embryonic lethality young adult hermaphrodites were microinjected with sterile dH_2O, *pqn-85* dsRNA, *scc-3* dsRNA or *mau-2* dsRNA. Injected worms were placed on fresh NGM plates (Section 2.4.4) and incubated at 20°C for 24 hours. After 24 hours the adult injected hermaphrodites were placed onto fresh NGM plates (Section 2.4.4) and were incubated for a further 24 hours, this was repeated until 72 hours after injection at which time the injected hermaphrodites were discarded. After removal of the adult injected hermaphrodites each plate was incubated for a further 24hrs to allow eggs to hatch. The number of eggs that had not hatched after 24hrs on each plate was counted and were considered to be dead whilst the number of larvae was counted to represent the eggs that were not dead.

3.2.2 Time-lapse Imaging of C. elegans Embryos

To analyse the effect of depleting *pqn-85*, *mau-2* and *scc-3* on chromosome segregation, *pqn-85*, *mau-2* and *scc-3* double stranded RNA for microinjection was produced as per Section 2.4.7. Young adult hermaphrodites were microinjected (Section 2.4.11) with sterile dH_2O, *pqn-85* dsRNA, *scc-3* dsRNA or *mau-2* dsRNA or a 1:1 mixture of two different dsRNA sequences. Embryos to be analysed were dissected from adult injected hermaphrodites (Section 2.4.13) 48 hours after microinjection and were mounted (Section 2.4.15) on microscope slides containing fresh agarose pads (Section 2.4.12). Differential interference contrast (DIC) and GFP images were obtained by microscopy (Section 2.4.16) at appropriate intervals. DIC and GFP images were overlaid using Zeiss Axiovision 4.6 software.

3.3 Results

3.3.1 Production of Double Stranded RNA for Microinjection

To produce gene specific double stranded RNA (dsRNA) a small fragment of the *pqn-85*, *scc-3* and *mau-2* genes were amplified by PCR from *C. elegans* genomic DNA. The PCR primers used contained a T7 promoter and T3 promoter sequence such that the PCR products would be flanked by T7 and T3 promoters. The PCR products were size fractionated by agarose gel electrophoresis and bands of the expected size (*scc-3* 742bp, *pqn-85* 693bp, *mau-2* 937bp) were observed (Figure 3.1A). The PCR products were purified from the gel and were used in separate T7 and T3 transcription reactions to create single stranded sense and antisense RNA populations. The corresponding single stranded RNA populations were mixed to create dsRNA. To confirm that the T7 and T3 reactions produced single stranded RNA and to visualise the dsRNA 1µl of each reaction was size fractionated by agarose gel electrophoresis. Bands were observed in all T7 and T3 single stranded RNA production reaction suggesting at all the reactions were successful (Figure 3.1B). The bands appeared smaller in size on the agarose gel than expected due to the secondary structure adopted by single stranded RNA. Unlike single stranded RNA, dsRNA does not form a secondary structure therefore will run as a linear molecule through an agarose gel. Single stranded RNA also binds less Ethidium Bromide than dsRNA, so is much fainter. Bands of the correct size were observed in lanes containing dsRNA (Figure 3.1B) confirming the presence of dsRNA.

3.3.2 Analysis of the Effect of Microinjection on Embryonic Mortality

To study the effect of microinjecting *C. elegans* on the survival of the eggs laid from the injected worms, 10 young adult *histone::gfp* hermaphrodites were injected with sterile dH_2O and were recovered on fresh NGM plates overnight (one worm per plate). The injected worms were transferred to fresh NGM plates every day for three days and the eggs laid on each plate were allowed to develop for a further 24 hrs. Eggs that had not hatched after the 24 hr period were considered to be dead. The number of eggs laid on each day that had not hatched and the number of larvae on each plate was counted, the number of dead eggs was calculated as a percentage of the overall number of eggs laid. At the time points 0-24hrs, 24-48 hrs and 48-72 hrs after injection of dH_2O no dead eggs were observed (Table 3.1) suggesting that the microinjection procedure has no effect on the mortality of developing eggs.

A

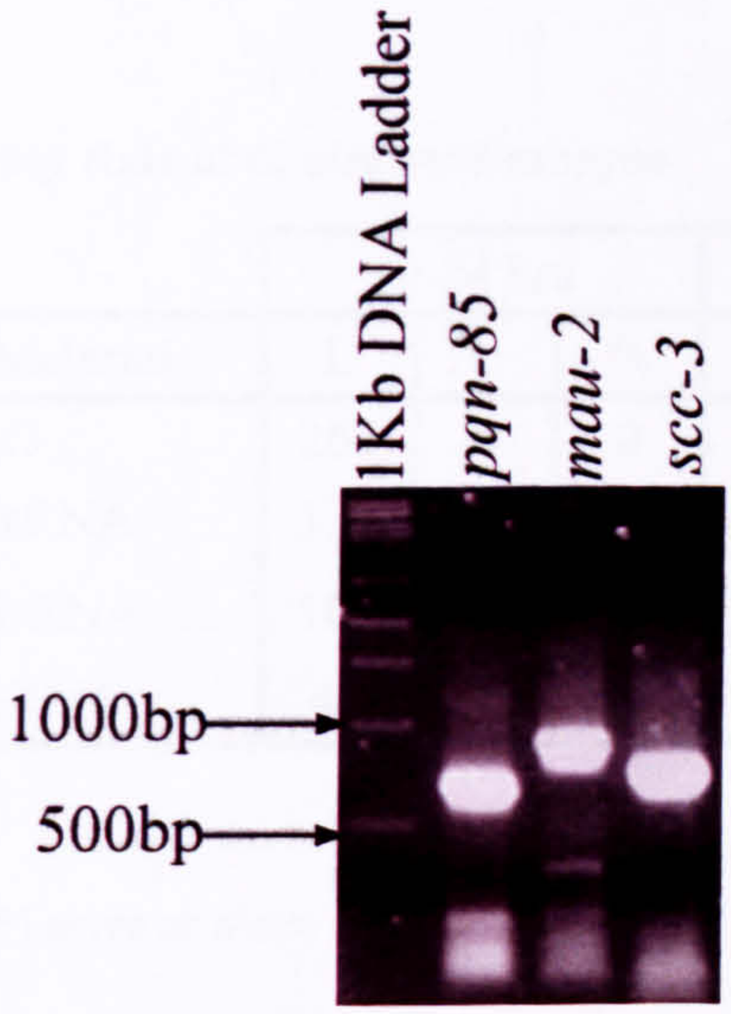

B

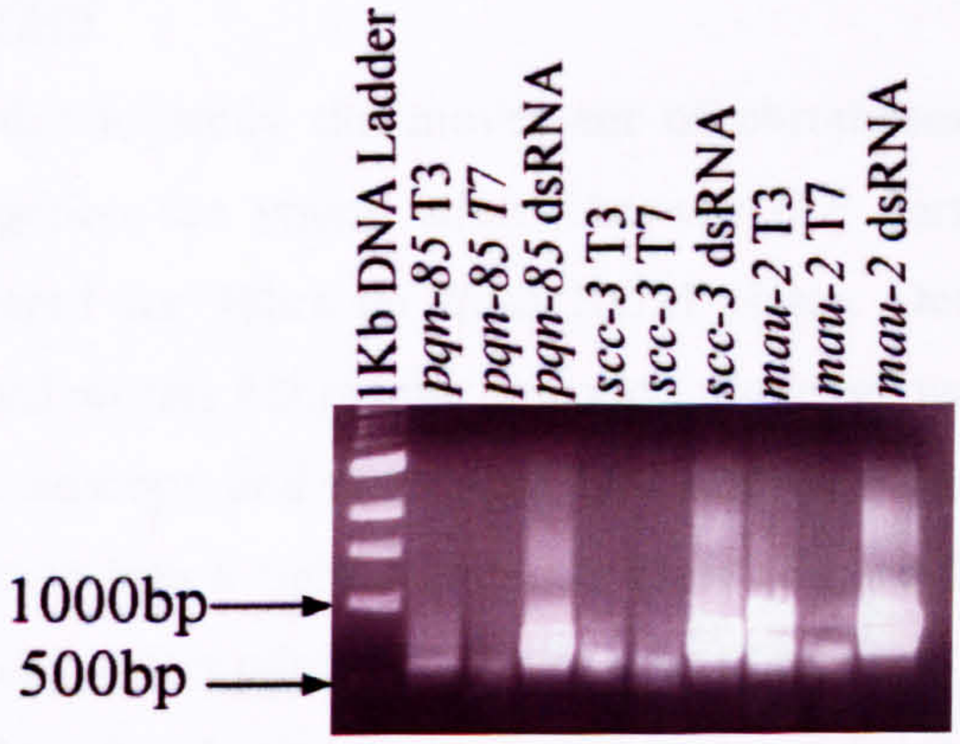

Figure 3.1 Double Stranded RNA Production for RNAi

A) Small fragments of *scc-3* (742bp), *pqn-85* (693bp) and *mau-2* (937bp) genomic sequence were amplified by PCR. The PCR products were size fractionated by agarose gel electrophoresis and bands of the expected size were observed. **B)** The *mau-2*, *scc-3* and *pqn-85* PCR products from **A)** were excised from the gel and used as template in separate T7 and T3 reactions to produce *mau-2, pqn-85* and *scc-3* sense and antisense single stranded RNA populations. The sense single stranded RNA was mixed with the corresponding antisense RNA to produce double stranded RNA. The single stranded reactions were size fractionated by agarose gel electrophoresis alongside the corresponding double stranded RNA and 1Kb DNA ladder to confirm the size of the bands on the gel.

Table 3.1 Mortality Rate of *C. elegans* Embryos

	0-24 hrs			24-48hrs			48-72hrs		
Injection Material	L	U	%	L	U	%	L	U	%
dH_2O	265	0	0	352	0	0	95	0	0
mau-2 dsRNA	138	0	0	368	0	0	288	0	0
pqn-85 dsRNA	100	0	0	200	111	36	0	173	100
scc-3 dsRNA	49	162	77	14	327	96	0	174	100

L Number of Larvae on plates

U Number of Unhatched eggs

% Percentage of eggs laid that did not hatch

3.3.3 Visualisation of the First Mitotic Chromosome Segregation in C. elegans Embryos

In order to study the movement of chromosomes through the first mitotic chromosome segregation ten young adult *histone::GFP* hermaphrodites were injected with dH_2O and recovered for 48hrs on fresh NGM plates. Developing embryos were dissected from the injected worms 48hrs after injection, the eggs were mounted on a fresh agarose pad, viewed by microscopy and time lapse DIC and GFP images were taken. The chromosomes clearly condense into a tight metaphase plate (Figure 3.2 A) followed by anaphase in which two distinct bundles of chromosomes start to separate to opposite poles of the cell (Figure 3.2 B, C and D). The chromosomes begin to decondense (Figure 3.2 E, F, G, H and I) as the cells move toward interphase and the embryo undergoes cytokinesis (Figure 3.2 E, F, G, H and I) to form two daughter cells. Cell division is non-symmetrical as a result of the slight posterior placement of the spindle (Albertson, 1984), always producing a larger anterior cell and a smaller posterior cell (Sulston et al., 1983). This data is consistent with that observed in previous studies (Mito et al., 2003, Strome et al., 2001) and suggests that this assay is appropriate for the purpose of tracking chromosome movement.

3.3.4 Depletion of scc-3 by RNA Interference Results in Abnormal Anaphase During Mitotic Chromosome Segregation

Previous RNAi studies against *scc-3* had shown an embryonic lethality phenotype with 100% penetrance (Mito et al., 2003). To confirm the effectiveness of RNAi against *scc-3*, 10 young

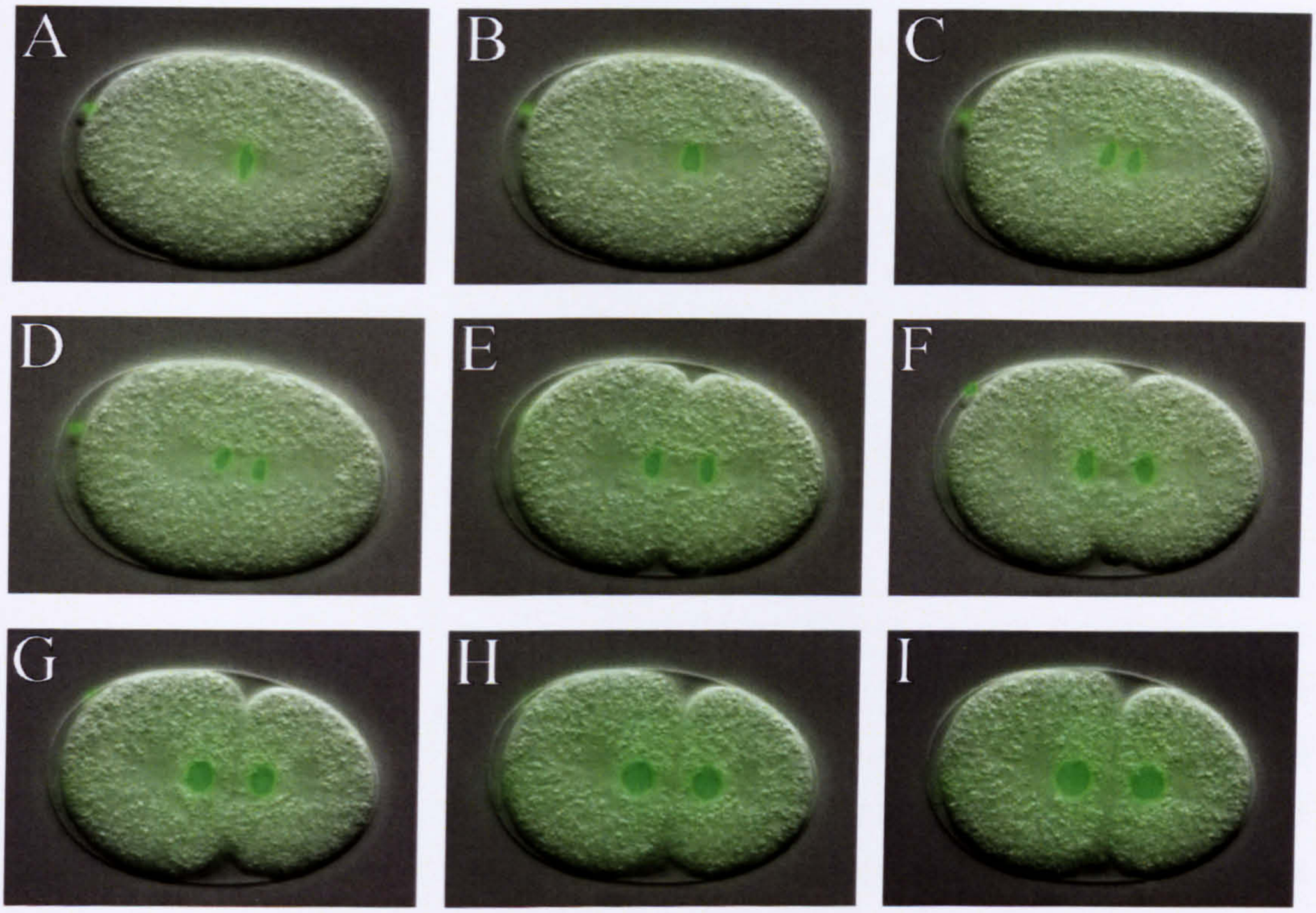

Figure 3.2 Movement of Chromosomes Throughout the First Mitotic Cell Division of *C. elegans* Embryos

Time lapse DIC and GFP images of an embryo dissected from an adult hermaphrodite *histone::GFP C. elegans* 48hrs after injection of dH_2O showing the movement of chromosome during the first mitotic cell division (anterior left and posterior right). A clearly defined metaphase plate **(A)** is visible before chromosomes segregate to opposite poles into two tight bundles during anaphase **(B-E)**. Chromosomes decondense as the embryo undergoes cytokinesis **(E-I)** dividing asymmetrically into daughter cells that differ in size with a larger anterior cell and a smaller posterior cell **(I)**.

adult *histone::GFP* hermaphrodites were injected with *scc-3* dsRNA and were recovered overnight on fresh NGM plates. The injected worms were transferred to fresh plates every 24 hours and the number of progeny hatched from each replica plate was counted and compared to the overall number of embryos laid. Of the embryos laid in between 0-24hrs after injection 77% did not hatch into larvae and were considered dead. This figure rose to 96% for those embryos laid between 24-48hrs after injection and to 100% for embryos laid between 48-72hrs (Table 3.1). This result is in concordance with previous RNAi studies with *scc-3* dsRNA that showed embryonic lethality with 100% penetrance (Mito et al., 2003, Wang et al., 2003) and suggests that *scc-3* was successfully depleted.

To view the effect of depleting *scc-3* on chromosome segregation, embryos were dissected from adult hermaphrodites 48 hrs after injection of *scc-3* dsRNA. Time lapse DIC and GFP images were taken to observe chromosome movement during the first mitotic chromosome segregation. No obvious effect on metaphase was apparent and a tight bundle of chromosomes aligning in the middle of the cell was observed (Figure 3.3A) as was the case for wild type. Defects in chromosome segregation became apparent at anaphase however when a chromosomal bridge between the two dividing bundles of chromosomes was observed (Figure 3.3C, D and E). This phenomenon was observed in 10 of 10 embryos studied. Eventually the chromosome bridge is broken as the cell divides into two (Figure 3.3F). The chromosomes decondense and the embryo undergoes cytokinesis dividing asymmetrically into two differently sized daughter cells (Figure 3.3F, G, H and I) as observed in the wild type.

Embryos that had developed further than the two cell stage were examined for chromosome segregation defects. Embryos were consistently observed with micronuculei (Figure 3.3J and K white arrows) and unresolved chromosomal bridges (Figure 3.3J and K white arrow head) between individual nuclei indicative of chromosome segregation defects. These phenotypes and the ones described in the previous paragraph are consistent with results obtained from previous RNAi experiments directed against cohesin subunits (Mito et al., 2003, Pasierbek et al., 2003). This further suggests that the RNAi against *scc-3* was successful and that visualising chromosome movement in *histone::GFP* embryos is an effective test of chromosome segregation defects in response to defects in the cohesin pathway.

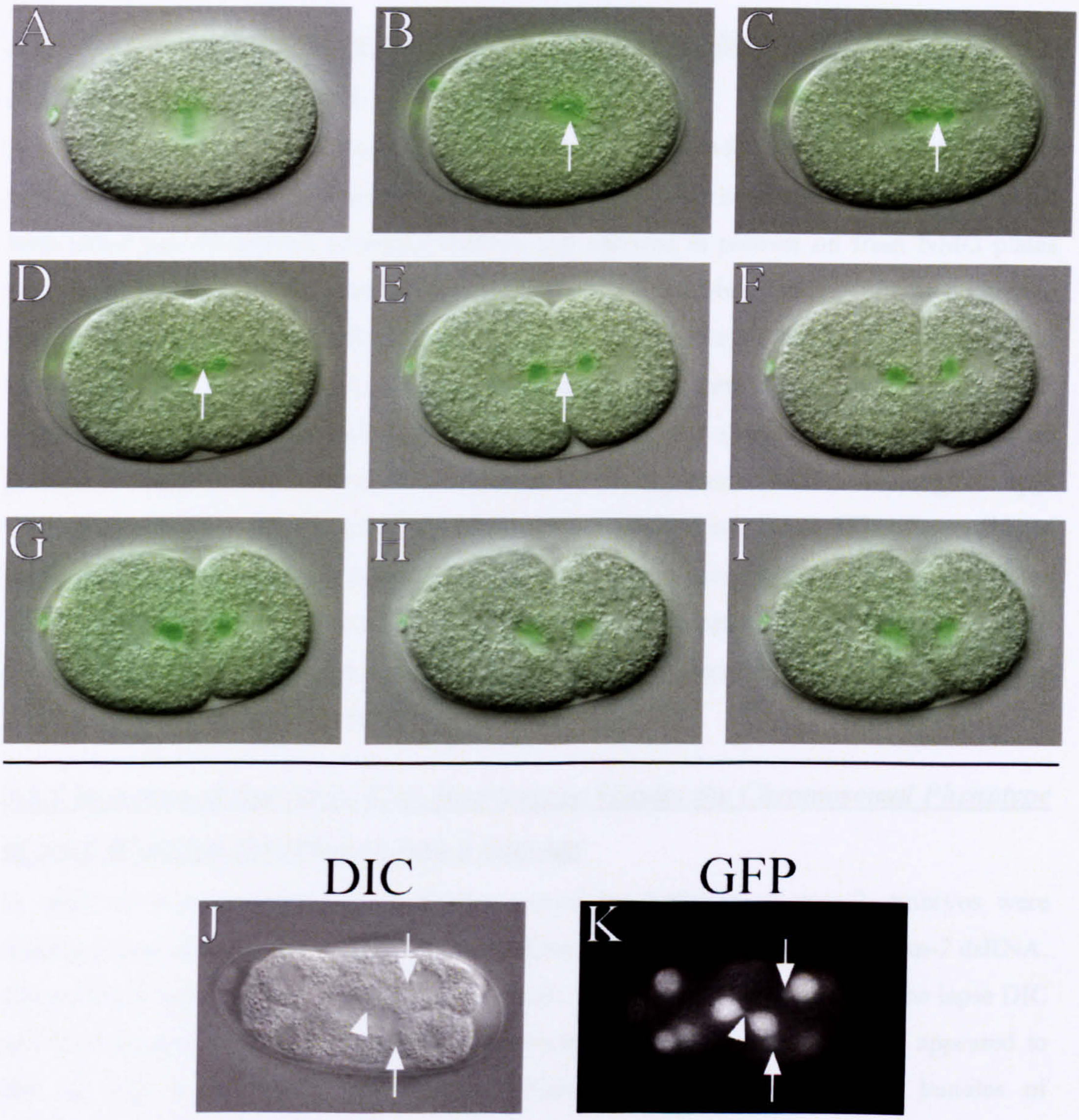

Figure 3.3 RNAi Against *scc-3* Results in Lagging Anaphase Chromosomes

Time lapse DIC and GFP images of an embryo dissected from an adult *histone::GFP C. elegans* hermaphrodite 48hrs after injection of *scc-3* dsRNA showing the movement of chromosome during the first mitotic cell division (anterior left and posterior right). A clearly defined metaphase plate is visible **(A)** however a chromosomal bridge becomes apparent between segregating chromosomes as anaphase progresses **(B-E white arrows)** which disappears as the cell divides into two **(F)**. Chromosomes decondense as the embryo undergoes cytokinesis **(F-I)** and the cell undergoes asymmetric cell division resulting in daughter calls that differ in size with a larger anterior cell and a smaller posterior cell **(I)**. **(J and K)** Embryos that had undergone further development and had been laid as eggs were picked from the NMG plates 48 hrs after injection of the dsRNA and visualised by DIC and GFP imaging. As the embryos developed further clear evidence of aberrant chromosome segregation was apparent with cells containing micronuclei **(white arrows)** and unresolved chromosomal bridges **(white arrow heads)** were observed.

3.3.5 Depletion of pqn-85 by RNA Interference Causes Embryonic Lethality Whilst Depletion of mau-2 does not

An initial aim of this project was to determine whether the *pqn-85* or *mau-2* genes function in chromosome segregation. Therefore ten adult *histone::GFP* hermaphrodites were injected with either *pqn-85* dsRNA or *mau-2* dsRNA and allowed to recover on fresh NMG plates overnight. The worms were transferred to fresh plates every 24 hrs, the eggs laid on each plate were allowed to develop for a further 24 hrs and the number of eggs that had not hatched after the 24 hr period were counted. No unhatched (dead) eggs were found when *histone::GFP* worms were injected with *mau-2* dsRNA (see Table 3.1) it should also be noted that no postembryonic phenotypes could be observed in worms depleted of *mau-2*. Although all eggs laid between 0-24hrs after injection of *pqn-85* dsRNA hatched into larvae 36% of eggs did not hatch between 24 and 48 hrs after injection and this figure rose to 100% between 48-72 hrs after injection (Table 3.1). The results obtained suggest that depleting *pqn-85* by RNAi had a similar but less potent effect on embryo mortality than RNAi against *scc-3* but depleting *mau-2* appears to have no effect on embryo mortality.

3.3.6 Depletion of pqn-85 by RNA Interference Mimics the Chromosomal Phenotype of scc-3 RNAi but Depletion of mau-2 does not

In order to observe chromosomal defects caused by depletion of *mau-2,* embryos were dissected from adult *histone::GFP* hermaphrodites 48 hours after injection of *mau-2* dsRNA. The embryos were mounted on fresh agarose pads, viewed by microscopy and time lapse DIC and GFP images were taken to follow chromosome movement. Chromosomes appeared to line up into a defined metaphase plate (Figure 3.4A) and two distinct bundles of chromosomes segregated at anaphase with no chromosomal bridge (Figure 3.4B, C and D), unlike embryos depleted of *scc-3*. The chromosomes begin to decondense and cytokinesis occurs as the cell divides asymmetrically to produce daughter cells of differing sizes (Figure 3.4F-I). This lack of observable chromosomal phenotypes is in concordance with the results observed in Section 3.3.5 in which depletion of *mau-2* does not cause embryonic lethality.

To determine if chromosome segregation defects are present in *pqn-85* depleted embryos, hermaphrodites were dissected 48 hrs after injection of *pqn-85* dsRNA to remove the embryos. The embryos were mounted on fresh agarose pads and the first mitotic chromosome segregation was viewed by time lapse DIC and GFP microscopy. The chromosomes condense into a tight metaphase plate in the middle of the cell (Figure 3.5A) as in wild type. In a similar fashion to that observed in the *scc-3* depleted embryos a bridge between the dividing bundles

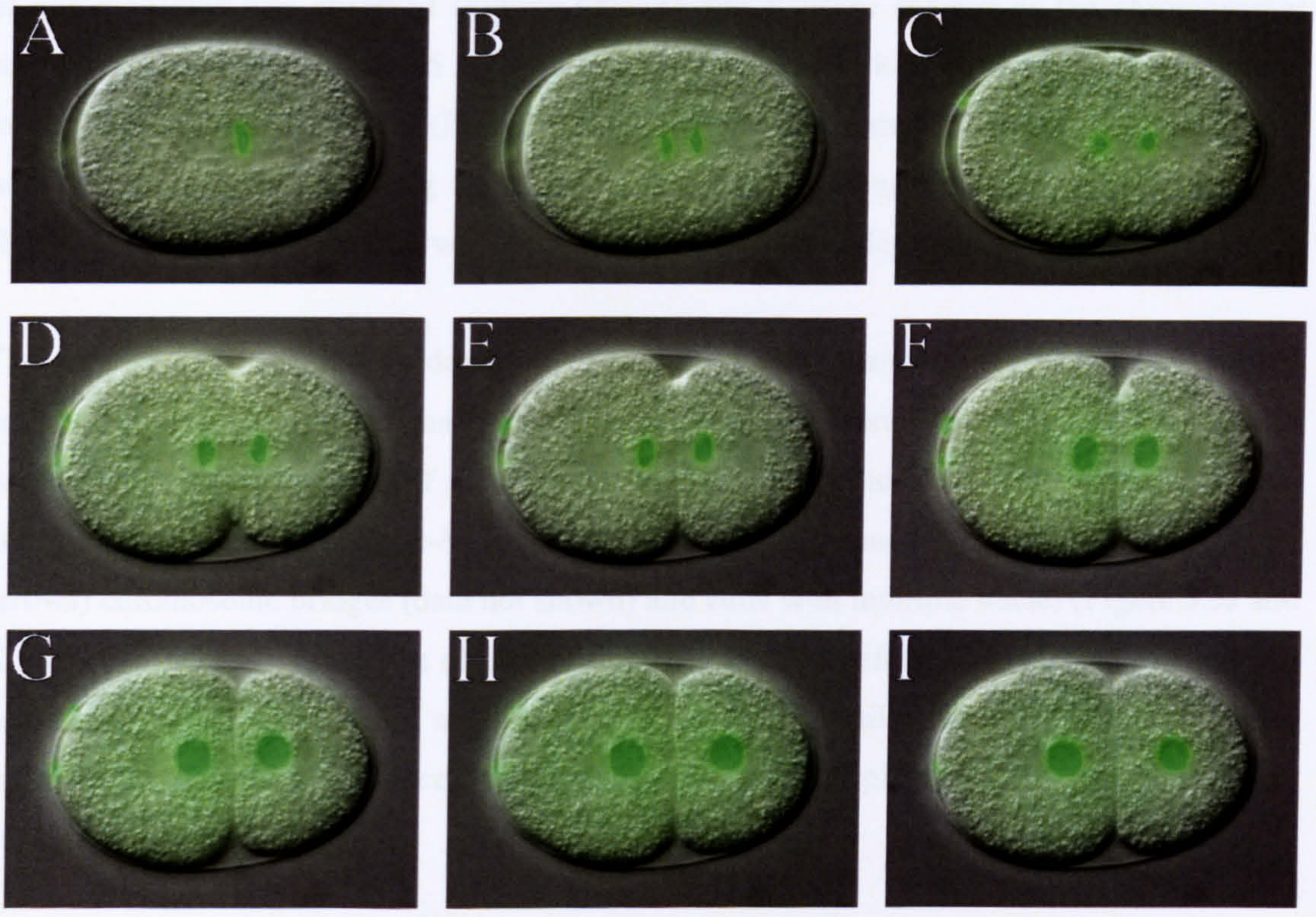

Figure 3.4 RNAi Against *mau-2* Causes no Defects in Chromosome Segregation

Embryos were dissected from a *histone::GFP* adult hermaphrodite 48hrs after injection of *mau-2* dsRNA and chromosome movement was visualised by time lapse DIC and GFP imaging. Chromosomes align on a metaphase plate **(A)** and two distinct bundles of chromosomes segregate as anaphase progresses without the presence of chromosomal bridges **(B-E)**. The chromosomes decondense as cytokinesis occurs **(F-I)** and the cell undergoes asymmetric cell division producing daughter cells of differing sizes with a larger anterior cell and a smaller posterior cell **(I)**.

of chromosomes was observed (Figure 3.5C, D and E white arrows) as the chromosomes begin to separate in anaphase (5 out of 10 embryos studied). This chromosome bridge breaks as the cell divides into two (Figure 3.5 F), the chromosomes decondense and the cell undergoes cytokinesis dividing asymmetrically producing daughter cells of differing sizes (Figure 3.5 G, H and I) as observed in the wild type and *scc-3* depleted embryos.

The cellular defect caused by depletion of *pqn-85* is not severe enough to preclude further embryonic development and many multicellular embryos were observed. As was the case when embryos were depleted of *scc-3* (Figure 3.3J and K) (Mito et al., 2003, Pasierbek et al., 2003) embryos depleted of *pqn-85* were observed with micronuclei (Figure 3.5J and K white arrows) chromosome bridges (data not shown) and cells with multiple nuclei (Figure 3.5J and K white arrow head), indicative of chromosome segregation defects. The phenotypes detailed here when *pqn-85* is depleted are very similar to those detailed from section 3.3.4 where embryos were depleted of *scc-3* suggesting that *pqn-85* plays a role in chromosome segregation.

3.3.7 Depletion of pqn-85 and scc-3 or mau-2 and scc-3 by RNA Interference Causes Very Severe Chromosome Segregation Defects

The chromosomal defects observed when *scc-3* is depleted by RNAi are not as severe as would be expected given its key role in the cell cycle but are consistent with results from previous studies (Mito et al., 2003, Pasierbek et al., 2003). One such paper showed that conducting RNAi against two members of the cohesin complex at the same time results in much more severe chromosome segregation defects than when RNAi is conducted against either singularly (Chan et al., 2002). If *pqn-85* and *mau-2* are involved in loading the cohesin complex then it is feasible that depleting the expression level of *scc-3* with either *pqn-85* or *mau-2* by RNAi would result in a much more severe chromosome segregation phenotype.

To asses whether this was the case young adult *histone::GFP* hermaphrodites were injected with a mixture of either *scc-3* and *pqn-85* dsRNA or *scc-3* and *mau-2* dsRNA. Injected hermaphrodites were recovered on fresh NGM plates for 48hrs after which embryos were dissected from the worms and mounted on fresh agarose pads. The dynamics of chromosome segregation during the first mitotic chromosome segregation were assessed as before using time lapse DIC and GFP imaging. In both experiments the result is a catastrophic failure in chromosome segregation with similar phentoypes. Whilst metaphase does occur, the chromosomes are more diffuse (Figure 3.6A and Figure 3.7A) when compared to wild type

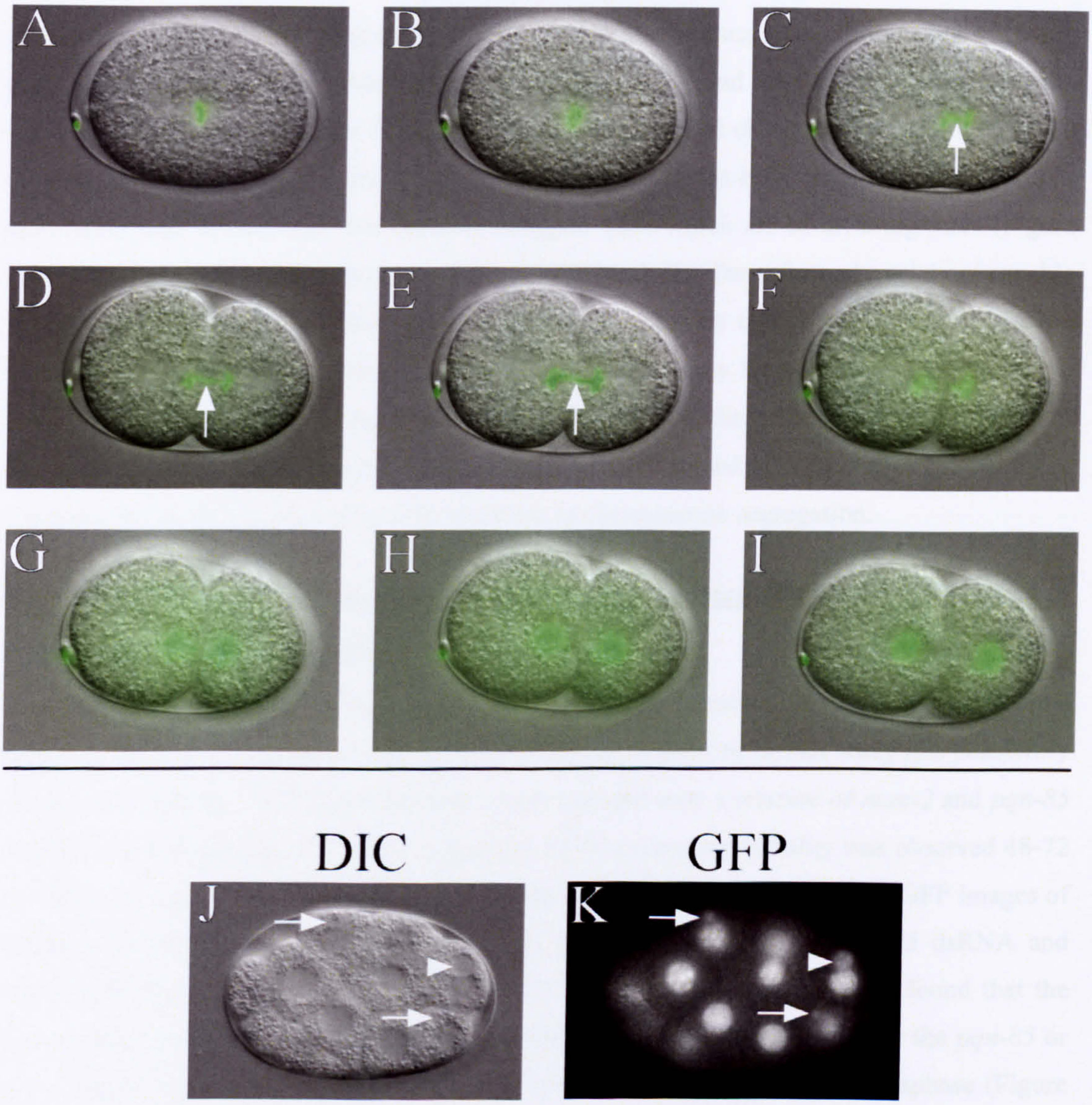

Figure 3.5 RNAi Against *pqn-85* Causes Lagging Anaphase Chromosomes Similar to RNAi Against scc-*3*

Embryos were dissected from a *histone::GFP* adult hermaphrodite 48hrs after injection of *pqn-85* dsRNA and chromosome movement was visualised by time lapse DIC and GFP imaging. Chromosomes align on a metaphase plate **(A)** but as was observed in RNAi against *scc-3* a chromosomal bridge is apparent between segregating chromosomes as anaphase progresses **(C-E white arrows)** which is broken as the cell divided into two **(F)**. The chromosomes decondense as cytokinesis occurs **(F-I)** and asymmetric cell division produces daughter cells of differing sizes a large anterior cell and a smaller posterior cell **(I)**. **(J and K)** Embryos that had undergone further development and had been laid as eggs were picked from the NMG plates 48 hrs after injection of the dsRNA and visualised by DIC and GFP imaging. As the embryos developed further clear evidence of aberrant chromosome segregation was apparent with cells containing micro nuclei **(white arrows)** and multiple nuclei **(white arrow heads)** were observed.

metaphase chromosomes (Figure 3.2A). As mitosis continues the chromosomes do not segregate but remain in the centre of the cell (Figure 3.6B-I and Figure 3.7B-I). Defining the stage of the cell cycle becomes difficult but the non-segregated chromosomes decondense and nuclei can form (Figure 3.6J and K and Figure 3.7J and K). In both cases the cell undergoes cytokinesis and divides into two separate daughter cells which are of differing sizes (Figure 3.6I and Figure 3.7I) as observed in wild type (Figure 3.2I). The reformed nuclei are capable of undergoing further replication and embryos with multiple nuclei were commonly seen. However, due to the lack of chromosome segregation the newly formed nuclei are often in the same cell (Figure 3.6 J and K and Figure 3.7J and K). The finding that depletion of *pqn-85* or *mau-2* with *scc-3* exacerbates that chromosomal defect observed when *scc-3* is depleted alone suggests that *mau-2* as well as *pqn-85* functions in chromosome segregation.

3.3.8 Depletion of mau-2 and pqn-85 by RNA Interference Mimics the Phenotype of Depleting scc-3 or pqn-85 Alone

The finding that both *mau-2* and *pqn-85* function in chromosome segregation suggests that they may form a *C. elegans* cohesin loading complex. In order to further study this possibility young adult *histone::GFP* hermaphrodites were injected with a mixture of *mau-2* and *pqn-85* dsRNA. As with the *pqn-85* dsRNA injections 100% embryonic lethality was observed 48-72 hrs after injection of *mau-2* dsRNA with *pqn-85* dsRNA. Time lapse DIC and GFP images of embryos dissected from adult hermaphrodites 48hrs after injection of *pqn-85* dsRNA and *mau-2* dsRNA were analysed for defects in chromosome segregation. It was found that the chromosome segregation phenotype was indistinguishable to that observed for the *pqn-85* or *scc-3* single injections. A tight bundle of chromosomes was observed in metaphase (Figure 3.8 A) but a defect in anaphase with chromosomal bridging was evident (Figure 3.8 B-F white arrows). As with the *scc-3* or *pqn-85* single injection the chromosomal bridge was broken as the cell divides into two (Figure 3.8 G) and the chromosomes decondense as the cells undergo cytokinesis to divide asymmetrically into two daughter cells as observed in wild type and the *pqn-85* and *scc-3* single injections.

As was the case in the *pqn-85* and *scc-3* single injections this cellular defect does not preclude further development and many multicellular embryos were observed. These embryos frequently had a nuclear defect such as unresolved chromosomal bridges (Figure 3.8 J and K white arrow head) and micro nuclei (Figure 3.8 J and K white arrow) indicative of chromosome segregation defects and similar to those observed in embryos depleted of either *scc-3* or *pqn-85*.

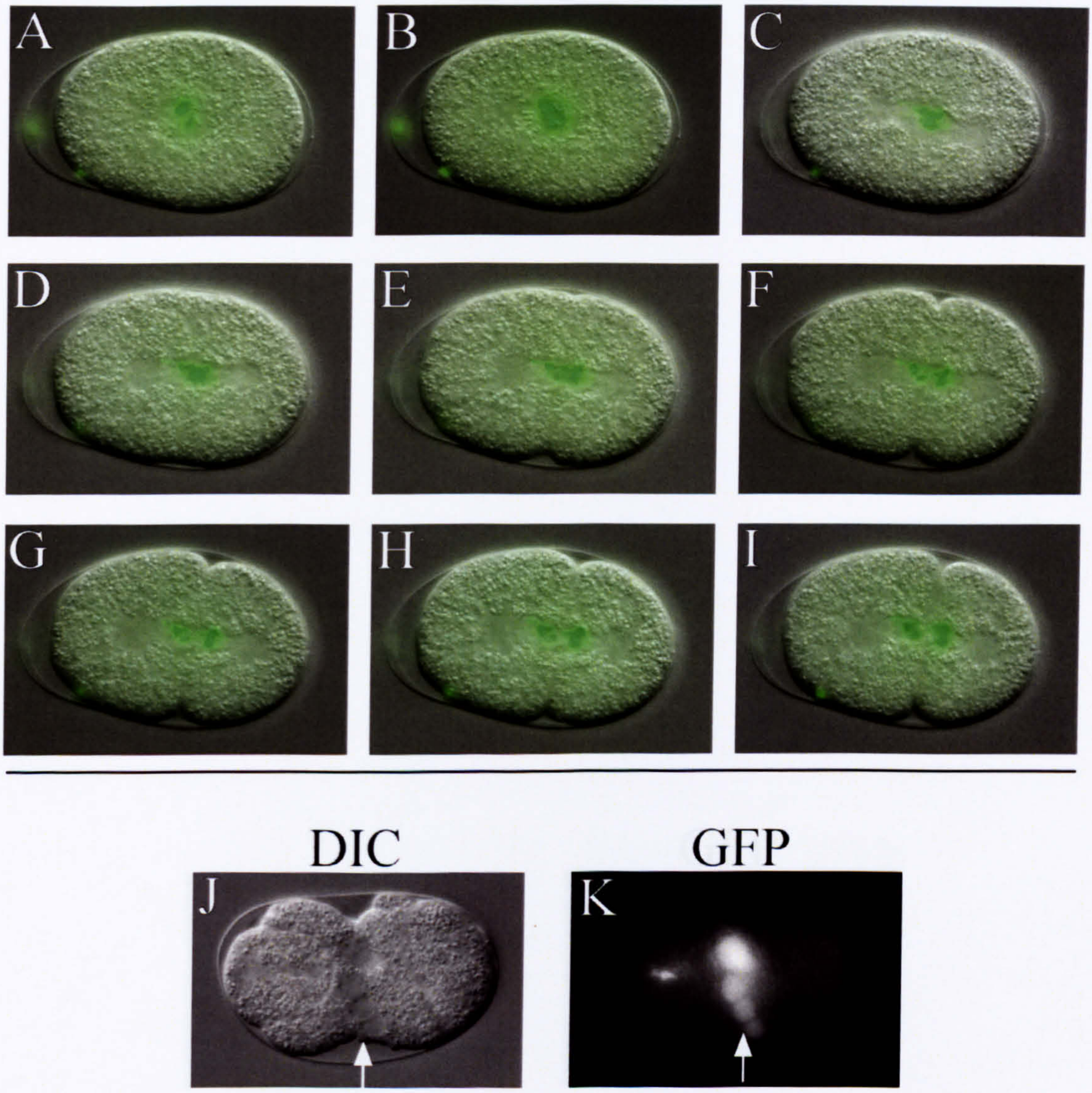

Figure 3.6 RNA Interference Against both *pqn-85* and *scc-3* Causes Severe Chromosome Segregation Defects

Time lapse DIC and GFP imaging of embryos dissected from an adult *histone::GFP C. elegans* hermaphrodite injected with both *scc-3* and *pqn-85* dsRNA. At metaphase the chromosomes appear diffuse **(A)** when compared to wild type and as cell division progresses very little chromosome movement occurs **(B-H)**. The cell divides asymmetrically producing two unequally sized daughter cells **(I)** as in wild type, however unlike wild type the undivided chromosomes are split into two separates bundles one in either cell. **(J and K)** Embryos that had undergone further development and had been laid as eggs were picked from the NMG plates 48 hrs after injection of the dsRNA and visualised by DIC and GFP imaging. There was clear evidence of further nuclear division; however these nuclei were often found grouped together in one cell **(white arrows)**.

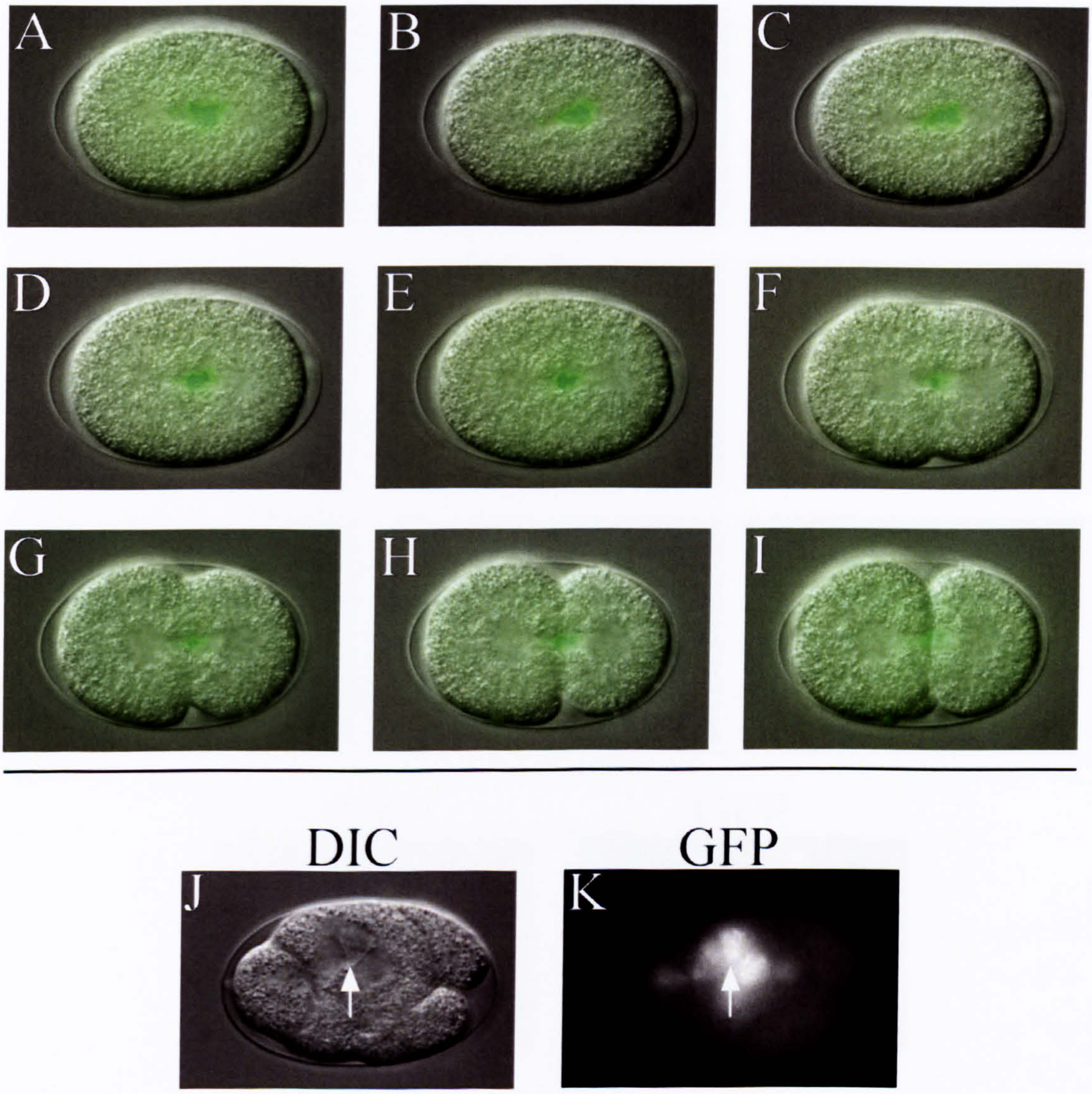

Figure 3.7 RNA Interference Against both *mau-2* and *scc-3* Causes Severe Chromosome Segregation Defects

Time lapse DIC and GFP imaging of embryos dissected from *histone::GFP C. elegans* hermaphrodites injected with both *scc-3* and *mau-2* dsRNA. At metaphase the chromosomes appear diffuse **(A)** when compared to wild type and as cell division progresses no or very limited chromosome movement occurs **(B-I)**. The cell divides asymmetrically producing two unequally sized daughter cells **(I)** as in wild type, however unlike wild type the undivided chromosomes appear to sit between both cells **(I)**. **(J and K)** Embryos that had undergone further development and had been laid as eggs were picked from the NMG plates 48 hrs after injection of the dsRNA and visualised by DIC and GFP imaging. There was clear evidence of further nuclear division; however these nuclei were often found grouped together in one cell **(white arrows)**.

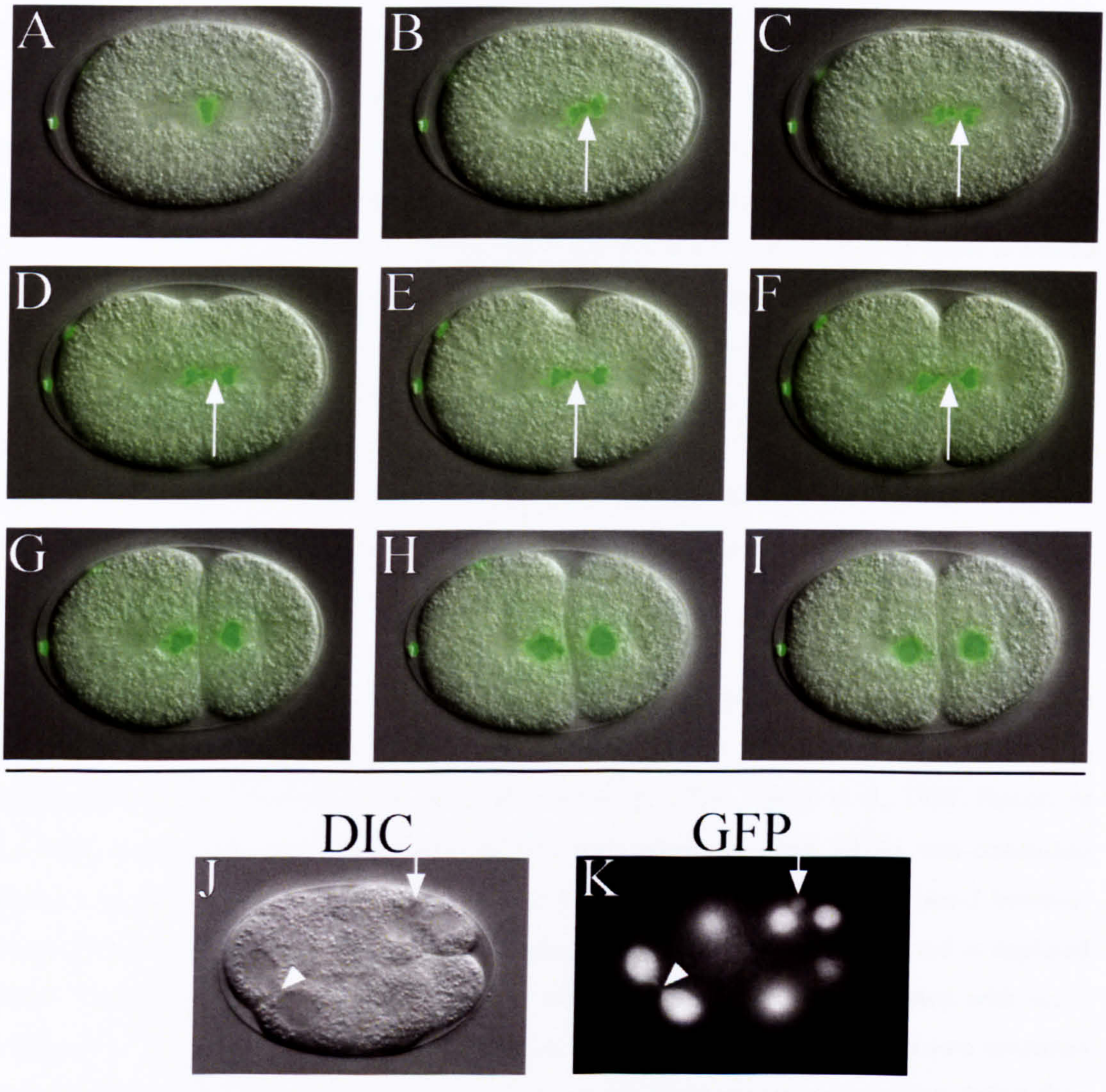

Figure 3.8 RNA Interference Against both *pqn-85* and *mau-2* Causes Lagging Anaphase Chromosomes

Embryos were dissected from a *histone::GFP* adult hermaphrodites 48hrs after injection of both *pqn-85* and *mau-2* dsRNA and chromosome movement was visualised by time lapse DIC and GFP imaging. Chromosomes align tightly on a metaphase plate **(A)** but a chromosomal bridge is apparent between segregating chromosomes as anaphase progresses **(B-F white arrows)**. The chromosomal bridge breaks as the cell divides into two **(G)** and chromosomes decondense as cytokinesis occurs. Asymmetric cell division producing daughter cells of differing sizes (I) occurs as in wild type. **(J and K**) Embryos that had undergone further development and had been laid as eggs were picked from the NMG plates 48 hrs after injection of the dsRNA and visualised by DIC and GFP imaging. As the embryos developed further clear evidence of aberrant chromosome segregation was apparent with cells containing micronuclei **(white arrows)** and unresolved chromosomal bridges **(white arrow heads)** were observed.

3.4 Discussion

The chromosomal phenotype observed when RNAi is carried out against *scc-3* or *pqn-85* is very similar and suggests that they have similar functions. In this study and others anaphase chromosome bridges are observed in embryos depleted of the cohesin complex member *scc-3* (Mito et al., 2003, Pasierbek et al., 2003) although this study goes further to show a similar defect is present in embryos depleted of *pqn-85*. Embryos depleted of *scc-3* are capable of further development but defects such as micronuclei and unresolved chromosomal bridges between adjoining cells are commonly observed (Figure 3.3). These phenotypes have been observed in previous RNAi studies into *scc-3* (Mito et al., 2003, Pasierbek et al., 2003) however this study also shows that such defects are present in embryos depleted of *pqn-85* (Figure 3.5). The similarity of the phenotypes suggests that they function in the same pathway in mitotic chromosome segregation.

No phenotypes were observed when *mau-2* was depleted alone; however there is evidence that *mau-2* functions in chromosome segregation. Neither the post embryonic defects commonly associated with *mau-2* mutants (Benard et al., 2004, Takagi et al., 1997, Hekimi et al., 1995) nor chromosome segregation defects were observed when RNAi was conducted against *mau-2* alone (Section 3.3.5 and Figure 3.4). Depletion of *mau-2* with *scc-3* however causes chromosome segregation defects of much greater severity than when *scc-3* is depleted alone. This phenotype is very similar to that observed when *pqn-85* is depleted with *scc-3* (Figure 3.6). Previous studies have also reported that conducting RNAi against two members of the cohesin complex results in a much more severe chromosome segregation defect than depleting either individually (Chan et al., 2003). This would suggest that *mau-2* as well as *pqn-85* functions in the same pathway as *scc-3* in chromosome segregation.

The increase in severity of the chromosomal phenotype when *scc-3* is depleted with either *mau-2* or *pqn-85* to that observed when *pqn-85*, *scc-3* or *mau-2* are depleted alone could be due to incomplete depletion of the targeted transcripts. Any residual SCC-3 protein left as a result of incomplete depletion of its transcript should be able to form cohesin complexes and even a low level of cohesin may be sufficient to complete cell division all be it with lagging chromosomes. Similarly any residual PQN-85 or MAU-2 as a result of incomplete depletion of *pqn-85* or *mau-2* mRNA transcripts could still potentially load cohesin complexes onto chromosomes although fewer cohesin complexes may be loaded. Certainly sister chromatid cohesion in metazoans can be maintained by only a fraction of the total cellular cohesin complement (Losada et al., 2000, Wazenegger et al., 2000, Warren et al., 2000). When *scc-3*

is depleted alongside either *pqn-85* or *mau-2* then a reduction in the number of functional cohesin complexes which would be expected by depletion of *scc-3* alongside a reduction in the efficiency of cohesin loading by depletion of *pqn-85* or *mau-2* could result in a catastrophic reduction in functional cohesin loaded onto chromosomes and led to the increase in phenotypes observed in these embryos.

When *mau-2* is co-depleted with *pqn-85* the chromosomal phenotype is no more severe than when either gene is depleted alone which goes against the result in which *mau-2* or *pqn-85* when depleted with *scc-3* increase the chromosomal phenotype over that observed when only one is depleted. Certainly there appears to be a difference in the relative importance of MAU-2 and PQN-85 in regulating chromosome segregation. Depletion of *pqn-85* by RNAi is embryonic lethal where as a *mau-2* null mutant is not. Further, *pqn-85* depletion causes chromosome segregation defects in embryos whereas *mau-2* depletion does not. A possible explanation for this could be that if *mau-2* and *pqn-85* do form a complex that functions in cohesin loading, then perhaps MAU-2 cannot function without PQN-85. Therefore when *mau-2* is depleted alone PQN-85 may be able to carry out its role in regulating chromosome segregation with similar efficiency to wild type. However, when *pqn-85* is depleted alone MAU-2 may no longer be able to carry out its role in regulating chromosome segregation therefore when you deplete *mau-2* as well the chromosome segregation phenotype would be no more severe as when *pqn-85* was depleted alone.

The lack of phenotypes observed when RNAi is carried out against *mau-2* may be because of the protection of *mau-2* expression within the nervous system. It has been previously established that genes expressed with in the *C. elegans* nervous system are protected for the effects of RNAi (Timmons et al., 2001). Certainly *mau-2* expression exclusively within the nervous system alone is sufficient to rescue all phenotypes observed in *mau-2* mutant strains (Benard et al., 2004).

Further experiments are required to confirm the role of *pqn-85* and *mau-2* in chromosome segregation. To confirm the authenticity of these results *scc-3* should be depleted by RNAi within a *mau-2* null background which would be predicted to have a very severe effect on chromosome segregation. To determine the affect of depleting *pqn-85* and *mau-2* on cohesin the localisation of various cohesin subunits should be monitored using antibodies against cohesin subunits by immunofluorescence. When the embryo is depleted of *scc-3* there should be a reduction in the level of the SCC-3 protein whilst the remaining cohesin subunits would

presumably not be able to form (or form very few) a stable complex. The majority of cohesin subunits should therefore not stably bind to the DNA and would be observed as extrachromosomal proteins. Similarly embryos depletion of *pqn-85* and *mau-2* would display cohesin complexes that were mostly unbound to chromosomes.

Cohesin and adherin mutations in other organisms often result in premature sister chromatid separation during mitosis (Section 1.1.6 and 1.17). RNAi experiments in this study and from others (Mito et al., 2003, Pasierbek et al., 2003) have shown that when cohesin genes are depleted in *C. elegans* the result is often chromosome bridges suggesting that the chromosome have not disjoined properly. This defect in chromosome segregation could be due to the holocentric nature of *C. elegans* chromosomes. The centromeric region of *C. elegans* chromosomes is not defined but instead is spread along the length of the chromosome which results in a diffuse kinetochore and binding of microtubules at different points along the chromosome (Maddox et al., 2004). As well as keeping sister chromatids together prior to anaphase in mitosis, cohesin is also responsible for bi-orientation of sister chromatids on the metaphase plate (Sonoda et al., 2001, Tanaka et al., 2000b) ensuring that both sister chromatids aligned at metaphase do not bind microtubules emanating from the same pole. This leads to an elegant theory proposed by Pasierbek et al (2001) as to the reason behind these chromosomal bridges. A defect in cohesion may result in a failure to bi-orient *C. elegans* chromosomes. The holocentric nature of these chromosomes means that the microtubules emanating from different poles could bind to different sites on the same chromatid. During anaphase the microtubules would attempt to pull the same chromatid to opposite poles and the resistance of the chromatid to this may result in the chromosome bridges.

The evidence presented in this chapter does not provide definitive evidence of the role of *pqn-85* and *mau-2* in cohesin loading during cell division however it does demonstrate that they function in mitotic chromosome segregation. Further experimentation in the form of cohesin loading assays is required to confirm this.

Chapter 4

Investigating the Interaction between PQN-85 and MAU-2

4.1 Introduction

In Chapter 3 of this thesis it was shown that *C. elegans pqn-85* and *mau-2* function in chromosome segregation. Whilst bioinformatic analyses has demonstrated that the PQN-85 protein belongs to the adherin protein family of which *S. cerevisiae* Scc2 is part (Section 1.2.3), MAU-2 is suspected to be only distantly related to *S. cerevisiae* Scc4 (Section 1.2.6 and Tom Strachan personal communication). The *S. cerevisiae* Scc2 and Scc4 proteins interact to form a complex that loads cohesin onto chromosomes (Ciosk et al., 2000). If *pqn-85* and *mau-2* represent true orthologues of *scc2* and *scc4* then it would be expected that the protein products of *pqn-85* and *mau-2* would interact.

Despite the apparent lack of homology between Scc4 and its proposed orthologues, the MAU-2 protein is well conserved amongst metazoans [(Benard et al., 2004) and Section 1.1.9]. The *Drosophila* orthologue of MAU-2 (encoded by the gene *CG4203*) has been shown to bind the *Drosophila* adherin Nipped-B by yeast two-hybrid analysis (Giot et al., 2003). In order to determine if PQN-85 and MAU-2 can interact and so to further analyse whether the *pqn-85* and *mau-2* genes represent orthologues of the *scc2* and *scc4* genes respectively, analysis of the interaction between the PQN-85 and MAU-2 protein was undertaken by directed yeast two hybrid assays.

The directed yeast two-hybrid assay seeks to confirm a possible interaction between two proteins. The yeast two hybrid assay utilises the ability of the regulatory protein GAL4 to control the expression of genes regulated by upstream GAL4 responsive elements in *S. cerevisiae* (Giniger et al., 1985). The GAL4 protein is comprised of two separate domains; the GAL4 binding domain which binds GAL4 responsive elements in the DNA sequence (Keegan et al., 1986) and the GAL4 activation domain which initiates transcription of genes regulated by the GAL4 responsive elements (Brent and Ptashne, 1985). In the yeast two hybrid assay the GAL4 activation domain and the GAL4 binding domain are supplied

separately and exogenously from two specific yeast two hybrid vectors. When these yeast two hybrid vectors are expressed in *S. cerevisiae* the GAL4 binding domain can bind GAL4 responsive elements in the DNA sequence. The GAL4 activation domain however cannot interact with the GAL4 binding domain and cannot as a result initiate transcription of genes regulated by the GAL4 responsive elements (Figure 4.1A). To directly test the interaction between two proteins, cDNAs encoding the proteins to be analysed are cloned into the specific yeast two hybrid vectors. One cDNA is cloned into a yeast two hybrid vector containing the GAL4 binding domain sequence and the other cDNA is cloned into a yeast two hybrid vector containing the GAL4 activation domain sequence. The cloning is designed such that when the vectors containing the cDNA inserts are expressed in *S. cerevisiae,* one protein will be produced fused to the GAL4 binding domain and the other protein will be produced fused to the GAL4 activation domain. The GAL-4 activation domain and the GAL4 binding domain will only be brought into close proximity on the GAL4 responsive elements if the proteins encoded by the cDNA insert interact. Bringing the GAL4 activation and binding domain together result in a functional GAL4 transcription factor as detected by the expression of specific reporter genes (Figure 4.1B).

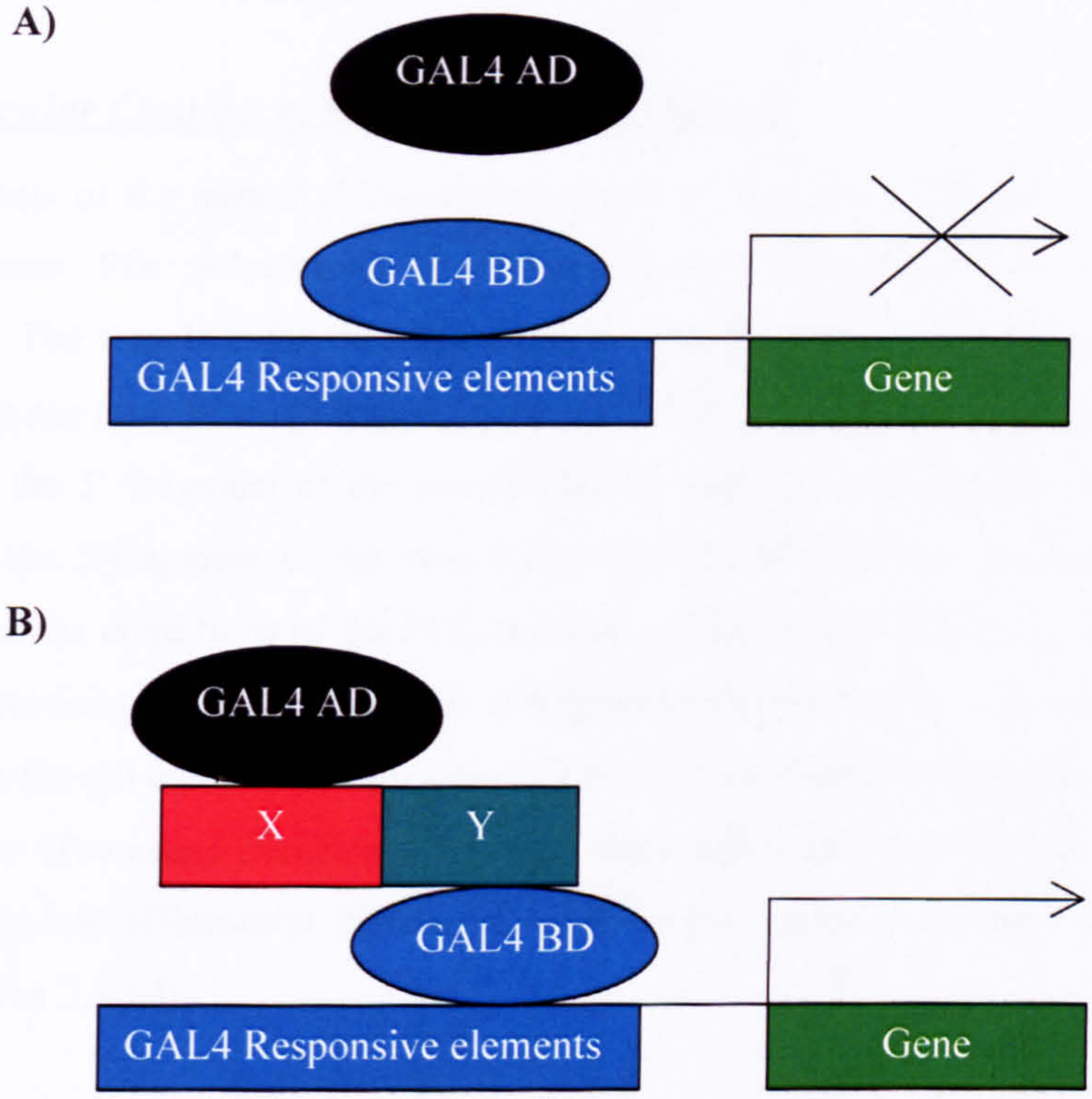

Figure 4.1 Schematic of the GAL4 Yeast Two-Hybrid Protein Interaction System

A) The GAL4 binding domain (GAL4 BD) exogenously supplied from a yeast two hybrid vector binds to GAL4 responsive elements within the DNA sequence. The GAL4 activation domain (GAL4 AD) exogenously supplied from a yeast two hybrid vector cannot bind to the GAL4 BD and cannot therefore initiate transcription of gene under the control of GAL4 responsive elements. **B)** The GAL4 binding domain fused to a protein of interest (Y) is exogenously supplied from a yeast two hybrid vector and can bind to GAL4 responsive elements within the DNA sequence. The GAL4 activation domain fused to a protein of interest (X) is exogenously supplied from a yeast two hybrid vector. If proteins X and Y interact then the GAL4 activation domain will be brought into close proximity with the GAL4 binding domain bound to the GAL4 responsive elements which allows GAL4 to function in transcription

4.2 Materials and Methods

4.2.1 Molecular Cloning of mau-2 into pGEM-t easy

Two fragments of the *mau-2* cDNA called mau-2-5' and mau-2-3' were amplified by PCR using Platinum Pfx polymerase (Invitrogen and Section 2.2.3) as per manufacturers instructions. The template for the PCR reaction was first strand DNA (Section 2.2.2) made using *C. elegans* total RNA (Section 2.2.1). The PCR primers used were SL1 with mau-2 5' reverse (for the 5' fragment of the *mau-2* cDNA) and mau-2 3' forward with mau-2 whole reverse (for the 3'fragment of the *mau-2* cDNA). The PCR primer sequences as detailed in Table 4.3 and the conditions of the PCR reaction are detailed in Table 4.1. The PCR products were size fractionated by agarose gel electrophoresis (Section 2.2.4) and the bands were excised from the gel and purified (Section 2.2.5). The purified PCR products were cloned into pGEM-t easy (Promega) (Section 2.3.2) and were subcloned together via the unique *Nco*I restriction site into pBluescript (Stratagene and Section 2.3.3). The clones were sequenced by MWG (Section 2.2.10).

Table 4.1 PCR Cycling Conditions for Amplification of *mau-2* cDNA Fragments

Step	Temperature	Time	Number of Cycles
Initial Denaturation	94	10 minutes	1
Denaturation	94	30 seconds	
Annealing	60	30 seconds	35
Extension	68	2 minutes	
Final Extension	68	10 minutes	1

4.2.2 Molecular Cloning of mau-2 into pGBKT7

The *mau-2* cDNA was amplified by PCR using Phusion DNA polymerase (Finnzymes and Section 2.2.3) as per the manufacturers' instructions. The template for the PCR reaction was *mau-2* cDNA made in Section 4.3.1. The primers used were Y2Hmau-2 forward with Y2Hmau-2 reverse which contained the restriction sites *Eco*RI and *Bam*HI respectively to allow sub-cloning of *mau-2* into the pGBKT7 vector (Section 4.2.5). The PCR primer sequences are detailed in Table 4.3 and the conditions of the PCR reaction are detailed in

Table 4.2. The PCR products were size fractionated by agarose gel electrophoresis (Section 2.2.4) and a band of the expected size was excised from the gel and purified (Section 2.2.5). The purified PCR product was cloned into the pGEM-t easy vector (Promega) (Section 2.3.2) and was subcloned into pGBKT7 (Clontech) via the *Eco*RI and *Bam*HI restriction sites (Section 2.3.3). The clone was sequenced by MWG (Section 2.2.10).

Table 4.2 PCR Cycling Conditions for Amplification of Full Length *mau-2* cDNA

Step	Temperature	Time	Number of Cycles
Initial Denaturation	98	10 minutes	1
Denaturation	98	10 seconds	
Annealing	60	30 seconds	34
Extension	72	1 minute	
Final Extension	72	10 minutes	1

4.2.3 Molecular Cloning of pqn-85 Fragments P1, P2 and P3

The P1, P2 and P3 cDNA fragments were amplified by PCR using Phusion DNA polymerase (Finnzymes and Section 2.2.3) as per the manufacturers' instructions. The template for the PCR reaction was first strand DNA (Section 2.2.2) made using *C. elegans* total RNA (Section 2.2.1). The PCR primers used were P1 forward with P1 reverse (for the P1 fragment), P2 forward with P2 reverse (for the P2 fragment) and P3 forward with P3 reverse (for the P3 fragment) and contained the restriction sites *Nco*I and *Xma*I at the 5' and 3' end respectively to allow cloning of the PCR products in the pACT2 vector (Section 4.2.5). The PCR primer sequences are detailed in Table 4.3 and the conditions of the PCR reaction are detailed in Table 4.4. The PCR products were size fractionated by agarose gel electrophoresis (Section 2.3.4) and bands of the expected size were excised from the gel and purified (Section 2.2.5). The purified PCR product was cloned into the pGEM-t easy vector (Promega) (Section 2.3.2) and was subcloned into pACT2 (Clontech) via the *Nco*I and *Xma*I restriction sites (Section 2.3.3). The clone was sequenced by MWG (Section 2.2.10)

Table 4.3 Sequence of PCR Primers used in Amplification of *mau-2* and *pqn-85* cDNA Sequences

Gene specific sequences are italicised and linker sequences are in bold, the *NcoI* restriction site is highlighted in red, the *Eco*RI restriction site is highlighted in blue, the *Bam*HI restriction site is highlighted in green and the *Xma*I restriction site is highlighted in yellow. The *mau-2* mRNA sequence used for reference was GenBank sequence number NM_059827.3. The *pqn-85* mRNA sequence used for reference was GenBank sequence number NM_061286.2.

Primer name	Primer sequence (5'-3')	Position of 5' base within mRNA
SL1	*CGTTTAATTACCCAAGTTTGAG*	See Figure 4.2
Mau-2 5' reverse	*TAATCTCATCGGCGTGTTTG*	904
Mau-2 3' forward	*GAACTTCCCGGCAACTTTTA*	704
Mau-2 whole reverse	*GAGGAAGCAGCTTGAATGGA*	1768
Y2H mau-2 forward	**AGTGAATTCC***ACCAAGATGCAGTTGCGAAAGC*	11
Y2H mau-2 reverse	**ATGGATCC***CGAGGAAGCAGCTTGAATGGA*	1769
P1 forward	**GCCATGGA***GGATCCGAATAACTTGCAAAA*	3
P1 reverse	**ACCCGGGTG***AATCTGGCGGATCCTCTTCT*	2270
P2 forward	**GCCATGGAG***ATGCCGAAGAACAAGAAACG*	2110
P2 reverse	**ACCCGGGTG***AGGATGAGCTGCTCCAGGTA*	4475
P3 forward	**GCCATGGAG***AGACGGGTGACTGATGAGGAAG*	4291
P3 reverse	**ACCCGGGTG***TTAATGCTCCATTTGCTCCA*	6612

Table 4.4 PCR Cycling Conditions for Amplification of *pqn-85* cDNA Fragments P1, P2 and P3

Step	Temperature	Time	Number of Cycles
Initial Denaturation	94	10 minutes	1
Denaturation	94	30 seconds	
Annealing	60	30 seconds	35
Extension	72	90 seconds	
Final Extension	72	10 minutes	1

4.2.4 Yeast strains

Yeast strain AH109 - *MATa, trp1-901, leu2-3,112,ura3-52,his3-200, gal4?, gal80?, LYS2::GAL1$_{UAS}$-GAL1$_{TATA}$-HIS3, GAL2$_{UAS}$-GAL2$_{TATA}$-ADE2 URA3::MEL1$_{UAS}$-MEL1$_{TATA}$-LacZ MEL1*

Yeast strain Y187 - *MATa, ura3-52, his-200, ade2-101, trp-901, leu2-3,112, gal4?, gal80?, met-, URA3::GAL1$_{UAS}$-GAL1$_{TATA}$-LacZ MEL1*

The AH109 and Y187 strains contain inactivating mutations in *his3*, *leu2* and *trp1*. Y187 also contains an inactivating mutation in the *ade2* gene whilst *ade2* has been removed from AH109. In order to survive, Y187 and AH109 cells require an exogenous source of histidine, leucine, tryptophan and adenine. The Y187 and AH109 strains both contain the *lacZ* reporter gene under the control of a promoter driven by GAL4 responsive elements (Section 4.1) and the AH109 strain also contains the *his3* and *ade2* reporter genes under the control of a promoter driven by GAL4 responsive elements (Section 4.1). To inhibit endogenous expression of the reporter genes the Y187 and AH109 strains have had the *gal4* and *gal80* genes (GAL80 is an inhibitor of GAL4 function) removed and as a result the *lacZ*, *ade2* and *his3* genes should not be expressed without exogenously supplied GAL4. The AH109 and Y187 strains are opposite mating types and when mated (Section 4.2.8) the resultant diploids are deficient for growth on SD media lacking adenine, histidine, leucine and tryptophan. When an exogenous source of GAL4 is provided however the reporter genes *ade2*, *his3* and *lacZ* should be expressed. Expression of the *his3* and the *ade2* genes will confer on yeast the ability to grow on SD media lacking adenine and histidine, whilst expression of *lacZ* results in production of ß-galactosidase an enzyme that can cleave the chemical X-gal yielding

galactose and 5-bromo-4-chloro-3-hydroxyindole. The 5-bromo-4-chloro-3-hydroxyindole oxidizes into 5,5'-dibromo-4,4'-dichloro-indigo, an insoluble blue product.

4.2.5 Yeast Plasmids

pGBKT7 The vector supplied by Clontech contains the kanamycin resistance gene for bacterial manipulation, the *trp1* gene which confers the ability to grow on SD agar lacking tryptophan (Sections 2.1.6 and 2.1.7) when transformed into yeast and the GAL4 DNA binding domain sequence under the control of the ADH1 constitutive yeast promoter upstream of the MCS

pACT2 The vector supplied by Clontech contains the ampicillin resistance gene for bacterial manipulation, the *leu2* gene which confers the ability to grow on SD agar lacking leucine when transformed into yeast (Sections 2.1.6 and 2.1.7) and the GAL4 activation domain sequence under the control of the ADH1 constitutive yeast promoter upstream of the MCS.

pTD1-1 The vector supplied by Clontech contains the SV40 large T antigen cDNA sequence (GenBank locus SV4CG) cloned into the multiple cloning site of pACT2 and produces the SV40 large T antigen fused to the GAL4 activation domain sequence.

pGBKT7-53 The vector supplied by Clontech contains the murine p53 cDNA sequence (GenBank accession number K01700) cloned in to the multiple cloning site of pGBKT7 and produces murine p53 fused to the GAL4 DNA binding domain sequence.

4.2.6 Yeast Transformation

A microcentrifuge tube with 1ml of YPDA (Section 2.1.3) was inoculated with several colonies of the appropriate yeast strain and vortexed briefly to disperse the cells. The contents

of the tube were transferred to a sterile flask containing 50mls YPDA (Section 2.1.3) and the yeast culture was incubated for 16-18hrs at 30°C to stationary phase (OD600>1.5). The culture was diluted in 300mls of fresh YPDA (Section 2.1.3) to an OD600 of 0.2-0.3. The culture was incubated at 30°C until log phase when the OD600 measured 0.4-0.6 before being transferred to sterile 50ml falcon tubes and centrifuged at 1000 x g for 5mins at room temperature. The supernatant was discarded and the pellets were resuspended in 5mls sterile TE buffer (Section 2.1.9) before being pooled in one 50ml Falcon tube (BD Biosciences). The resuspended cells were once again centrifuged at 1000 x g for 5mins and the supernatant was discarded. The pelleted cells were resuspended in 1.5ml fresh sterile 1X TE/1X LiAc (Section 2.1.21). In a fresh microcentrifuge tube 0.1µg of plasmid DNA was added to 0.1mg of herring testis carrier DNA (Sigma D6898) and mixed by vortexing. 0.1ml of the competent yeast cells resuspended in 1.5ml fresh sterile 1X TE/1X LiAc (Section 2.1.21) were added to the plasmid and herring testis carrier DNA and the microcentrifuge tube was vortexed briefly before adding 0.6 ml of sterile PEG/LiAc (Section 2.1.22) and vortexing again. The tube was incubated at 30°C for 30mins with shaking at 200rpm. Following the incubation, 70µl of DMSO was added and the contents were gently mixed by inversion. The yeast were heat shocked for 15 minutes in a 42°C water bath and then chilled on ice for 2 minutes. The cells were centrifuged at 14000rpm for 5seconds and the supernatant was discarded. The pelleted cells were resuspended in 0.5ml sterile 1X TE buffer (Section 2.1.9). The cells were spread onto SD agar containing the appropriate supplements and grown for 3-5 days at 30°C

4.2.7 Filter Lift Colony Assay

A Whatman No. 5 filter was placed over the yeast colonies to be tested and the filter was gently pressed down to allow the yeast to attach to the filter. The filter was removed from the yeast colonies and placed in liquid nitrogen for 10 seconds before being removed and thawed at room temperature. The filter was placed colony side uppermost onto another Whatman No. 5 filter in a clean 90mm petri dish that had been presoaked in 2.5ml Z buffer/X-gal solution (Section 2.1.18). The filter was incubated at 30°C for three hours.

4.2.8 Yeast Mating Assay

One colony of each yeast strain to be mated were resuspended in the same microcentrifuge containing 0.5ml YPDA broth (Section 2.1.3), the tube was vortexed and the cells were incubated for 24hrs at 30°C with shaking at 200rpm. The yeast was resuspended, spread onto the appropriate SD agar (section 2.1.6) and were grown at 30°C for 3-5 days.

4.3 Results

4.3.1 Molecular Cloning of mau-2

Total RNA extracted from 100µl of packed *C. elegans* was used as a template in an oligo-dT primed reverse transcription reaction to produce first strand cDNA. Two overlapping fragments of the *mau-2* cDNA called mau-2-5' and mau-2-3' (Figure 4.2 A) sharing a unique *Nco*I restriction site were amplified from the first strand cDNA population by PCR. The PCR products were size fractionated by agarose gel electrophoresis and bands of the expected size were observed (Figure 4.2B), The purified PCR products were initially cloned separately into pGEM-t easy and to create the full length *mau-2* cDNA the mau2-5' and mau-2-3' fragments were cloned together via the unique *Nco*I restriction site into pBluescript. The *mau-2* cDNA was verified by sequencing and the sequence was found to be >99% identical to the *mau-2* mRNA from base 11 to base 1769 (GenBank sequence number NM_059827.3) with only one base out of 1759 being different. The change affects base 56 of the sequence corresponding to the *mau-2* mRNA (GenBank sequence number NM_059827.3) and changes a guanine to an adenine. The codon affected by this base changes from CUG to CUA however both sequences code for the amino acid leucine. The discrepancy in the DNA sequence therefore does not affect the sequence at the protein level suggesting that it is likely to be a polymorphism and would not affect future experiments.

4.3.2 Molecular Cloning mau-2 into the pGBKT7 Yeast Two-Hybrid Vector

The *mau-2* cDNA corresponding to bases 11 to 1769 of *mau-2* mRNA (GenBank sequence number NM_059827.3) was amplified by PCR from the cDNA created in Section 4.3.1 using *mau-2* specific oligonucleotide primers. The PCR primers used contained restriction sites which were not found in the *mau-2* cDNA sequence to allow sub-cloning of the PCR product into the yeast two hybrid vector pGBKT7. The position of the restriction sites within the PCR primers was designed to allow in frame translation of the *mau-2* transcript with the GAL4 DNA binding domain sequence. The PCR products were size fractionated by agarose gel electrophoresis (Figure 4.3A) and a band of the expected size (~1700bp) was excised from the gel and purified. The purified PCR product was cloned into pGEM-t easy then sub-cloned into the yeast two hybrid vector pGBKT7 MCS with the appropriate restriction enzymes. The finished construct (called M1) was sequenced and was found to be to be 100% identical to that of the *mau-2* cDNA created in 4.3.1 and was also in frame with the GAL-4 DNA binding domain sequence confirming that the construct was suitable to use for the yeast two hybrid assay.

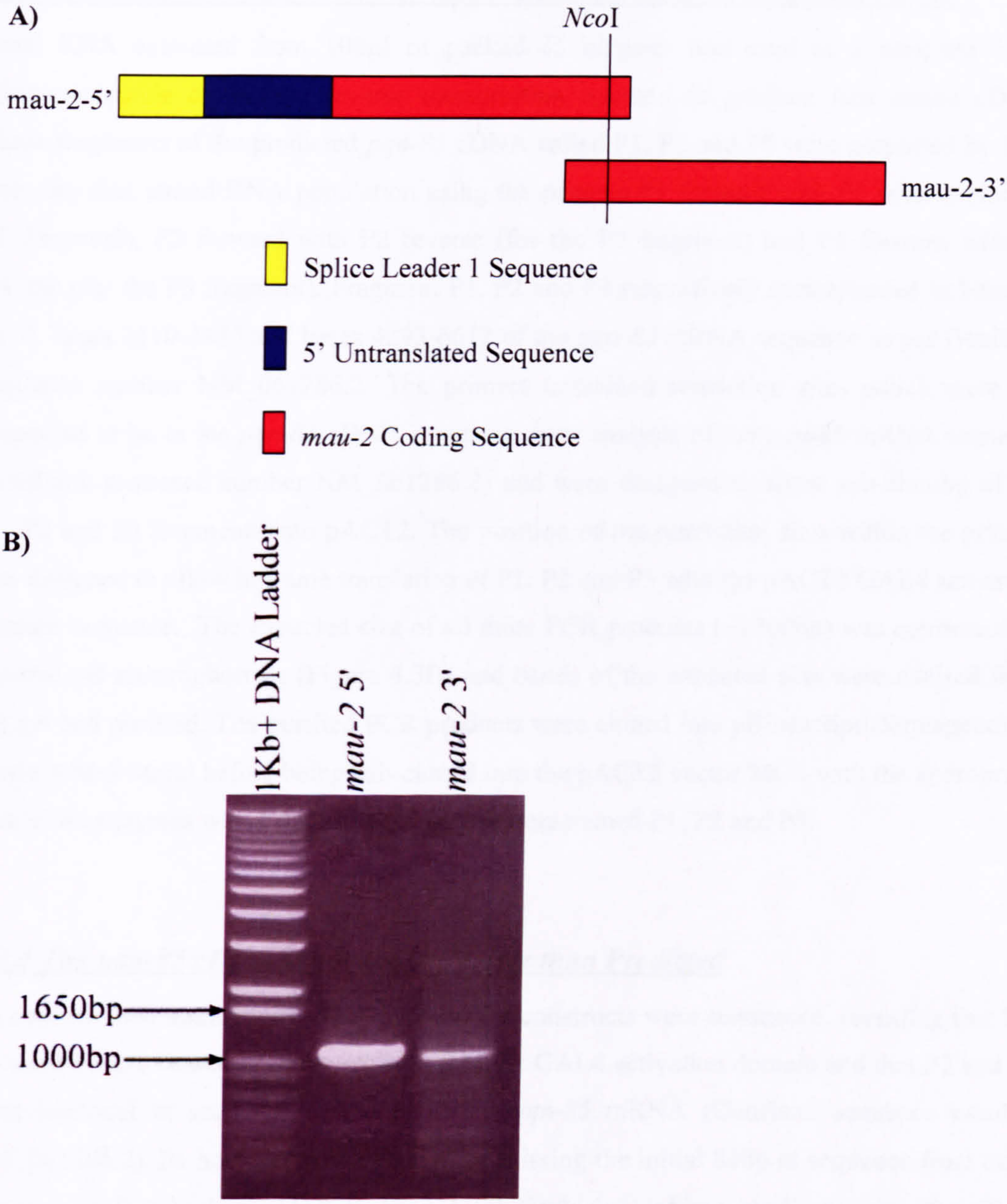

Figure 4.2 Cloning of *mau-2* cDNA

A) The structure of the PCR products amplified by PCR in 4.3.1. Fragment mau-2-5' comprises the SL1 splice leader sequence which is attached to the 5' end of the *C. elegans mau-2* mRNA sequence (Benard et al., 2004), 5' UTR and 898bp of *mau-2* coding sequence. The mau-2-3' fragment comprises 1068bp of the *mau-2* coding sequence; both fragments share a unique *Nco*I restriction site. **B)** The mau-2-5' and mau-2-3' PCR products visualised by agarose gel electrophoresis. Specific bands of the correct size (~1Kb) can be seen.

4.3.3 Molecular Cloning of pqn-85 into the pACT2 Yeast Two-Hybrid Vector

Total RNA extracted from 100µl of packed *C. elegans* was used as a template in an oliogonucleotide dT-primed reverse transcription reaction to produce first strand cDNA. Three fragments of the predicted *pqn-85* cDNA called P1, P2 and P3 were amplified by PCR from the first strand DNA population using the primers P1 forward with P1 reverse (for the P1 fragment), P2 forward with P2 reverse (for the P2 fragment) and P3 forward with P3 reverse (for the P3 fragment). Fragment P1, P2 and P3 respectively corresponded to bases 3-2270, bases 2110-4475 and bases 4293-6612 of the *pqn-85* mRNA sequence as per GenBank sequence number NM_061286.2. The primers contained restriction sites which were not suspected to be in the *pqn-85* cDNA sequence upon analysis of the *pqn*-85 mRNA sequence (GenBank sequence number NM_061286.2) and were designed to allow sub-cloning of the P1, P2 and P3 fragments into pACT2. The position of the restriction sites within the primers was designed to allow in frame translation of P1, P2 and P3 with the pACT2 GAL4 activation domain sequence. The expected size of all three PCR products (~2300bp) was confirmed by agarose gel electrophoresis (Figure 4.3B) and bands of the expected size were excised from the gel and purified. The purified PCR products were cloned into pBluescript (Stratagene) by Nazia Abdul-Majid before being sub-cloned into the pACT2 vector MCS with the appropriate restriction enzymes where upon the constructs were named P1, P2 and P3.

4.3.4 The pqn-85 cDNA Sequence is Shorter than Predicted

To confirm their authenticity the P1, P2 and P3 constructs were sequenced, revealing that P1, P2 and P3 were cloned in frame with the pACT2 GAL4 activation domain and that P2 and P3 were identical in sequence to the predicted *pqn-85* mRNA (GenBank sequence number NM_061286.2). P1 however was shown to be missing the initial 81bp of sequence from exon 6 corresponding to base 1119 to base 1199 (inclusive) of the predicted *pqn-85* mRNA sequence (GenBank sequence number NM_061286.2) (Figure 4.4 A and B). The removal of the 81bp sequence would not affect the frame of the mRNA translation but would result in the deletion of a 27 amino acid sequence from PQN-85. Base 1119 was predicted to form the 5' start of exon 6 which suggested the possibility that the splice site had been incorrectly predicted. To assess this possibility a BLASTn search of the 81bp missing sequence against the *C. elegans* EST database was carried out and showed no evidence of expression. The 27 amino acid sequence encoded by this 81bp segment was used in a TBLASTN search to search for predicted proteins from translated sequences and a BLASTP search against a non redundant sequence database. Only the PQN-85 protein sequence shares

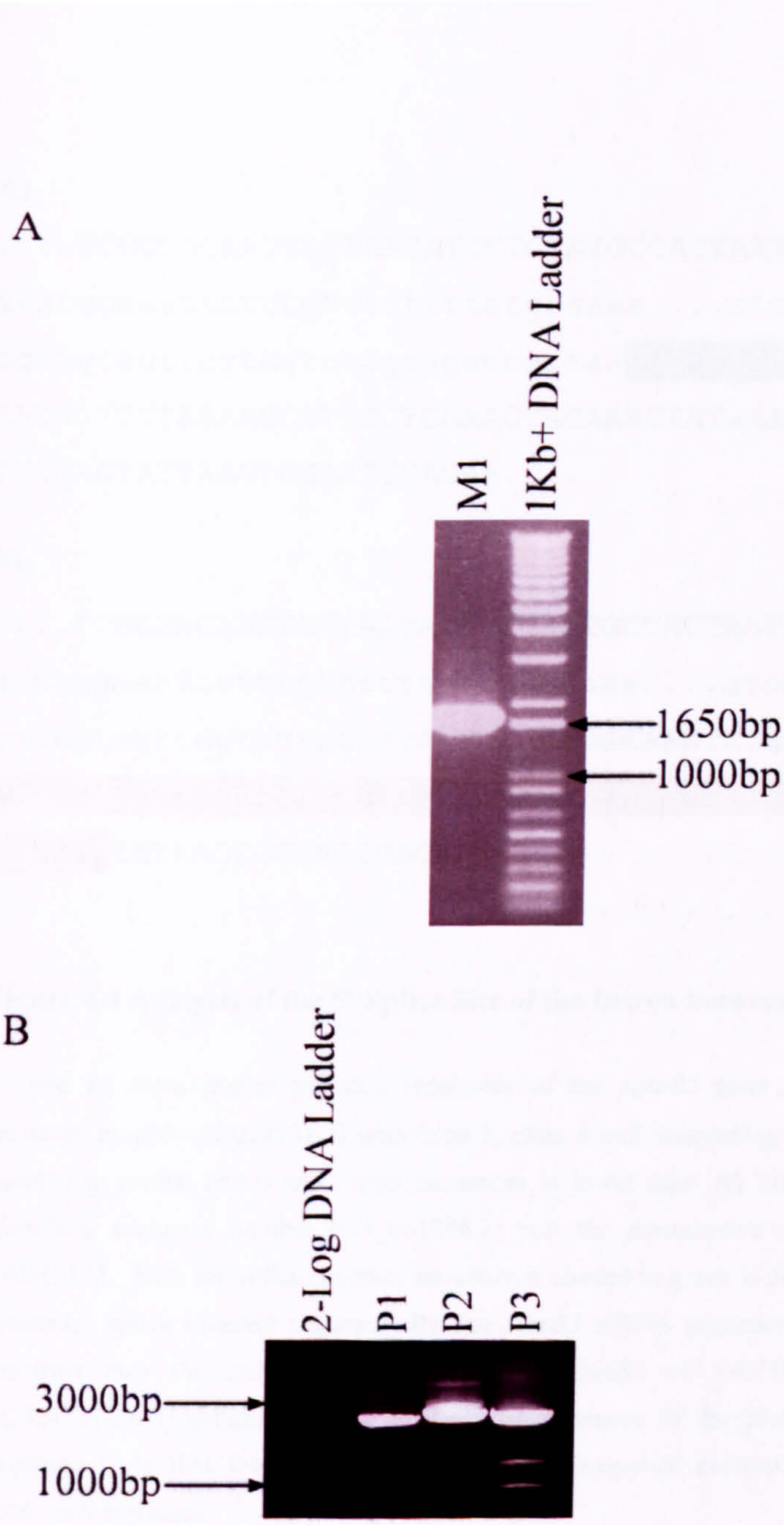

Figure 4.3 PCR Amplification of *mau-2* and *pqn-85* Fragments for Yeast Two-Hybrid Constructs

A) The *mau-2* cDNA was amplified corresponding to base 11-1769 of the *mau-2* mRNA sequence (GenBank sequence number NM_059827.3) by PCR and the products size fractionated by agarose gel electrophoresis. A band of the expected size (1759bp) can be seen. **B)** Fragments P1, P2 and P3 as detailed in section 4.3.3 were amplified by PCR and products were size fractionated by agarose gel electrophoresis. Specific bands of the expected size (P1 2267bp, P2 2365bp and P3 2319bp) can be seen

A)

....TCGCCACAATTAGTAATATCCTGAATGCCACTAATATTGATGATATgtaagttgga
atatggaaatttttgtttttttttctgaaaaa....atcacttgggtctgctaaatcgag
agttgtagttcgtagtctagcagaccaaaaaaaaaatttaattcagAATAAGTTCTGTTAC
AACTGTTTTAAAAGCGTTGCTCAAACTACAAACTATAAAATATTTCACATATCTCTTTTC
TTCCAGTATTAACTCGAATGGACAA....

B)

....TCGCCACAATTAGTAATATCCTGAATGCCACTAATATTGATGATATgtaagttgga
atatggaaatttttgtttttttttctgaaaaa....atcacttgggtctgctaaatcgag
agttgtagttcgtagtctagcagaccaaaaaaaaaatttaattcagaataagttctgttac
aactgttttaaaagcgttgctcaaactacaaactataaaatatttcacatatctcttttc
ttccagTATAACTCGAATGGACAA....

Figure 4.4 Analysis of the 5' Splice Site of the Intron between *pqn-85* Exon 5 and Exon 6

A) and **B)** show partial genomic sequences of the *pqn-85* gene from cosmid Y42H11AL (GenBank sequence number AC024781.2) with exon 5, exon 6 and intervening intron sequnces. Exon sequences are annoted in capital letters and intron sequences in lower case. **A)** The predicted *pqn-85* mRNA sequence (GenBank sequence number NM_061286.2) puts the presumptive splice acceptor at position 30683 of Y42H11AL. Note the splice acceptor sequence is shaded in green is poorly related to the $(T/C)_{10}N(T/C)AG$ consensus splice acceptor sequence. **B)** The *pqn-85* mRNA sequence confirmed by sequencing of the P1 construct puts the splice acceptor at position 30682 of Y43H11AL (Genbank accession number AC024781.2). Highlighted in red is the 81bp sequence of the predicted exon 6 missing from the P1 sequence Note that the inferred splice acceptor sequence corresponds well to the $(T/C)_{10}N(T/C)AG$ consensus sequence.

any homology to this 27 amino acid sequence. Wormbase (Wormbase) also reports no expression of this sequence suggesting that the 81bp sequence may have been incorrectly attributed to the *pqn-85* mRNA sequence.

To assess the likelihood of each sequence forming a splice site, the end of the intron sequence preceding exon 6 (as predicted in the *pqn-85* mRNA: GenBank sequence number NM_061286.2) and the end of the missing 81bp sequence were compared to the consensus splice acceptor sequence. Both sequences end in the splice acceptor dinucleotide AG, however the splice acceptor site at the end of the 81bp fragment is almost identical to the consensus sequence whereas the splice acceptor site within the predicted intron upon analysis of the *pqn-85* genomic sequence from (Genbank accession number AC024781.2) is rather diverged from the consensus. This suggests that the 81bp is more likely to form the end of the intron preceding exon 6 than the sequence that had been previously predicted. Taken together this evidence suggests that the 81bp previously predicted as belonging to exon 6 actually forms part of the intron preceding exon 6 and that the overall length of PQN-85 is 2176 amino acids and not the predicted 2203 amino acids. This means that the P1, P2 and P3 constructs respectively correspond to bases 3-2189 bases 2129-4394 and bases 4210-6531 of the *pqn-85* mRNA sequence as confirmed by sequencing. Further this confirms that the P1 construct as with the P2 and P3 constructs were suitable for use in the yeast two hybrid assay.

4.3.5 Testing the MAU-2 PQN-85 Interaction Using Yeast Two-Hybrid Analyses

To test the interaction of MAU-2 with PQN-85, the M1, P1, P2 and P3 constructs were transformed into the *S. cerevisiae* AH109 and Y187 strains to be used in a directed yeast two hybrid assay. Table 4.5 illustrates the specific detail of the transformation experiments. Yeast transformants were incubated at 30°C on SD agar lacking the appropriate amino acid for 3 days to select for yeast containing the corresponding constructs. To obtain diploid yeast with two plasmids in one cell the Y187 and AH109 which are opposite mating types yeast were mated. Table 4.6 illustrates the specific detail of the transformation experiments. The mated yeast were grown on SD agar lacking both leucine and tryptophan at 30°C for 3 days to select for the presence of the corresponding constructs.

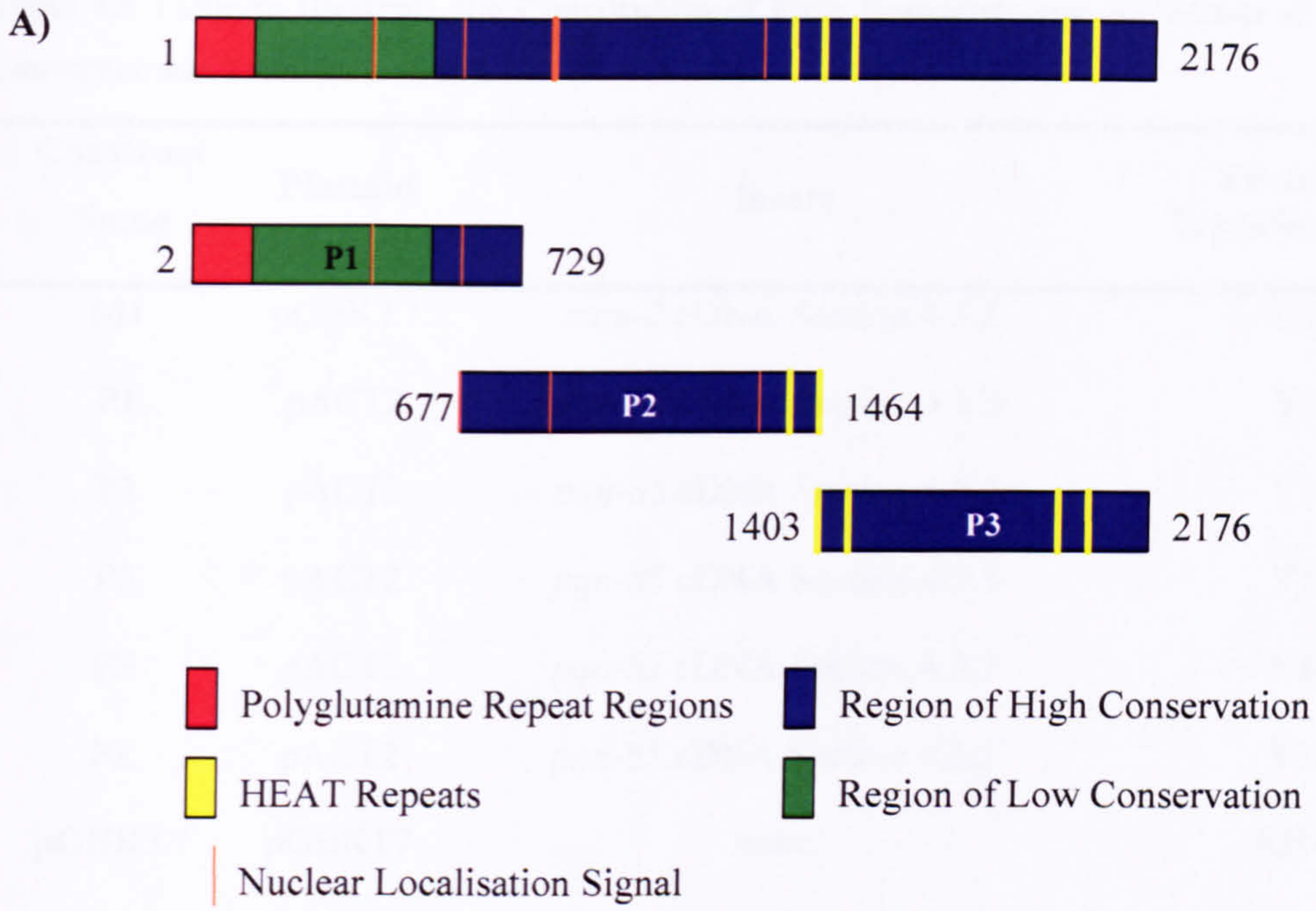

Figure 4.5 Schematic of the Yeast Two-Hybrid Constructs

A) The *C. elegans* PQN-85 protein is 2176 amino acids long as confirmed in Section 4.3.4. The P1, P2 and P3 constructs were designed to be partially overlapping as shown. The positions of the predicted HEAT repeats within the sequence are detailed (Figure 1.5 and 1.6). Also shown are the location of the nuclear localisation signals and the regions of the protein demonstrating high of low levels of sequence conservation (Section 1.) **B)** The *C. elegans* MAU-2 protein is 593 amino acids long and the M1 construct spans most of the sequence.

Table 4.5 Table to Illustrate the Constitution of Each Construct and the Strain of Yeast Each Construct was Transformed into

Construct Name	Plasmid	Insert	Yeast Strain Transformed Into
M1	pGBKT7	*mau-2* cDNA Section 4.3.2	AH109
P1	pACT2	*pqn-85* cDNA Section 4.3.3	Y187
P2	pACT2	*pqn-85* cDNA Section 4.3.3	Y187
P3	pACT2	*pqn-85* cDNA Section 4.3.3	Y187
PS	pACT2	*pqn-85* cDNA Section 4.3.7	Y187
PE	pACT2	*pqn-85* cDNA Section 4.3.3	Y187
pGBKT7	pGBKT7	none	AH109
pACT2	pACT2	none	Y187
pGBKT7-p53	pGBKT7	murine p53 Section 4.2.5	AH109
pTD1-1	pACT2	SV40 large T antigen Section 4.2.5	Y187

4.3.6 MAU-2 Interacts with the N-terminal Region of PQN-85

The diploid yeast containing two plasmids in one cell were streaked onto SD agar lacking leucine and tryptophan and incubated at 30°C for 3 days to obtain fresh yeast colonies. To test for expression of the *lacZ* gene a colony filter lift assay was performed on the fresh yeast and the filter was incubated at 30°C for 3 hours. Within one hour of the assay being performed yeast containing pGBKT7-53 and pTD1-1 turned blue (Figure 4.6 and summarised in Table 4.7) as expected indicting that an interaction occurred confirming that the colony filter lift assay could report positive interactions. Yeast containing P1 and M1 also turned blue (Figure 4.6 and summarised in Table 4.7) around 1 hour after the assay was performed suggesting that this was a positive interaction. The yeast containing P2 or P3 with M1 however did not turn blue (Figure 4.6 and summarised in Table 4.7) three hours after the colony filter lift assay was performed suggesting that no interaction occurred. Yeast containing the empty vectors pGBKT7 and pACT2 also did not turn blue three hours after the assay was performed confirming that no background level of interaction occurred.

Table 4.6 Table to Illustrate the Yeast Mating Experiments Set up to Obtain Diploid Yeast and the Objective of the Mating Experiments

Negative Control – The GAL4 DNA binding and activation domain sequences will be expressed from empty pGBKT7 and empty pACT2 respectively but they cannot interact with each other to produce functional GAL4 and should not induce expression of the reporter genes.

Positive Control – The SV40 large T antigen fused to the GAL4 activation domain sequence is known to interact with p53 fused to the GAL4 DNA binding domain sequence bringing together the GAL4 DNA BD and AD inducing expression of the reporter genes.

Mating Experiment	Objective of Mating Experiment
M1 in AH109 x P1 in Y187	Analysis of the interaction between PQN-85 and MAU-2
M1 in AH109 x P2 in Y187	Analysis of the interaction between PQN-85 and MAU-2
M1 in AH109 x P3 in Y187	Analysis of the interaction between PQN-85 and MAU-2
M1 in AH109 x PE in Y187	Analysis of the interaction between PQN-85 and MAU-2
M1 in AH109 x PS in Y187	Analysis of the interaction between PQN-85 and MAU-2
pGBKT7 in AH109 x pACT2 in Y187	Negative control (see above)
pGBKT7-p53 in AH109 x pTD1-1 in Y187	Positive control (see above)

In order to further confirm the result obtained by the colony filter lift assay, expression of the *ade2* and *his3* reporter genes was analysed. The diploid yeast containing two plasmids in one cell were streaked onto SD agar lacking histidine, adenine, leucine and tryptophan and incubated at 30°C for 3 days. The yeast containing pGBKT7-53 and pTD1-1 grew (Figure 4.7 and summarised in Table 4.7) confirming that the *ade2* and *his3* genes were expressed in response to a positive interaction. In concordance with the results obtained from the colony filter lift assay yeast containing M1 and P1 also grew on plates lacking leucine, tryptophan, histidine and adenine (Figure 4.7 and summarised in Table 4.7) indicating a positive interaction whereas yeast containing M1 and PS, M1 and P2 and M1 and P3 did not grow

(Figure 4.7 and summarised in Table 4.7) indicating that an interaction does not occur. This suggests that the N terminal 729 amino acids of PQN-85 are required for the interaction with MAU-2 but the remaining 1447 amino acids are not required.

4.3.7 M1 Interacts with a Smaller Segment of the P1 Construct

To further localise the interaction domain of PQN-85, the P1 construct was used to create two smaller constructs named PE and PS. To make the PE construct purified P1 plasmid was restriction digested with *Eco*RI which cuts twice within the *pqn-85* cDNA sequence (Figure 4.8A) and once in the MCS of the pACT2 producing bands of approximate size 100bp, 750bp and ~9.5Kb. To make the PS construct purified P1 plasmid was restriction digested with *Sac*I which cut twice within the *pqn-85* cDNA sequence and once with in the MCS of the pACT2 removing segments of approximate size 700bp, 850bp and 8.7Kb. The products of the restriction digest were size fractionated by agarose gel electrophoresis and bands of the expected size were observed (Figure 4.9). The largest band from each restriction digest corresponding to the remaining segment of P1 was excised from the gel, purified and religated using standard cloning techniques. Figure 4.8B details the specific amino acids covered by the PE and PS constructs.

Table 4.7 Summary of Yeast Two-Hybrid Results

Mating Experiment	Colour of Filter Colony Assay	Growth on SD agar Lacking Adenine and Histidine	Interaction Between the Proteins Encoded by the Constructs
M1 x P1	Blue	Yes	Yes
M1 x P2	Colourless	No	No
M1 x P3	Colourless	No	No
M1 x PE	Blue	Yes	Yes
M1 x PS	Colourless	No	No
pGBKT7 x pACT2	Colourless	No	No
pGBKT7-p53 x pTD1-1	Blue	Yes	Yes

The PE and PS constructs were transformed into the Y187 yeast strain and were incubated on SD agar lacking leucine at 30°C for three days to select for the presence of the PE and PS

constructs (summarised in Table 4.5). The Y187 strain containing the PE and PS constructs was then mated to the AH109 strain containing the M1 construct (summarised in Table 4.6). The yeast was then grown on SD agar lacking leucine and tryptophan for three days at 30°C to select for the presence of the M1 and either the PE or PS constructs. The yeast colonies were streaked onto fresh SD agar and grown for three days at 30°C and the resultant colonies were tested for expression of the *lacZ* gene by colony filter lift assay. Yeast containing the M1 construct with the PE construct turned blue (Figure 4.6 and summarised in Table 4.7) when the assay was performed, whereas the yeast containing the PS construct with M1 did not (Figure 4.6 and summarised in Table 4.7). To further confirm this result the yeast was streaked onto SD agar lacking histidine, adenine, leucine and tryptophan to test for expression of the *ade2* and *his3* genes. The yeast containing PE with M1 grew but the yeast containing PS with M1 did not. This suggests that the first 450 amino acids of PQN-85 are required for the interaction with MAU-2 however the first 210 amino acids are not sufficient for the interaction to occur.

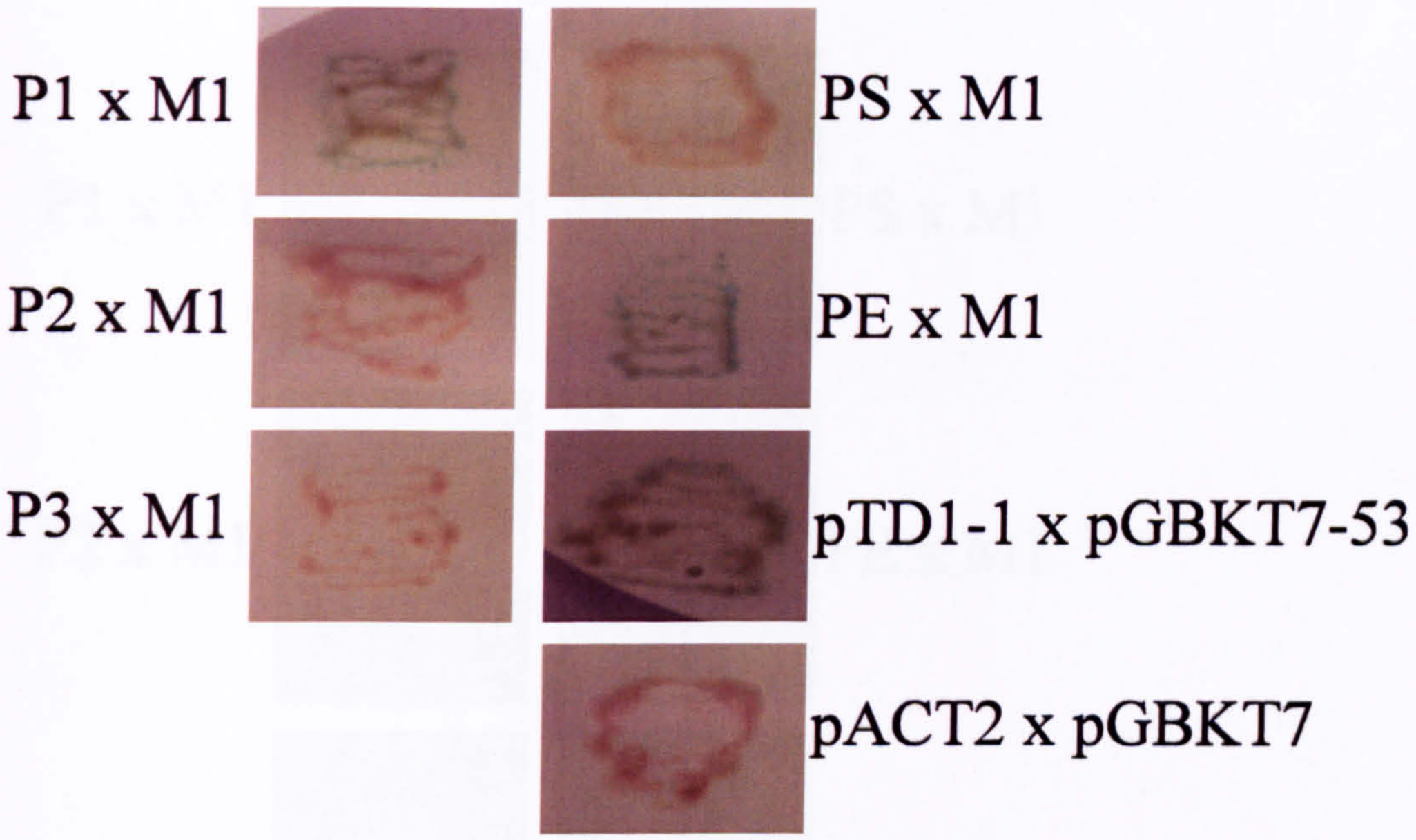

Figure 4.6 Interaction between MAU-2 and PQN-85 Revealed by Directed Yeast Two-Hybrid Assays

A directed yeast two hybrid assay was used to analyse the interaction between the MAU2 and PQN-85 proteins. A positive interaction inducing expression of the *lacZ* gene was assessed by colony filter lift assay. Positive interactions were denoted by blue colonies whereas colonies that were not blue indicated no interaction. Yeast strains carrying the P1 and M1 constructs (Figure 4.5 and P1 x M1 below) or PE and M1 constructs (Figure 4.8 and PE x M1 below) turned blue 1 hour after the filter lift assay was conducted indicating a positive interaction. Yeast strains carrying the P2 and M1 constructs (Figure 4.5 and P2 x M1 below), P3 and M1 constructs (Figure 4.5 and P3 x M1 below) and the PS and M1 constructs (Figure 4.8 and PS x M1 below) did not turn blue three hours after the colony filter lift assay was conducted, consistent with a lack of interaction. The yeast carrying the pGBKT7-53 and pTD1-1 which are known to produce a positive result turned blue; yeast carrying the empty pGBKT7 and pACT2 vectors (which are unable to interact) remained colourless.

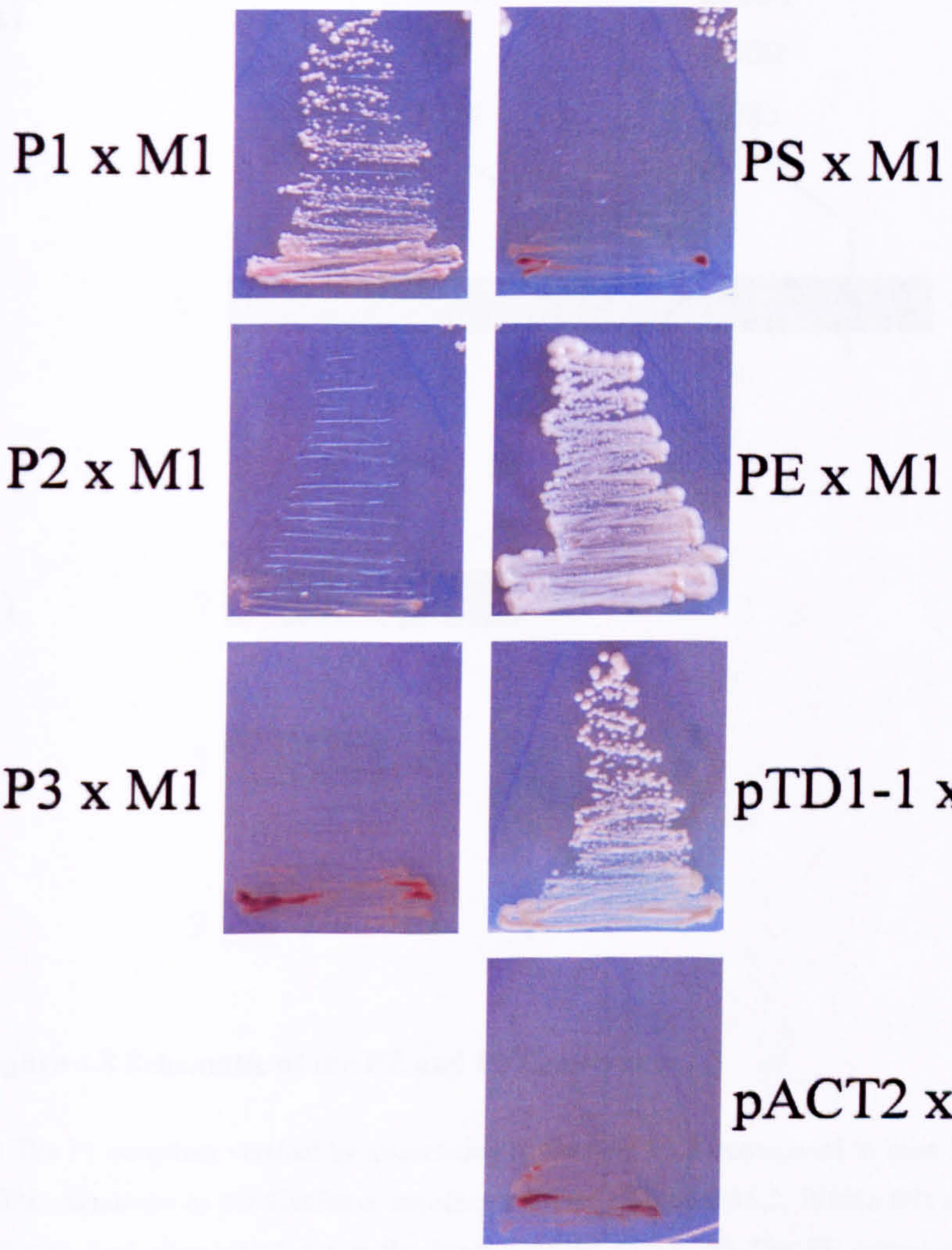

Figure 4.7 Verification of the Interaction between MAU-2 and PQN-85

A directed yeast two hybrid assay was used to analyse the interaction between the MAU2 and PQN-85 proteins. A positive interaction inducing expression of the *ade2* and *his3* genes was assessed by growth of the yeast on SD agar lacking adenine and histidine. Yeast strains carrying the P1 and M1 constructs (Figure 4.5 and P1 x M1 below) or PE and M1 constructs (Figure 4.8 and PE x M1) grew on SD agar lacking adenine and histidine indicating a positive interaction. Yeast strains carrying the P2 and M1 constructs (Figure 4.5 and P2 x M1 below), P3 and M1 constructs (Figure 4.5 and P3 x M1 below) and the PS and M1 constructs (Figure 4.8 and PS x M1 below) did not grow on SD agar lacking adenine and histidine indicating no interaction occured. Yeast carrying the pGBKT7-53 construct and the pTD1-1 construct (P53 x PTD1) that are known to interact also grew on SD agar lacking histidine and adenine. Yeast carrying the empty pACT2 and PGBKT7 vectors (pACT2 x pGBKT7) were unable to grow on the SD agar lacking leucine, tryptophan, histidine and adenine.

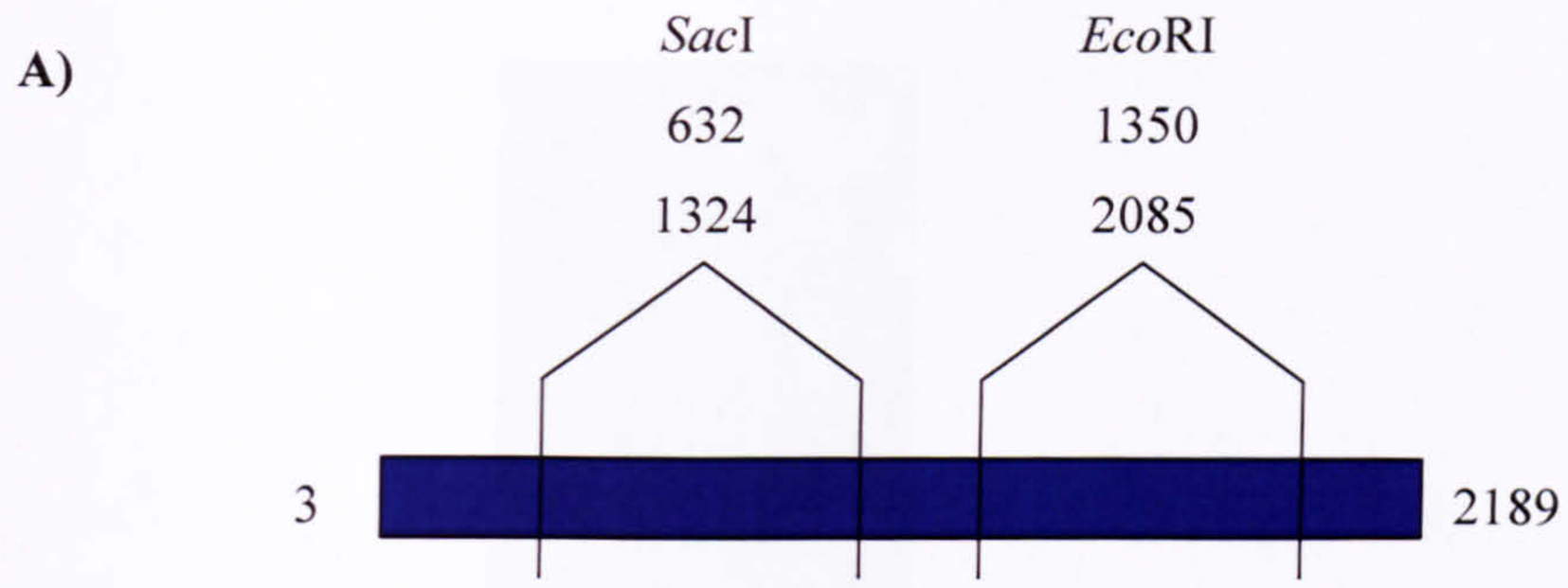

Figure 4.8 Schematic of the PE and PS Constructs

A) The P1 construct verified by sequencing in Section 4.3.3 correspond to base 3 to base 2189 of the *pqn-85* mRNA sequence as per GenBank sequence number NM_061286.2. Within this sequence are two *Eco*RI sites and two *Sac*I sites which cut at the bases detailed above. **B)** The PE covers amino acids 2-450 of the *C. elegans* PQN-85 protein whilst the PS construct covers amino acids 2-210 of the *C. elegans* PQN-85 protein. **C)** The P1 construct was restriction digested with *Eco*RI and *Sac*I and the products were size fractionated by agarose gel electrophoresis. Most bands of the expected size can be observed for the *Eco*RI digest (approximate sizes - 100bp, 750bp and ~9.5Kb) and all bands of the expected size can be observed for the *Sac*I digest (approximate sizes - 700bp, 850bp and 8.7Kb).

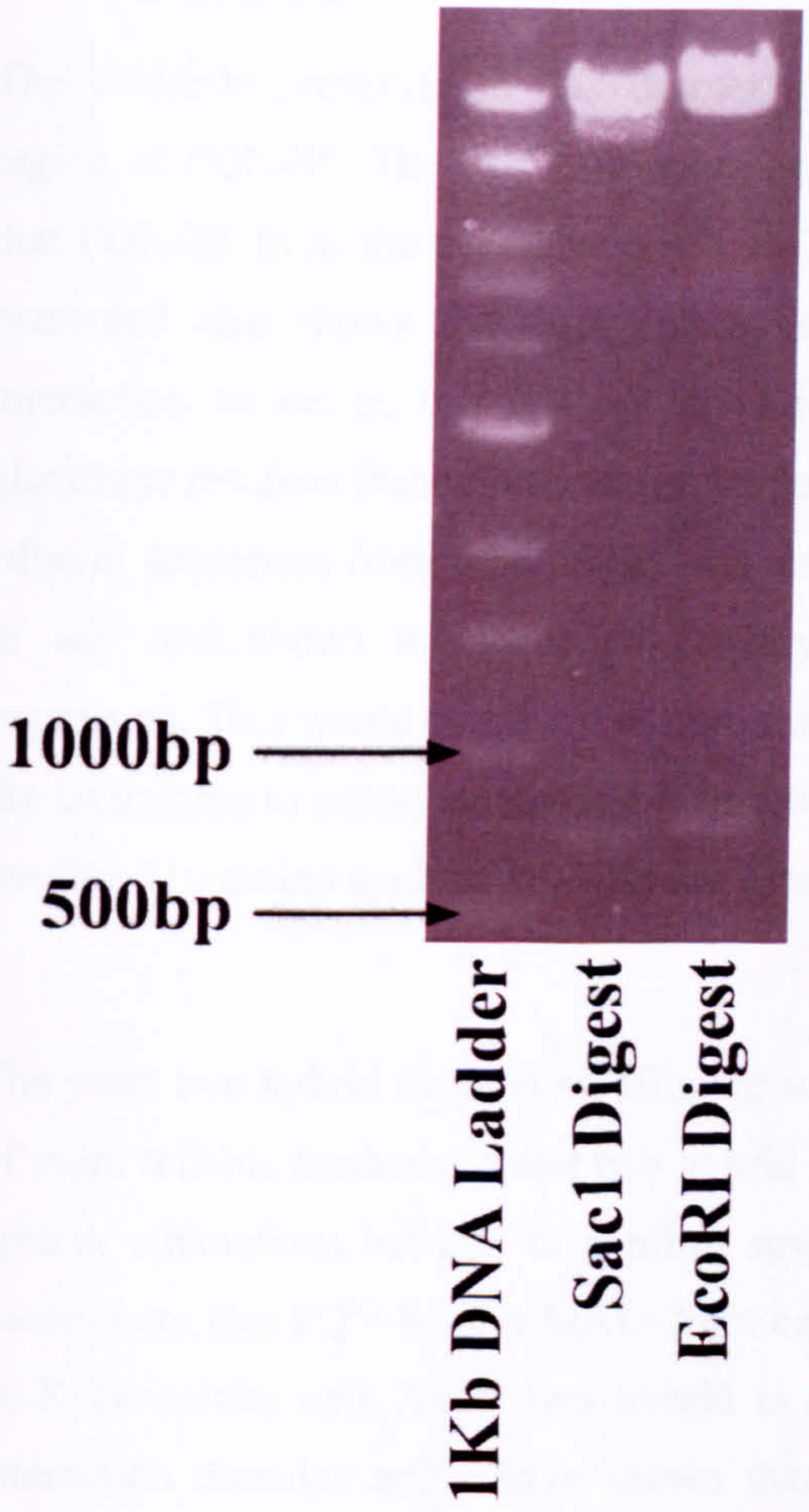

Figure 4.9 Restriction Digest of the P1 Construct

The P1 construct was restriction digested with *Eco*RI and *Sac*I and the products were size fractionated by agarose gel electrophoresis. Most bands of the expected size can be observed for the *Eco*RI digest (approximate sizes - 100bp, 750bp and ~9.5Kb) and all bands of the expected size can be observed for the *Sac*I digest (approximate sizes - 700bp, 850bp and 8.7Kb).

4.4 Discussion

The evidence presented in this chapter shows that MAU-2 interacts with the N-terminal region of PQN-85. The first 450 amino acids of PQN-85 are sufficient to bind MAU-2 and that PQN-85 from the amino acid 451 to 2176 is not required for the interaction. The data presented also shows that first 210 amino acids of PQN-85 are not sufficient for this interaction to occur, this 210 amino acid region contains a highly repetitive series of glutamine residues (henceforth called the polyglutamine rich region). Rudimentary analysis of adherin sequences from other organisms suggests that no polyglutamine rich region is found in any and shows no sequence conservation with orthologous sequences from other organisms. This would suggest therefore that the polyglutamine rich region is dispensable for the interaction to occur, however it cannot be ruled out that specific residues or regions within the first 210 amino acids of PQN-85 are vital to the interaction with MAU-2.

The yeast two hybrid assay is an efficient way of detecting protein interaction in the absence of more reliable methods. Yeast two hybrid has been used for many years to determine novel protein interactions but also to confirm suspected interactions between two proteins. I have shown here that PQN-85 and MAU-2 are capable of binding to one another in the context of an *S. cerevisiae* cell. Yeast two hybrid is also particularly useful for determining specific interaction domains and I have shown that this interaction requires only a stretch of 450 amino acids from the extreme N terminus of PQN-85. Every effort has been made to ensure that the results are genuine and no background level of interaction was detected in the assay using yeast vectors expressing only the GAL4 activation domain and GAL4 binding domain. MAU-2 did not interact with peptides from the C-terminal end of PQN-85 suggesting that the interaction is specific and that MAU-2 does not indiscriminately interact with any protein sequence. To further analyse the interaction domain within PQN-85 and MAU-2 required for the interaction to occur, the size of the cDNA construct within the yeast two hybrid vectors should be reduced in size to find the minimum amino acid requirements for the interaction to occur.

The Yeast two-hybrid assay does not provide evidence of an in vivo interaction and despite the interaction MAU-2 and PQN-85 may not interact in *C. elegans*. To further confirm the biological relevance of the interaction between PQN-85 and MAU-2 further evidence in the form of coimmunoprecipitation or immunofluorescent co-localisation studies is required.

Currently no antibodies specific to PQN-85 and MAU-2 exist and generating antibodies to MAU-2 at least appears to be especially difficult (this study unpublished data and S. Hekimi personal communication). Alternative strategies such as creating strains of *C. elegans* expression PQN-85 fused to a fluorescent protein or a small peptide tag such as polyhistidine or FLAG. Such small peptide tags can be recognised by commercially supplied monoclonal antibodies allowing immunofluorescence detection of the fusion proteins. Unfortunately the *pqn-85* cDNA sequence was only recently created whilst the *pqn-85* genomic sequence is over 14Kb in size which lends certain technical difficulties in cloning, time constrains did not allow the creation of such a strain.

Chapter 5

MAU-2::GFP is a Nuclear Protein Whose Nuclear Localisation is Dependent on PQN-85

5.1 Introduction

In Chapter 3 of this thesis it was shown that *C. elegans pqn-85* and *mau-2* function in chromosome segregation whilst in Chapter 4 it was shown that the PQN-85 and MAU-2 proteins can interact. If *pqn-85* and *mau-2* play a role in cohesin loading then it would be expected that PQN-85 and MAU-2 would be nuclear proteins. The PQN-85 protein sequence demonstrates contains four nuclear localisation signals (NLS), three simple and one bipartite NLS as predicted by NLSdb (http://cubic.bioc.columbia.edu/db/NLSdb). Orthologues of PQN-85 from all organisms studied have been shown to localise to the nucleus (Ciosk et al., 2000, Furuya et al., 1998, Gillespie and Hirano, 2004, Rollins et al., 2004, Takahashi et al., 2004) suggesting that PQN-85 is a nuclear protein. No nuclear localisation signals can be identified using the online prediction programme NLSdb (http://cubic.bioc.columbia.edu/db/NLSdb/) to analyse the MAU-2 protein sequence. As previously mentioned a MAU-2::GFP fusion protein was reported to be cytoplasmic in *C. elegans* [(Benard et al., 2004) and Section 1.2.6]. In Chapter 3 of this thesis it was shown that both *pqn-85* and *mau-2* function in chromosome segregation suggesting that the function of these genes in cohesin loading may be conserved. In order to determine if MAU-2::GFP is found in the nucleus of *C. elegans* we sought to recreate the original *mau-2::GFP* strain (Benard et al., 2004).

The process of transforming *C. elegans* hermaphrodites is a useful method to manufacture stable transgenic *C. elegans* lines. Heritably transformed hermaphrodites can be obtained by microinjecting linear or plasmid DNA sequences with a gene of interest into the cytoplasm of the adult hermaphrodite gonad (Mello et al., 1991, Stinchcomb et al., 1985). Following microinjection, the injected DNA forms a large highly repetitive extra chromosomal array which can be passed from generation to generation (Mello et al., 1991, Stinchcomb et al., 1985). Co-injection of two different DNA sequences in hermaphrodite results in progeny with extra chromosomal arrays containing both injected sequences thus allowing co-injection of a dominant marker gene with a gene of interest (Mello et al., 1991). The size of the extra

chromosomal array varies between progeny from the same injected parent with some animals containing more copies of the injected DNA in extra chromosomal arrays than others (Stinchcomb et al., 1985, Mello et al., 1991). The extra chromosomal arrays display a non-Mendelian inheritance pattern which varies between transformed animals (Stinchcomb et al., 1985, Mello et al., 1991). Analysis of transformed hermaphrodites demonstrates that the extra chromosomal DNA resides in all cells within transformed animals (Stinchcomb et al., 1985). Therefore *C. elegans* transformation by this manner can be used to obtain a stably transformed strain.

The pRF4 plasmid contains 4Kb of the dominant *rol-6(su1006)* collagen gene genomic sequence cloned into pBluescribe (Mello et al., 1991). When present in *C. elegans* the *rol-6(su1006)* collagen gene results in animals with a helically twisted body and cuticle (Kramer et al., 1990). Worms containing the *rol-6(su1006)* gene move in a distinctive circular motion instead of the characteristic sinusoidal motion and have been called 'rolling' worms (Kramer et al., 1990). Transformation of *C. elegans* with the pRF4 plasmid result in heritable progeny with an easily identifiable rolling phenotype (Mello et al., 1991) thus allowing the identification of transformed worms with ease. Introduction of the pRF4 plasmid with a second plasmid carrying a gene of interest means that worms transformed for both genes can be selected for by picking rolling worms (Mello et al., 1991).

In order to create a *mau-2::GFP* strain we obtained the pCB37 construct used to make the original *mau-2::GFP strain.* The pCB37 construct contains the bases 22063-32154 of the CO9H6 cosmid (GenBank accession number Z81466.1) corresponding to the *mau-2* genomic sequence from the initiating ATG up to but excluding the stop codon and 6Kb of the regulatory sequence upstream of the *mau-2* start site, the *mau-2* genomic sequence was cloned in frame to the *gfp* sequence in the plasmid pPD95.77 (Benard et al., 2004). Transformation of the pCB37 construct (Figure 5.1) into *C. elegans qm4* and *qm160 mau-2* mutant hermaphrodites (Section 1.2.6) results in production of a MAU-2::GFP fusion protein which is capable of rescuing all mutant phenotypes observed in the in these strains (Benard et al., 2004)

5.2 Materials and Methods

5.2.1 Creation of Transgenic C. elegans

The pRF4 [section 5.1 (Mello et al., 1991)] and pCB37 [Section 5.1, Figure 5.1 and (Benard et al., 2004)] plasmids were purified (see Section 2.2.8) and mixed in a fresh microcentrifuge to a final concentration of 100µg/ml (pRF4) and 25µg/ml (pCB37) diluted with dH_2O. The plasmid mixture was microinjected into young adult hermaphrodites (see Section 2.4.11) and injected worms were recovered and allowed to self-fertilise on fresh NGM plates (Section 2.4.4) at 20°C. The injected hermaphrodites were transferred to fresh NGM plates every 24 hours and the eggs (F1 progeny) lain on each plate were incubated at 20°C to allow F1 progeny to hatch. The injected hermaphrodites were discarded after 96 hours. The F1 progeny from injected hermaphrodites that displayed a circular pattern of movement were individually transferred to fresh NGM plates, incubated at 20°C for sufficient time to allow them self-fertilise and lay eggs (F2 progeny). The plates containing F2 progeny showing a similar circular movement were considered to contain stably transformed *C. elegans* and were subsequently maintained for analysis of GFP expression.

5.2.2 Maintenance of C. elegans mau-2::GFP Hermaphrodites

To maintain *mau-2::GFP* hermaphrodite lines, ten rolling worms were transferred to fresh NGM plates every week and were maintained as per Section 2.4.5.

5.2.3 Analysis of MAU-2::GFP Localisation

To analyse the localisation of MAU-2::GFP, embryos were removed from adult hermaphrodite rolling worms (Section 2.4.13) and were mounted on fresh agarose pads (Section 2.4.15). The mounted embryos were analysed by microscopy (Section 2.4.16).

5.2.4 PCR Amplification of the mau-2 Genomic Sequence

Genomic DNA was extracted from a mixed age population of *C. elegans* (see Section 2.4.6). The extracted genomic DNA was used as template to amplify a small region of the *mau-2* genomic sequence by PCR using Taq polymerase (Promega and see Section 2.2.3). The PCR primers used were Mau-2 forward with Mau-2 reverse and the sequences are detailed in Table 2.1 and the PCR reaction conditions used are detailed in Table 2.2. The PCR products were size fractionated by agarose gel electrophoresis (see Section 2.2.4).

5.2.5 RT-PCR of pqn-85 and ama-1

Total RNA was extracted from 50 adult *C. elegans* hermaphrodites using the QIAGEN RNeasy mini RNA extraction kit as per manufacturers' instructions. To make first strand cDNA the total RNA extracted from adult worms was used as a template in a reverse transcription reaction (see Section 2.2.2). A small fragment of the *ama-1* and *pqn-85* cDNA sequences was amplified by duplex PCR (two PCR reactions within the same tube) using Taq polymerase (Promega and see Section 2.2.3). The PCR primers used were pqn-85 RT-PCR forward with pqn-85 RT-PCR reverse (*pqn-85*) and ama-1 RT-PCR forward with ama-1 RT-PCR reverse (*ama-1*). The sequences of the primers are detailed in the Table 5.1 and the PCR reaction conditions used are detailed in Table 5.2. The PCR products were size fractionated by agarose gel electrophoresis (see Section 2.2.4).

Table 5.1 Sequence of Primers used in RT-PCR of *pqn-85* and *ama-1*

The *ama-1* mRNA sequence used for reference was GenBank sequence number NM_068122.4. The *pqn-85* mRNA sequence used for reference was GenBank sequence number NM_061286.2.

Primer name	Primer sequence (5'-3')	Position of 5' base within mRNA
pqn-85 RT-PCR forward	GCTTGACGCAGTTGTCAAAA	3447
pqn-85 RT-PCR reverse	GCACTTTCAAGGTCCTCAGC	3674
ama-1 RT-PCR forward	TGTCTCACGCGTTCAGTTTG	41
ama-1 RT-PCR reverse	AATTTCCAGCACTCGAGGAG	372

Table 5.2 PCR Cycling Conditions for RT-PCR Reactions Using Primers in Table 5.1

Step	Temperature °C	Time	Number of Cycles
Initial Denaturation	94	10 minutes	1
Denaturation	94	30 seconds	
Annealing	60	30 seconds	24, 27 or 30
Extension	72	20 seconds	
Final Extension	72	10 minutes	1

5.3 Results

5.3.1 pCB37 – mau-2::GFP Construct

To examine the sub-cellular localisation of MAU-2 we obtained the pCB37 construct that was used to make the original *mau-2::gfp* strain [Section 5.1, Figure 5.1 and (Benard et al., 2004)]. In order to confirm that the pCB37 construct was correct, six individual restriction digests were carried out on purified pCB37 using *Bam*HI, *Pst*I, *Sac*I, *Sma*I and *Xho*I and one negative control reaction that contained no restriction enzymes. The restriction map of the construct (Figure 5.1) demonstrates that *Bam*HI, *Sma*I and *Xho*I all cut pCB37 once linearising the construct. *Pst*I and *Sac*I cut the construct two and four times respectively producing bands of ~11.5kb and 3kb (*Pst*I digest) and ~13Kb, ~1.6Kb, 200bp and 100bp (*Sac*I digest). The restriction digests were size fractionated by agarose gel electrophoresis, the *Bam*HI, *Pst*I, *Sma*I and *Xho*I restriction digests produced bands running as expected for a linear DNA molecule and different from uncut pCB37 (Figure 5.2A). The *Sac*I digest produced the expected bands at 1.6Kb and a larger band (too large to accurately size on gel of this type) but the smaller bands at 100bp and 200bp were not visible (Figure 5.2A). Due to the small size of these fragments in relation to the pCB37 construct they would not make up a large part of the overall quantity of DNA. As a result, agarose gel electrophoresis may not be sensitive enough to visualise these small bands.

To further confirm the authenticity of the pCB37 construct two PCR assays were carried out using the PCR primers Mau-2 forward with Mau-2 reverse. The first PCR used the pCB37 construct as a template and the second PCR used *C. elegans* genomic DNA as a template. The PCR products were size fractionated by agarose gel electrophoresis and the products of both reactions were found to be of the expected size of 937bp (Figure 5.2B) confirming the presence of the *mau-2* genomic sequence in the pCB37 construct. These results suggest that the pCB37 construct was a faithful copy of the original pCB37 clone (Benard et al., 2004) and was suitable for use in creating the *mau-2::gfp* transgenic line.

5.3.2 Creating the mau-2::GFP Strain

To create the *C. elegans mau-2::gfp* strain a mixture of purified pCB37 construct and pRF4 construct was injected into the gonad of young adult N2 hermaphrodites. Adult worms expressing the dominant *rol-6(su1006)* marker move in a rolling circular motion (Section 5.1) and are easily distinguishable from their non transformed counterparts. The injected worms

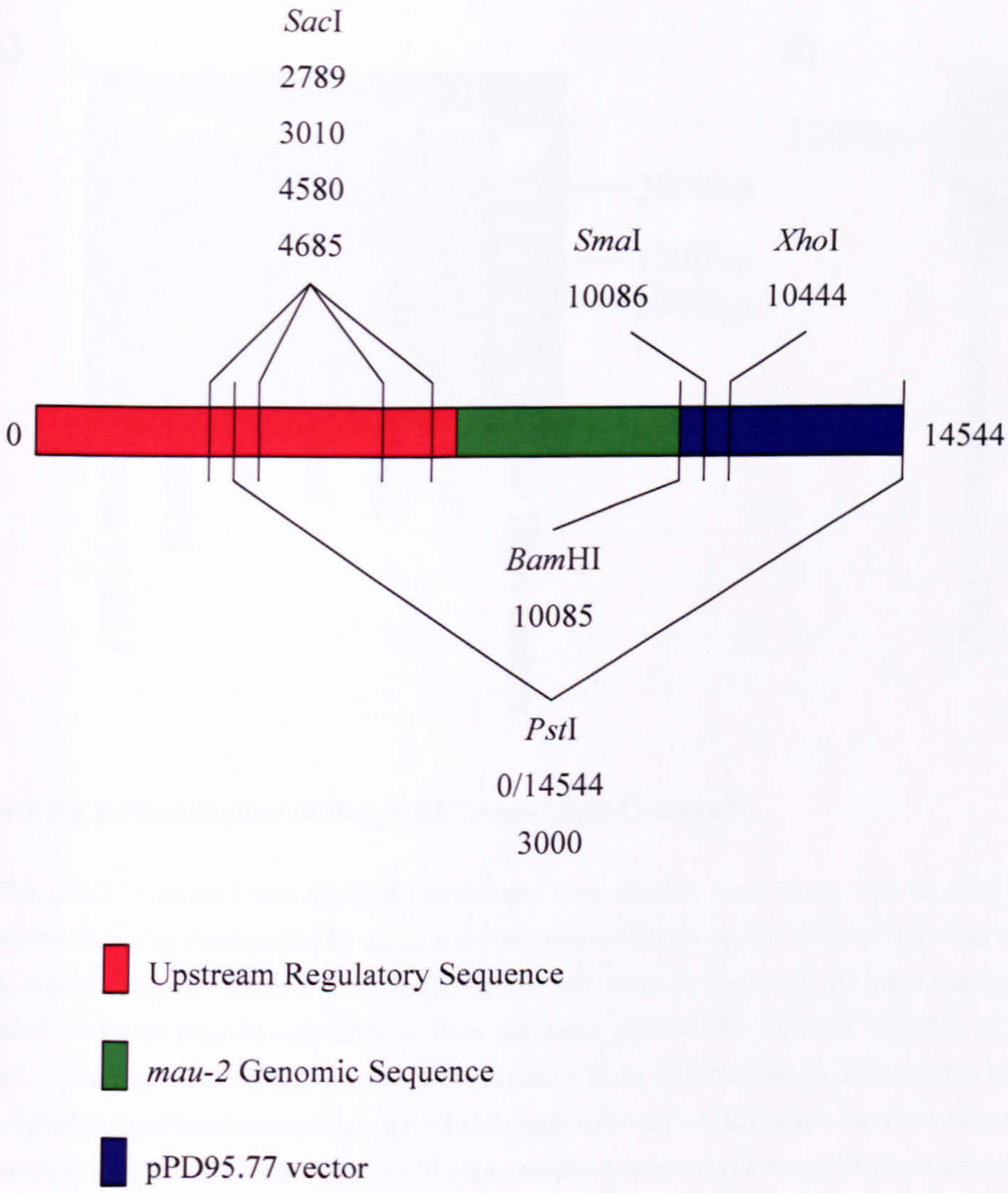

Figure 5.1 Schematic of the pCB37 *mau-2::gfp* Construct

Restriction map of the pCB37 plasmid [(Benard et al., 2004) and Section 5.1], the schematic shows a linearised plasmid such that the *Pst*I site at 0 and 14544 is the same site. The position of the various restriction sites within the plasmid are shown.

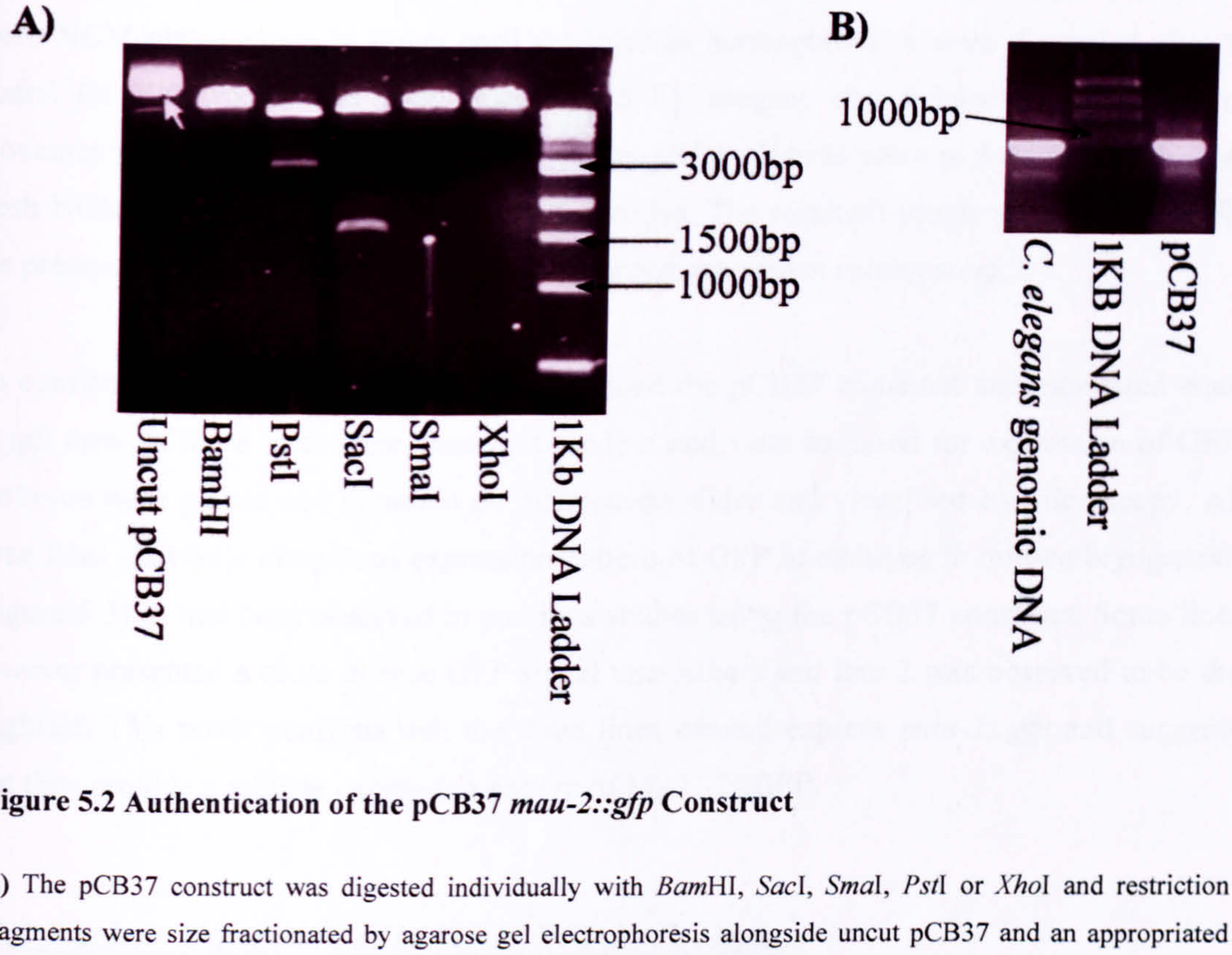

Figure 5.2 Authentication of the pCB37 *mau-2::gfp* Construct

A) The pCB37 construct was digested individually with *Bam*HI, *Sac*I, *Sma*I, *Pst*I or *Xho*I and restriction fragments were size fractionated by agarose gel electrophoresis alongside uncut pCB37 and an appropriated DNA marker. Plasmid digested with *Bam*HI, *Sma*I, and *Xho*I all produced one band running at a position expected for linear plasmid and different from the uncut plasmid. As expected digesting pCB37 with *Pst*I produced two bands, a very large upper band (expected to be ~11.5Kb) and a smaller 3Kb lower band. The *Sac*I digest also produced a very large upper band (expected to be ~13Kb) and a band at 1.6Kb as expected but the smaller bands at 100bp and 200bp could not be resolved because of limited Ethidium Bromide binding. **B)** To confirm the presence of the *mau-2* genomic sequence within pCB37 a 937bp of *mau-2* was amplified by PCR using primers specific to the *mau-2* genomic sequence. Two separate PCR assays were carried out using either *C. elegans* genomic DNA or purified pCB37 plasmid as template. The PCR products were size fractionated by agarose gel electrophoresis alongside a DNA marker of the appropriate size. In both cases band of the expected size (937bp) were observed.

were recovered on fresh NGM plates and allowed to self fertilise before being transferred to fresh NGM plates every 24 hours until the injected hermaphrodites were discarded after 96 hours. Of 120 worms that were injected, 15 F1 progeny that demonstrated the rolling movement in accodance with expression of the pRF4 plasmid were picked separately onto fresh NGM plates and were allowed to self-fertilise. The resultant progeny were assayed for the presence of rollers and 8 of the 15 lines returned permanent rolling stock.

To confirm that the transformed worms contained the pCB37 construct and expressed *mau-2::gfp* three of the 8 lines were chosen at random and were assessed for expression of GFP. Embryos were picked and mounted on microscope slides and visualised by microscopy. All three lines showed a ubiquitous expression pattern of GFP in embryos in mid-embryogenesis (Figure 5.3) as had been observed in previous studies using the pCB37 construct. Some lines however presented a more intense GFP signal than others and line 2 was observed to be the brightest. This result confirms that the three lines created express *mau-2::gfp* and suggests that they provide a reliable expression pattern of MAU-2::GFP.

5.3.3 Nuclear Expression of MAU-2::GFP in C. elegans

Previous studies had suggested that MAU-2::GFP expression in the *C. elegans* embryo could be first detected from late gastrulation whereupon expression became ubiquitous by mid embryogenesis (Benard et al., 2004). To further analyse the expression pattern of MAU-2::GFP, *mau-2::gfp* line 2 which showed the brightest GFP signal was chosen for further study. Embryos were dissected from rolling worms, mounted on microscope slides and were visualised by DIC and GFP imaging. In accordance with previous results, GFP expression becomes apparent in a small subset of cells at late gastrulation. However, expression was predominantly observed in the nucleus although a low level of GFP signal in the cytoplasm could be seen (Figure 5.4). This may represent the first zygotic transcription of *mau-2* and is probably not indicative of a lack of requirement for MAU-2 in early development. As development progresses the number of cells expressing MAU-2::GFP increases until all cells contain GFP in the nucleus (Figure 5.4). This evidence confirms the cytoplasmic expression observed in previous studies but goes further to show that MAU-2::GFP is found in all nuclei of developing *C. elegans* embryos.

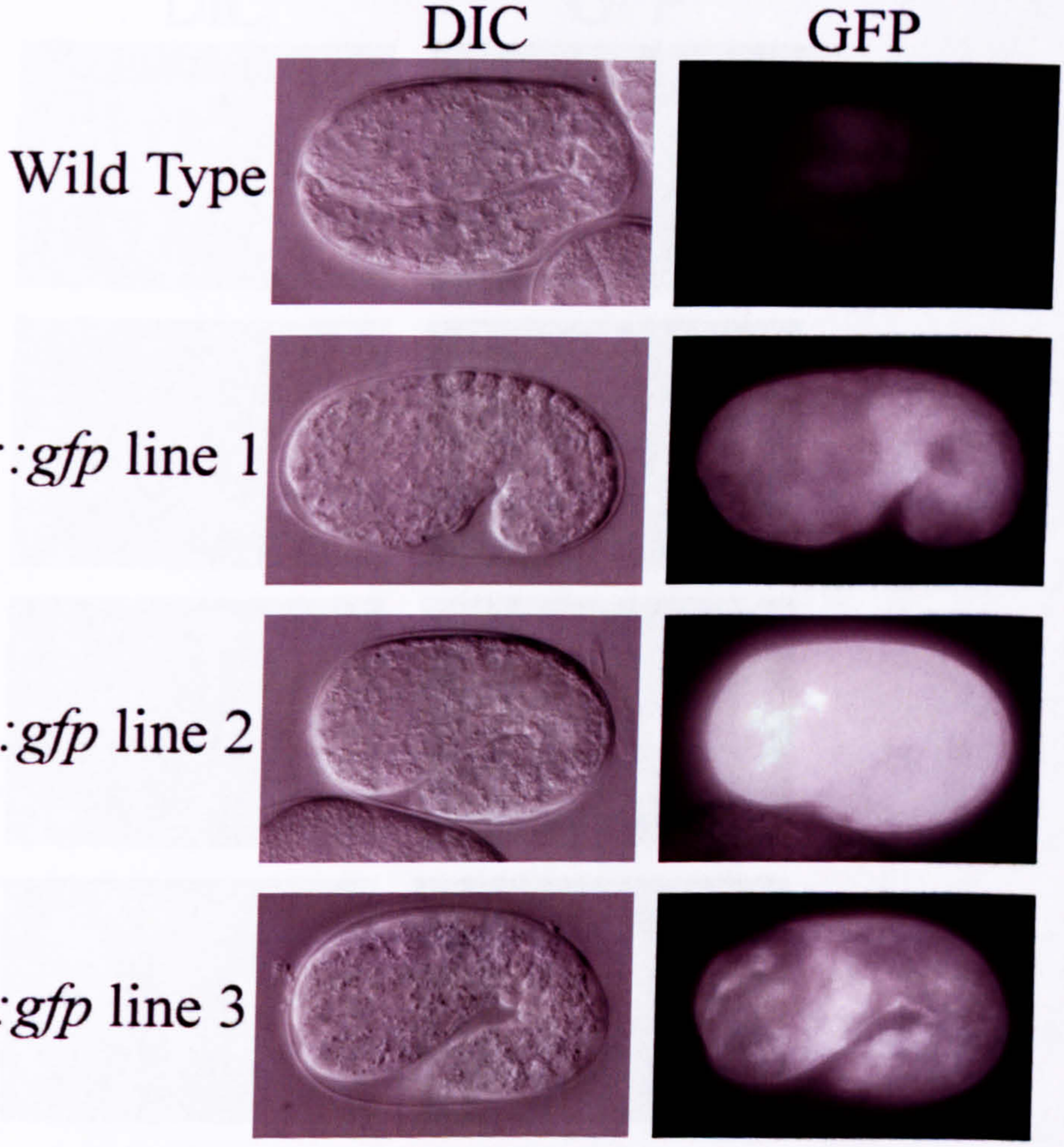

Figure 5.3 MAU-2::GFP is Ubiquitously Expressed in Mid-embryogenesis in all *C. elegans* Lines

Following injection of young adult wild type N2 *C. elegans* with a mixture of the pCB37 and pRF4, rolling F1 hermaphrodite progeny were picked and allowed to self-fertilise. Of the 8 permanent rolling lines three were chosen at random and were analysed for expression of MAU-2::GFP at mid embryogenesis. All three lines showed ubiquitous expression of MAU-2::GFP when compared to wild type which showed no GFP expression. It was also observed that expression of MAU-2::GFP was at a greater level in line 2.

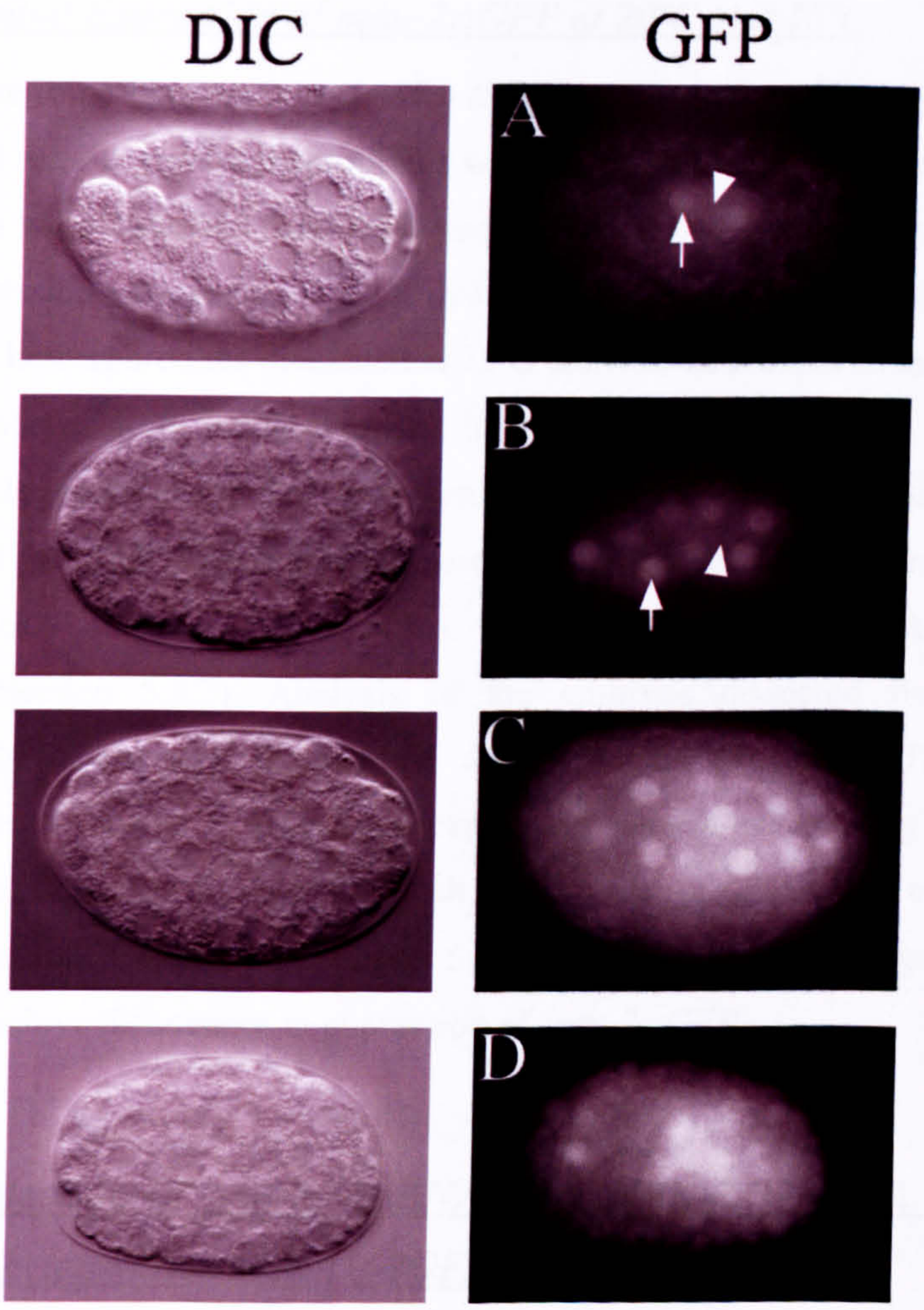

Figure 5.4 MAU-2::GFP is Located in the Nucleus in *C. elegans* Embryos

MAU-2::GFP is first expressed shortly after gastrulation where it is mainly found in the nucleus of a small number of cells (Panel A and B white arrows) although a faint cytoplasmic expression is also be observed (Panel A and B white arrow heads). As the embryo develops MAU-2 expression is found in more and more cells (Panel C) until all cells are found to contain nuclei with a GFP signal (Panel D).

5.3.4 Differential Expression of mau-2::GFP at 20°C and 15°C

In order to determine temperature-specific differences in expression levels of MAU-2::GFP 10 young adult *mau-2::gfp* hermaphrodites were incubated on fresh NMG plates at 20°C and 15°C. Embryos were dissected from adult hermaphrodites 48hrs after incubation was initiated and GFP expression was analysed by microscopy. Of 29 embryos analysed, 37% of those dissected from hermaphrodites incubated at 15°C showed GFP expression and this figure rose to 62% for embryos from hermaphrodites incubated at 20°C (from 37 embryos analysed). Analysis of embryos dissected from hermaphrodites incubated at 15°C that did demonstrate a GFP signal (11 in total) 5 showed clear nuclear expression whilst 6 embryos that were in midembryogenesis showed a ubiquitous expression pattern consistent with previous observations (Section 5.3.2). Analysis of the embryos dissected from hermaphrodites incubated at 20°C that did demonstrate a GFP signal (26 in total) 13 that were in midembryogenesis showed a ubiquitous expression pattern whilst only 1 showed nuclear expression. The remaining 8 showed a much higher level of GFP in the cytoplasm than seen in embryos incubated at 15°C (Section 5.3.3 and 5.3.4). This suggests that there are temperature-sensitive differences in expression of *mau-2::GFP*.

5.3.5 Microinjection of pqn-85 dsRNA into MAU-2::GFP C. elegans Causes Cytoplasmic Accumulation of MAU-2GFP

Having established that MAU-2::GFP is a nuclear protein it was unclear how it was translocated into the nucleus. Standard bioinformatic analysis of the MAU-2 protein sequence does not demonstrate any NLS consensus sequences (Section 5.1). An obvious way for MAU-2 to enter the nucleus would be bound to PQN-85 which contains several candidate NLS consensus sequences (Figure 1.5 and Section 1.1.7) and which is expected to be found in the nucleus. To analyse the effect of *pqn-85* on the localisation of MAU-2::GFP, RNAi was conducted on *mau-2::GFP* line 2 hermaphrodites. Young adult roller worms were injected with *pqn-85* dsRNA (Section 3.3.1) and recovered on fresh NGM plates at 15°C. To assess the effect of depleting *pqn-85* on embryo mortality the injected worms were transferred to fresh plates every day and the number of progeny hatching from each plate was counted. As observed in section 3.3.4 no embryos hatched that were laid 48hrs after injection of *pqn-85* dsRNA, confirming the effectiveness of the RNAi.

To analyse the localisation of MAU-2::GFP, embryos were dissected from the injected hermaphrodite 48hrs after injection and were mounted on microscope slides. The embryo

stage and localisation of MAU-2::GFP was visualised by DIC and GFP imaging. As in section 5.3.3 clear nuclear expression of MAU-2::GFP could be observed (Figure 5.5) however following injection of the *pqn-85* dsRNA no nuclear expression was observed, whilst extensive cytoplasmic expression was observed. This suggests that whilst expression of MAU-2::GFP is relatively unaffected its localisation is affected and it is no longer translocated into the nucleus. This suggests that *pqn-85* is involved in translocating MAU-2 in the nucleus, providing further evidence of the formation of a PQN-85 MAU-2 complex.

5.3.6 Confirmation of pqn-85 and mau-2 Knockdown

To confirm that the knockdown of the *pqn-85* transcript by RNAi was successful semi quantitative RT-PCR was carried out on worms depleted of *pqn-85*. 50 young adult *histone::gfp C. elegans* hermaphrodites were injected with *pqn-85* dsRNA and were allowed to recover on NGM plates. Total RNA was extracted from the worms 48 hrs after injection of the *pqn-85* dsRNA and separately from 50 uninjected *histone::gfp* worms. The total RNA from uninjected worms and those worms injected with dsRNA was used in separate oligo-dT primed RT-PCR reactions to produce two first strand cDNA populations. This first strand cDNA was used as a template to amplify a small segment of the *pqn-85* cDNA and a small segment of the *ama-1* cDNA (331bp) in six duplex PCRs. The *ama-1* gene of *C. elegans* encodes the large subunit of RNA polymerase II required for mRNA transcription and has been used in similar experiments in previous studies of this nature (Pocock et al., 2004). Three reactions used the first strand cDNA made from RNA extracted from uninjected controls as template whilst three reactions used first strand cDNA made from RNA extracted from worms injected with *pqn-85* dsRNA. To confirm that any major difference observed in the PCR was not due to PCR specific defects, the three PCRs containing each template DNA were cycled either 24, 27 or 30 times. The PCR products were size fractionated by agarose gel electrophoresis and bands of the expected size (228bp for *pqn-85* and 331bp for *ama-1*) were observed (Figure 5.6). At all numbers of cycles the level of *pqn-85* transcript in worms injected with *pqn-85* dsRNA is reduced when compared to the uninjected control worms whilst the level of *ama-1* remains similar for both at all cycle numbers (Figure 5.6). This confirms that the RNAi against *pqn-85* was successful.

To analyse the effectiveness of the *mau-2* RNAi young adult *mau-2::gfp C. elegans* were injected with *mau-2* dsRNA and the worms recovered at 20°C on fresh NGM plates. To analyse GFP expression the injected worms were dissected 48hrs after injection of the

dsRNA, the embryos were mounted on microscope slides and viewed by microscopy. Only 6% of embryos (of 49 embryos studied) showed GFP expression whereas 62% of embryos showed GFP expression previously at 20°C (section 5.3.4). This suggests that the depletion of *mau-2* by RNAi was successful.

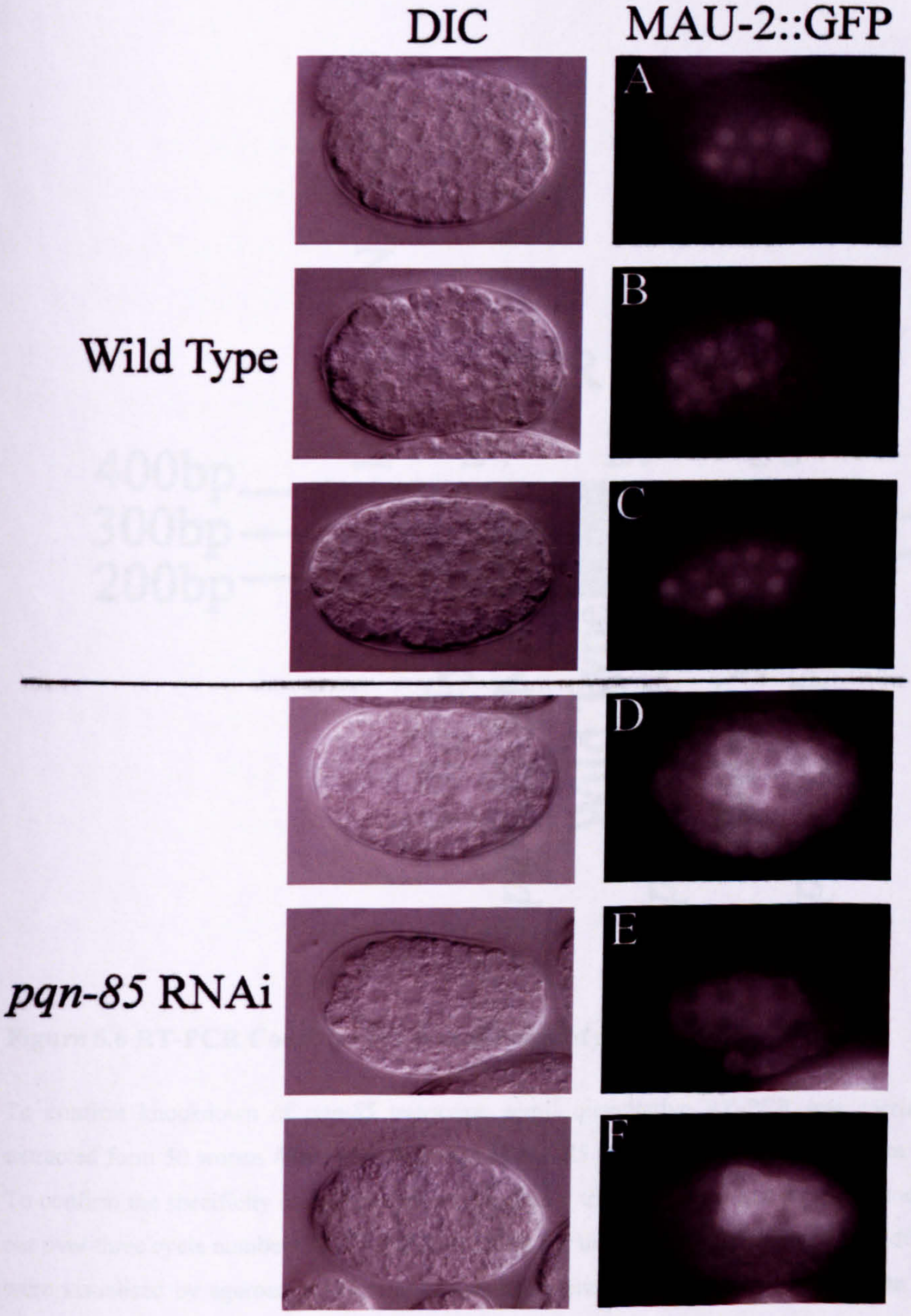

Figure 5.5 MAU-2::GFP is Predominantly Located in the Cytoplasm When *pqn-85* has been Depleted

Nuclear expression of MAU-2::GFP as observed in wild type embryos after gastrulation of developing *C. elegans* (panels A, B and C) becomes predominantly cytoplasmic following depletion of *pqn-85* by RNAi (panels D,E and F). The experiment was carried out at 15°C to allow nuclear localisation of MAU-2::GFP to be observed.

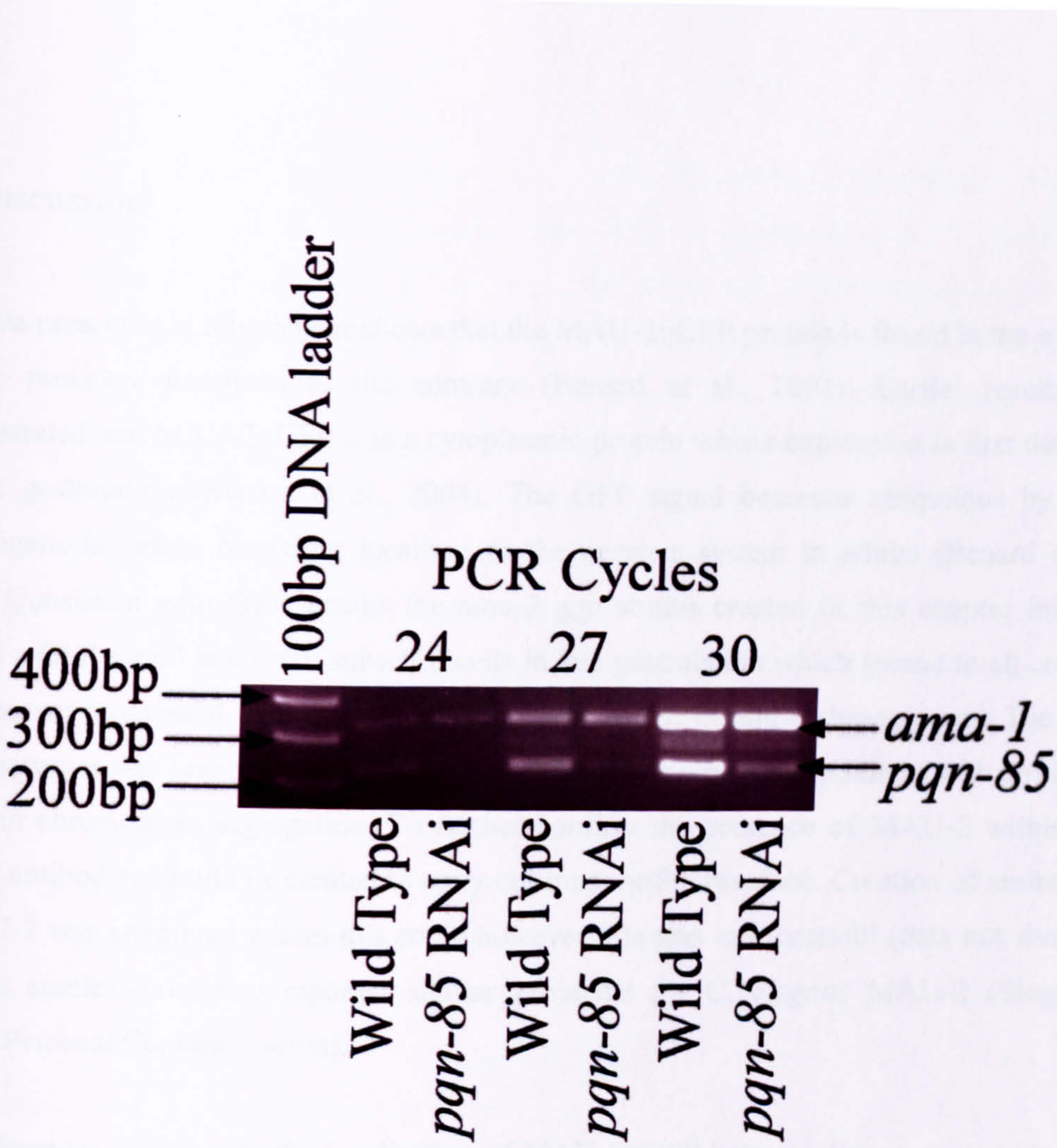

Figure 5.6 RT-PCR Confirms the Knockdown of *pqn-85*

To confirm knockdown of *pqn-85* transcript, semi- quantitative RT-PCR was carried out on total RNA extracted form 50 worms 48hrs after injection of pqn-85 and total RNA extracted from 50 uninjected worms. To confirm the specificity of the knockdown the *ama-1* transcript was used a control and the PCR was carried out over three cycle numbers 24, 27 and 30 to check for the exponential increase in product. The PCR products were visualised by agarose gel electrophoresis and were run alongside an appropriate DNA size marker. A knockdown in *pqn-85* can clearly be seen.

5.4 Discussion

The data presented in this chapter shows that the MAU-2::GFP protein is found in the nucleus despite previous assertions to the contrary (Benard et al., 2004). Earlier results had demonstrated that MAU-2::GFP was a cytoplasmic protein whose expression is first detected by late gastrulation (Benard et al., 2004). The GFP signal becomes ubiquitous by mid-embryogenesis before becoming localised to the nervous system in adults (Benard et al., 2004). Consistent with these results the *mau-2::gfp* strains created in this chapter initially showed a GFP signal in a small subset of cells in late gastrulation which spread to all cells as development progressed to a ubiquitous expression pattern in mid-embryogenesis. The GFP signal however was predominantly observed in the nucleus which is consistent with a role for *mau-2* in chromosome segregation. To further confirm the presence of MAU-2 within the nucleus antibodies should be created to carry out immunofluorescence. Creation of antibodies to MAU-2 was attempted within this study however this was unsuccessful (data not shown), previous studies have also reported similar problems for *C. elegans* MAU-2 (Siegfried Hekimi Personal Communication).

The differences observed in the localisation of MAU-2::GFP between the present study and the report by Benard et al (2004) could be due to temperature sensitivity of the construct. Here it has been shown that at 20°C the majority of embryos express MAU-2::GFP whereas at 15°C the majority of embryos do not express MAU-2::GFP. The embryos that had been incubated at 15°C showed clear evidence of nuclear expression although a low level of cytoplasmic GFP was also observed. Whilst embryos incubated at 20°C however showed nuclear expression, the level of cytoplasmic GFP was greatly increased and the nuclear expression was more difficult to identify than in embryos incubated at 15°C. This suggests that an increase in the temperature cause enhanced cytoplasm GFP signal and as a result may mask the nuclear localisation of MAU-2::GFP. Further experiments are required to confirm the altered expression levels of the *mau-2::GFP* construct including Western (using antibodies recognising GFP) and Northern blots to compare the level of MAU-2::GFP protein and *mau-2::GFP* mRNA respectively in worms incubated at 15°C and 20°C.

The initial observation of MAU-2::GFP at late gastrulation may represent the first zygotic transcription of *mau-2::gfp* and does not indicate that MAU-2 is not required in early embryos. A maternal contribution of MAU-2 is required for wild type development and is

present in high level in zygotes (Benard et al., 2004). Expression of the highly repetitive arrays that are formed when extra chromosomal DNA is introduced into *C. elegans* are silenced in the *C. elegans* germline (Kelly et al., 1997). In such strains expression of extra chromosomal DNA can be observed in the germline in initial generations after transformation but is progressively lost in the following generations until no germline expression of extra chromosomal DNA is observed (Kelly et al., 1997). The *mau-2::GFP* embryos within this thesis are not thought to contain a maternal contribution of MAU-2::GFP, therefore the expression of *mau-2::GFP* observed in late gastrulation likely represents the initial zygotic transcription of the *mau-2* gene. To further confirm the subcellular localisation of MAU-2::GFP within embryos that have not undergone gastrulation two principle mechanisms could be employed; first a strain of *C. elegans* expressing an integrated *mau-2::GFP* construct should be created. Bombardment of *C. elegans* with gold microparticles coated in DNA allows stable integration of the DNA coating the gold particles within the *C. elegans* genome allowing stable transgenics to be created (Praitis et al., 2001). Second, coinjection of the transgenic plasmids with restriction digested genomic DNA rescues expression of the extra chromosomal arrays within the germline (Kelly et al., 1997). It is thought that the genomic DNA reduces the repetitive nature of the extra chromosomal such that its expression is no longer silenced within the germline (Kelly et al., 1997).

Although no data is presented that PQN-85 is a nuclear protein it is likely to be found in the nucleus. Orthologues of PQN-85 in *Drosophila*, *S. cerevisiae* and *Xenopus* studied to date have been found in the nucleus (Ciosk et al., 2000, Gillespie and Hirano, 2004, Rollins et al., 2004, Takahashi et al., 2004) and the PQN-85 sequence contains four candidate nuclear localisation signals (NLS) as predicted by the online prediction programme NLSdb (http://cubic.bioc.columbia.edu/db/NLSdb/) (Section 5.1). Depletion of *pqn-85* by RNAi affects the sub-cellular localisation of MAU-2::GFP causing it to accumulate in the cytoplasm suggesting that PQN-85 plays a role in locating MAU-2::GFP to the nucleus. Given that the *mau-2* sequence contains no NLS it is easy to envisage that MAU-2::GFP would enter the nucleus bound to PQN-85. To further confirm that PQN-85 is found in the nucleus several experiments should be conducted. Firstly antibodies against the PQN-85 protein must be created; previous attempts at this have been unsuccessful in this study (data not shown). Second a transgenic *C. elegans* line expressing PQN-85 fused to a fluorescent protein (preferably an alternative colour to the green MAU-2::GFP to allow colocalisation studies) should be created. Unfortunately the *pqn-85* cDNA sequence was only recently created whilst

the *pqn-85* genomic sequence is over 14Kb in size which lends certain technical difficulties in cloning, time constrains did not allow the creation of such a strain.

Chapter 6

Discussion

The aim of this thesis was to establish a connection between the *C. elegans pqn-85* and *mau-2* genes providing evidence for the conservation of the cohesin loading complex in metazoans. The identification of a conserved cohesin loading complex in multicellular organisms would have potential implications in the pathogenesis of the human disease Cornelia de Lange Syndrome. This was accomplished in several ways. In Chapter 3 evidence is presented for the function of *mau-2* and *pqn-85* in mitotic chromosome segregation. In Chapter 4 evidence is presented that MAU-2 and PQN-85 interact with each other suggesting that they are capable of forming a complex. Finally in Chapter 5 evidence is presented that MAU-2::GFP is found in the nucleus and its nuclear localisation is dependent on PQN-85 suggesting that they also form a complex in vivo.

6.1 The Cohesin Loading Complex is Conserved Throughout Eukaryotic Evolution

The chromosome segregation defects observed in the RNAi experiments (Chapter 3) do not provide direct evidence that *pqn-85* and *mau-2* function in cohesin loading. However, corroborating evidence from other organisms suggest that it is likely that they do. Orthologues of *pqn-85* from a range of organisms have been previously shown to function in sister chromatid cohesion (Ciosk et al., 2000, Furuya et al., 1998, Gillespie and Hirano, 2004, Michaelis et al., 1997, Kaur et al., 2005) and more specifically in cohesin loading (Ciosk et al., 2000, Gillespie and Hirano, 2004, Takahashi et al., 2004, Seitan et al., 2006, Watrin et al., 2006). Several papers have now been published identifying *mau-2* orthologues in *S. pombe* as *ssl3* (Bernard et al., 2006), *Drosophila* as *CG4203* (Seitan et al., 2006) and humans as *KIAA0892* (Seitan et al., 2006, Watrin et al., 2006). These reports have also demonstrated that the cohesin loading function of *mau-2* orthologues is conserved in *S. cerevisiae*, *S. pombe* and humans (Bernard et al., 2006, Seitan et al., 2006, Watrin et al., 2006). This would suggest that the chromosome segregation defects observed in Chapter 3 of this thesis are likely the result of cohesin loading defects.

It seems likely that *pqn-85* and *mau-2* encode members of a *C. elegans* cohesin loading complex. Data presented in Chapter 4 of this thesis demonstrates that MAU-2 is capable of interacting with the N-terminus of PQN-85. Further evidence that the cohesin loading

complex is conserved amongst eukaryotes comes from observations that orthologues of the PQN-85 and MAU-2 proteins interact in several organisms. Previously the *S. cerevisiae* and Drosophila orthologues of PQN-85 and MAU-2 had been shown to interact with one another (Ciosk et al., 2000, Giot et al., 2003). More recently it has been shown that orthologues of PQN-85 in humans, *Xenopus* and *S. pombe* interact with their respective MAU-2 orthologues identified in each organism (Seitan et al., 2006, Watrin et al., 2006, Bernard et al., 2006). This suggests that the cohesin loading complex has been conserved throughout eukaryotic evolution.

If *mau-2* and its orthologues function in loading cohesin then it would be expected that they should be found in the nucleus. It has previously been reported that both *C. elegans* MAU-2 and its human orthologue hMAU-2 are cytoplasmic proteins (Benard et al., 2004). Data presented in Chapter 5 of this thesis however, demonstrates that a MAU-2::GFP fusion protein is found in the nucleus. Corroborating evidence that MAU-2 and its orthologues are found in the nucleus comes from recent reports demonstrating that endogenous hMAU-2 localises to the nucleus and binds to chromatin (Seitan et al., 2006, Watrin et al., 2006). A possible explanation for the difference observed in *C. elegans* MAU-2::GFP localisation between data presented in this thesis and that in previous reports (Benard et al., 2004) is presented in Section 5.4.

The PQN-85 protein is required for the nuclear localisation of the MAU-2 protein. Depletion of *pqn-85* from *C. elegans* embryos expressing *mau-2::GFP* by RNAi results in cytoplasmic accumulation of MAU-2::GFP. Similarly when the expression of the human orthologue of *pqn-85* (called *NIPBL*) is silenced in HeLa cells using small interfering RNAs (siRNA), hMAU-2 no longer localised to the chromatin (Watrin et al., 2006). It should be noted however due to methods used in visualising the hMAU-2 protein binding to chromatin, the accumulation of hMAU-2 in the cytoplasm of HeLa cells could not be observed.

The mechanism by which PQN-85 affects the localisation of MAU-2 could either be direct by keeping MAU-2 and hMAU-2 in the nucleus after their translocation into the nucleus by other means (Figure 6.1A) or by chaperoning MAU-2 and hMAU-2 into the nucleus (Figure 6.1B), or indirect by altering the function of proteins that are involved in the localisation of MAU-2 and hMAU-2 (Figure 6.1C). Neither the direct nor indirect manner of MAU-2 localisation can be excluded as the sub-cellular localisation in which PQN-85 and MAU-2 first interact is not known. Further analysis to determine the manner in which PQN-85 and MAU-2 interact in

vivo is required perhaps by immunofluorescent localisation studies of the sub-cellular localisation of these proteins throughout the cell cycle.

6.2 The PQN-85 Interaction Domain

The N-terminus of PQN-85 and its human orthologue delangin appears to be important in binding MAU-2 and hMAU-2 respectively. The results detailed in Chapter 4 of this thesis show that only the first 450 amino acids of PQN-85 are required for its interaction with MAU-2. Yeast two-hybrid studies demonstrated that the first 139 amino acids of delangin are required to bind hMAU-2 (Seitan et al., 2006). However, further yeast two-hybrid analysis of PQN-85 in Chapter 4 demonstrated that the first 210 amino acids of PQN-85 are not sufficient for the interaction with MAU-2 to occur. PQN-85 contains runs of polyglutamine repeats up to ~200 amino acids into the protein sequence. Of the 164 glutamine residues found in the PQN-85 protein 67 are found in the first 210 amino acids representing over 40% of the total. No such clustering of glutamines can be found by rudimentary analysis of the delangin sequence. It seems unlikely therefore that the first 210 amino acids of PQN-85 are required for the interaction with MAU-2.

To further analyse the region of PQN-85 that is required for its interaction with MAU-2 in *C. elegans* the first 450 amino acids of PQN-85 was aligned with the first 139 amino acids of delangin that had been shown to be required for its interaction with hMAU-2 (Seitan et al., 2006) using the ClustalW program (http://www.ebi.ac.uk/Tools/clustalw/index.html and Figure 6.2). As observed in Figure 6.2 the first 139 amino acids of delangin show extensive alignment with a section of PQN-85 spanning amino acids 283 to 445. This further suggests that the first 210 amino acids of PQN-85 are not required for the interaction with MAU-2 and that the section of PQN-85 bounded by the amino acids 283 to 450 may only be required for the interaction to occur.

6.3 Sequence Divergence of PQN-85 and MAU-2

Despite the overall sequence conservation observed amongst PQN-85 and its orthologues, conservation is restricted largely to the C-terminal end of the proteins (Strachan, 2005). PQN-85 and its orthologues from other organisms have extended N-terminal sequences relative to yeast ancestors (Section 1.1.7 and Figure 1.3). On the whole this region is poorly conserved throughout

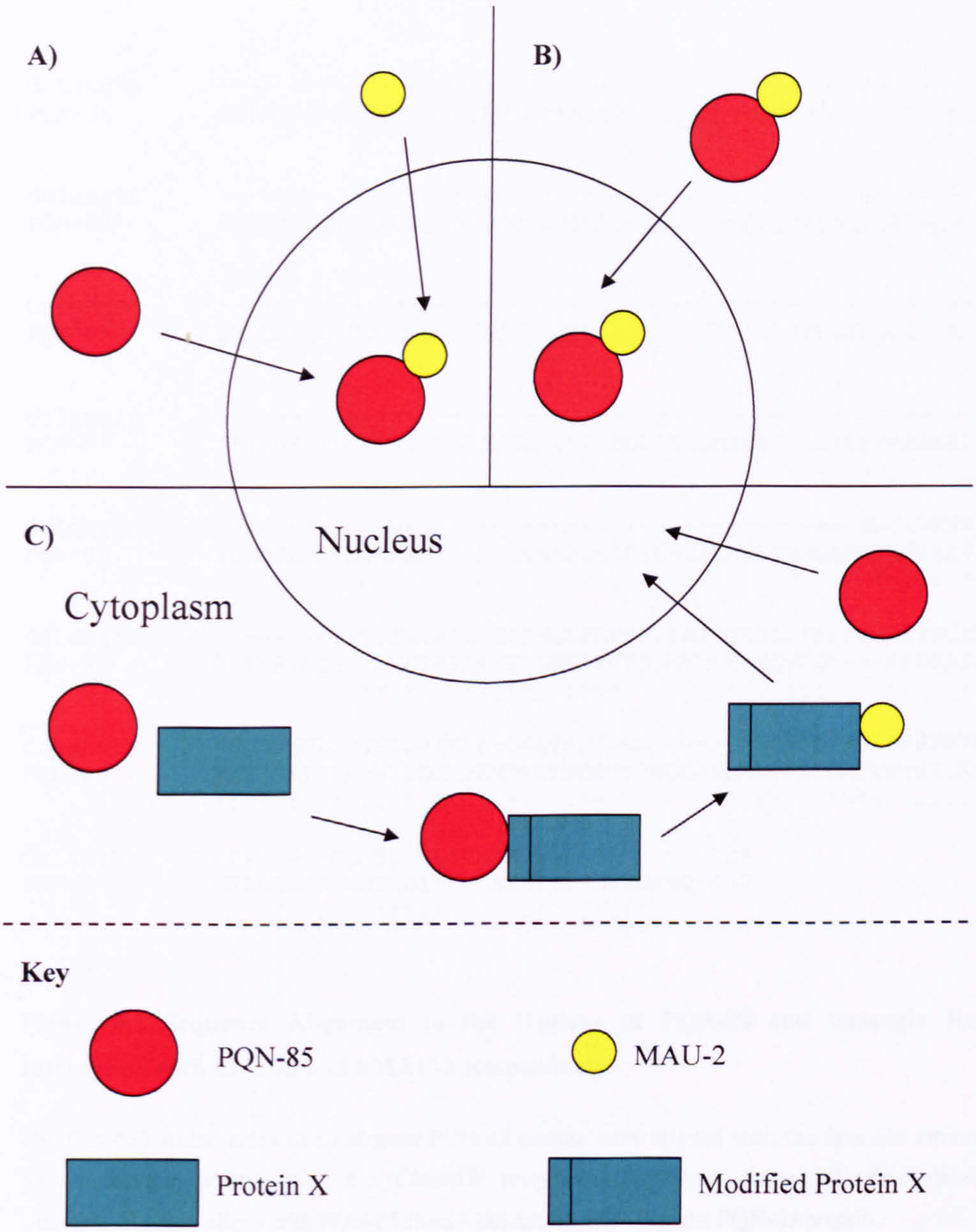

Figure 6.1 PQN-85 Could Affect the Subcellular Localisation of MAU-2 in Several Ways

A) the PQN-85 and MAU-2 proteins could be transported into the nucleus separately whereupon binding of PQN-85 retains MAU-2 in the nucleus. B) PQN-85 could bind to MAU-2 in the cytoplasm and chaperone it into the nucleus. C) PQN-85 could be required to modify another protein (here named Protein X for the sake of argument) to allow Protein X to bind MAU-2 and transports it into the nucleus.

```
delangin    ------------------------------------------------------------
PQN-85      MDPNNLQNSLNGTGNPNFQPVQTNAGGFGHQMAQTGAAAAAAATGQYNPMLLQQQYLNFG 60

delangin    ------------------------------------------------------------
PQN-85      FGMNYNNQLFDFQAQQQQQQQYLMQQQQQQQQLHHQQQQQHQNIAQPQAQHHQMNMFTQH 120

delangin    ------------------------------------------------------------
PQN-85      QMLQLMQQQQQQQQQQPVQQIQRQQPIAQPIPQHTIPPSTSNQFQQQIQSAASSIFDSSV 180

delangin    ------------------------------------------------------------
PQN-85      ISSHQKLYEEQCRQIEKERKEQEERKRKQELEEQRKRNEELKRLRIAEEKRLLEEQQRLR 240

delangin    ------------------------------------------MNGDMPHVP------- 9
PQN-85      EQMERERLAEIKRLEEAARLEDERRIAADIEAQKQAMLQKMQAEQNKHIAEVERQRSELE 300
                                                        * .:..*

delangin    --------ITTLAGIASLTDLLNQLPLPSPLPATTTKSLLFNARIAEEVNCLLACRDDNL 61
PQN-85      ERFARVSQPMTLVGTHFLPNFLDMIPFPYESMVDSTLPQVFDM---ERDSAILESCDPQM 357
                    **.*   *.::*: :*:*    . :* . :*:    *. ..:* . * ::

delangin    VSQLVHSLNQVSTDHIELK-DNLGSDDPEG------DIPVLLQAVLARSPNVFREKSMQN 114
PQN-85      VATISNILNATNIDDIITRMDKLRPDDKETNDLFLDKLPPIIQAVVNYNTSALDVDSHND 417
            *: : : ** .. *.*  : *:* .** *       .:* ::***:  ....:  .* ::

delangin    RYVQSG--MMMSQYKLSQNSMHSSPAS------ 139
PQN-85      MELLENEDVMMTEDITRTTAPSTSSSSYNNHHQ 450
                 : ..  :**::     .:  :*.:*
```

Figure 6.2 Sequence Alignment of the Regions of PQN-85 and Delangin Required for Interaction with MAU-2 and hMAU-2 Respectively

The first 450 amino acids of *C. elegans* PQN-85 protein were aligned with the first 139 amino acids of the human delangin protein using the (ClustalW programme(http://www.ebi.ac.uk/Tools/clustalw/index.html). Note that delangin aligns with PQN-85 from ~280 amino acids into the PQN-85 protein.

* denotes that the residues in that column are identical in both sequences in the alignment

: denotes conserved amino acid substitutions residues in both sequences in the alignment

. denotes semi-conserved amino acid substitutions are observed in both sequences in the alignment

evolution apart from a small section that appears to be required for the interaction with MAU-2 (Section 6.2). This suggests that the selective pressure for sequence conservation in the N-terminal region is low and as such may have allowed the extension of polyglutamine tracts in PQN-85. Rudimentary analysis of PQN-85 orthologue sequences shows that no polyglutamine regions can be found in human, *Drosophila* or *Xenopus* adherins. This suggests that during evolution the N-terminal region of PQN-85 and its orthologues may have evolved separate functions in different organisms.

The sequence of the *C. elegans* MAU-2 protein is very well conserved in metazoan orthologues (Benard et al., 2004); however until recently no orthologue of MAU-2 could be identified in budding yeast. It has now been recognised that the *S. cerevisiae* orthologue of MAU-2 is Scc4 (Seitan et al., 2006, Watrin et al., 2006). Sequence conservation between Scc4 and MAU-2 is low and it is interesting to wonder why the MAU-2 sequence has diverged so greatly from Scc4. One theory proposed by Seitan et al (2006) is that Scc4 in yeast binds only the Scc2 protein and therefore is not under a great level of selective pressure to maintain its sequence (Seitan et al., 2006). However as the sequences of Scc4 orthologues in higher eukaryote such as *C. elegans* diverged they may have taken on other roles such as axon migration that placed a high degree of selective pressure on the MAU-2 protein sequence, explaining the apparent well conserved nature of MAU-2 orthologues outside *S. cerevisiae*.

6.4 Consequences of These Results for CdLS Mutation Analysis

The low *NIPBL* mutation detection rate in CdLS patients is not due to undetected mutations. Several independent studies concentrated on detecting small changes in the coding sequence and have documented a *NIPBL* mutation detection rate of only ~40%-50% (Schoumans et al., 2007, Borck et al., 2004, Bhuiyan et al., 2006, Gillis et al., 2004, Krantz et al., 2004, Tonkin et al., 2004, Yan et al., 2006). An even lower mutation detection rate has been observed in the 5'UTR of *NIPBL* (Borck et al., 2006) whilst detection of large scale exon deletion or duplication within *NIPBL* using Multiple Ligation-dependent Probe Amplification (MLPA) has proved fruitless (Bhuiyan et al., 2007, Schoumans et al., 2007). The low mutation detection rate observed even though the *NIPBL* gene has now been extensively analysed in many CdLS patients suggests that mutations in other genes are involved in the pathogenesis of CdLS.

Recently members of the cohesin complex have been implicated in the pathogenesis of CdLS in a small number of cases. Mutations in the X linked *SMC1L1* gene which encodes the SMC1 subunit of cohesin have been found in CdLS patients with a prevalence of ~5% (Deardorff et al., 2007, Musio et al., 2006). Whilst initial reports stated that mutations in *SMC1L1* accounted for only male CdLS patients (Musio et al., 2006) it has been found that *SMC1L1* mutations affect both sexes (Deardorff et al., 2007). One CdLS causing mutation has also been found in the *SMC3* gene in a cohort of 96 patients (Deardorff et al., 2007) which suggests that the prevalence of mutations in *SMC3* is even lower than for *SMC1L1*. Interestingly in both reports it is stated that these mutations account for only mild cases (Deardorff et al., 2007, Musio et al., 2006) suggesting that there could be substantially different effects on CdLS phenotype between the mutations in *NIPBL* and those in *SMC3* and *SMC1L1*.

All mutations discovered in *SMC1L1* and *SMC3* are missense or amino acid deletions that affect a very small number of residues (Deardorff et al., 2007, Musio et al., 2006). The mutations retain the open reading frame of the mRNA sequence therefore affects on the protein sequence are predicted to be minor, it has therefore been predicted that functional cohesin complexes should be produced (Deardorff et al., 2007). This is unsurprising as chromosome segregation defects resulting from complete disruption of the cohesin complex would presumably be lethal early in development. This brings the overall CdLS causing mutation detection rate to only ~45%-55% and suggests that further genes are involved in causing CdLS. As structural components of the cohesin complex human orthologues of the *S. cerevisiae* *scc1* and *scc3* genes should be considered for mutational analysis.

Mounting evidence has suggested that mutations in the *PDS5B* gene which is also involved in cohesin regulation may cause CdLS. The *PDS5B* gene encodes one of two homologues of the *S. cerevisiae pds5* found in vertebrate genomes both of which function in sister chromatid cohesion and are found to bind cohesin (Losada et al., 2005, Sumara et al., 2000). Mice lacking the *PDS5B* gene display very similar physical defects to CdLS patients such as growth retardation, small head, shortened limbs, cleft palate and dysmorphic facial features (short snout, short low chin and thin upper lip) (Zhang et al., 2007). Further analysis of *PDS5B* deficient mice found evidence of congenital heart defects of a type commonly found in CdLS patients (Zhang et al., 2007). The significant link between *NIPBL* and *PDS5B* in cohesin dependent chromosome segregation, and the phenotypic overlap between CdLS

patients and *PDS5B* deficient mice suggests that mutations in human *PDS5B* may also contribute to a proportion of CdLS cases.

The finding that the cohesin loading complex is conserved in metazoans led to suggestions that mutations in the *KIAA0892* gene were involved in the pathogenesis of CdLS. As previously mentioned the product of the *KIAA0892* gene called hMAU-2 has been shown to partner delangin in loading cohesin onto chromosomes (Seitan et al., 2006, Watrin et al., 2006). Therefore, *KIAA0892* was analysed for mutations in a panel of classical CdLS patients that had no detectable *NIPBL* mutations. No mutations were detected in the *KIAA0892* coding region or immediate intronic region at the exon boundary of these patients (Seitan et al., 2006) suggesting that it is not involved in the pathogenesis of CdLS. This study did not look for large exon deletions or duplications within the gene or for gene rearrangements therefore some mutations may have been overlooked. Although this suggests that the *KIAA0892* gene is not involved in CdLS it cannot be discounted in the pathogenesis of CdLS. Mutations in *KIAA0892* may cause only a handful of CdLS cases and this study did not statistically cover a sufficient number of patients. Alternatively mutations in *KIAA0892* may only account for mutation in mild CdLS cases which were not analysed as part of the study.

6.5 PDS5B and KIAA0892 Link Neuron Migration to the Pathogenesis of CdLS

A common feature that links both *PDS5B* and *KIAA0892* to CdLS is defects in neuronal migration. Although neuropathological studies in CdLS patients are rare, abnormal placement of neurons in the brain indicative of neuronal migration defects have been observed (Hayashi et al., 1996). Mice lacking *PDS5B* display defects in the peripheral nervous system which controls the function of external sensory organs as well as skeletal and involuntary muscles. Abnormal positioning of the superior cervical ganglia (SCG; that supplies neurones to facial muscles) in mice lacking *PDS5B* results in ptosis (Zhang et al., 2007) a condition known to be common to CdLS patients. The enteric nervous system (ENS) is derived from neural crest cells (NCCs) migrating distally along the length of the bowel, *PDS5B* knockout mice display improper migration of NCCs and a consequent reduction in neuronal density at the distal end of the bowel (Zhang et al., 2007). Neuronal defects that affect aspects of bowel function such as smooth muscle contraction could be the underlying cause of the gastrointestinal defects observed in CdLS patients. Further, mutations in the *C. elegans mau-2* gene (the orthologue of *KIAA0892*) also display defects in axon migration (Benard et al., 2004, Takagi et al., 1997) which are the likely cause of the phenotypes associated with *mau-2* mutants strains (Section

1.2.6 and Table 1.5 and Table 1.6). This suggests that mutations in *PDS5B* or *KIAA0892* may cause CdLS and the defects in neuronal migration that may be a consequence of these mutations could explain the defects observed in CdLS patients.

It is currently unclear how *PDS5B* and *mau-2* mutations within mouse and *C. elegans* respectively lead to defects in neuronal migration. It seems unlikely that the defects are related to the function of these genes in sister chromatid cohesion. Mice lacking the PDS5B gene do not display defects in sister chromatid cohesion (Zhang et al., 2007) (possibly due to functional redundancy with its homologue identified in vertebrate genomes) suggesting that the defects observed in these mice are due to an as yet undiscovered function of *PDS5B*. The phenotypes observed in *C. elegans* homozygous for the null *qm160 mau-2* mutation can be rescued by expression of *mau-2* exclusively in the nervous system (Benard et al., 2004). Similarly expression of *mau-2* within individual neurons which are misplaced in *qm160* worms is sufficient to rescue the axon migration defects associated with this neuron (Benard et al., 2004). Further, expression of a functional *mau-2::GFP* within *qm160* mutants not only rescues all mutant phenotypes but also localises to the cytoplasm of neurons in adult worms (Benard et al., 2004) suggesting that the function of *mau-2* in axon migration is specific to neurons and not a result of a general defect in chromosome segregation.

6.6 Alternative Effects of NIPBL and Cohesin Mutations

Mutations in *NIPBL* and cohesin subunits may cause indirect effects on other members of the sister chromatid cohesion pathway. The cohesin complex has been shown to bind to and recruit PDS5B homologues to chromosomes in yeast, *Xenopus* and humans (Hartman et al., 2000, Losada et al., 2005, Noble et al., 2006, Panizza et al., 2000, Sumara et al., 2000, Tanaka et al., 2001, Wang et al., 2002, Mc Intyre et al., 2007) which in turn has been proposed to bind and recruit the yeast cohesion establishment factor Eco1 (Noble et al., 2006, Tanaka et al., 2001). Mutations in *NIPBL*, *SMC1L1* and *SMC3* genes that affect the level of cohesin bound to chromosomes may therefore affect the level of PDS5B and the human orthologue of Eco1 called ESCO2 that are bound to chromosomes.

A reduction in the level of ESCO2 bound to chromosomes may explain the phenotypic overlap between patients with CdLS and Roberts syndrome. Roberts syndrome is caused by mutations in the *ESCO2* gene (Schule et al., 2005, Vega et al., 2005) and patients share several physical characteristics with CdLS patients including growth retardation and

shortened limbs. Although the interaction between PDS5B and ESCO2 has not been assessed in humans, patients with Roberts syndrome consistently display defects in cohesion at centromeres suggesting that the function of ESCO2 is conserved in metazoans. A reduction in the level of chromosomally bound PDS5B as a result of *NIPBL*, *SMC1L1* or *SMC3* genes mutations could also conceivably cause a reduction in the level of chromosomally bound ESCO2 mimicking the effect of the mutations observed in Roberts syndrome. As a result CdLS patients could display a phenotypic overlap with Roberts syndrome patients.

6.7 CdLS Phenotypes as a Result of Defects in Cellular Proliferation

Only a small amount of cohesin is required to generate sister chromatid cohesion in metazoans. Therefore chromosome segregation defects may only be observed in CdLS patients where the *NIPBL* mutation is particularly severe. In metazoans the majority of cohesin is removed during prophase of the cell cycle in a phosphorylation dependent manner (Hauf et al., 2005). Early reports suggested that no cohesin remained on these chromosomes from prophase removal to anaphase when sister chromatid separate, however it was discovered that a small amount of cohesin persists at centromeric regions of the chromosomes (Wazenegger et al., 2000). This small population of centromeric cohesin appears to be sufficient to keep the sister chromatids together before anaphase and chromosome segregation. Mutations in *NIPBL* that cause only minor alterations to delangin protein function may still allow loading of enough cohesin to generate sister chromatid cohesion. More significant mutations in *NIPBL* however that cause truncations of the delangin protein or affect highly conserved residues may reduce cohesin loading to such a level that sister chromatid cohesion cannot be generated efficiently resulting in chromosome segregation defects.

Chromosome segregation defects likely play a role in the pathogenesis of CdLS. Studies have demonstrated that mutations in *NIPBL* cause PSCS in CdLS patients (Kaur et al., 2005) although it should be noted that this is currently the only study to have demonstrated this and others could find no evidence of this (Tonkin et al., 2004). No such analysis has been carried out on CdLS patients with mutations in cohesin genes as yet. A reduction in the number of progenitor cells as a result of aberrant chromosome segregation could feasibly cause some if not all of the phenotypes associated with CdLS such as growth retardation and limb reduction. It would be surprising given the role of delangin and the cohesin complex in sister chromatid cohesion that no chromosome segregation defects would be observed at all in CdLS patients.

It should be noted that any defect in chromosome segregation would likely be minor as a major defect in this process would likely be lethal early in development.

6.8 The Defects Found in CdLS Patients may be Caused by Aberrant Gene Expression

The defects observed in CdLS patients may be a result of aberrant developmental gene expression. There is no evidence as yet that human delangin or cohesin affects the regulation of developmentally important genes. However in *Drosophila*, Nipped B and cohesin have been shown to regulate expression of a gene involved in wing and limb development in a manner that is likely to affect chromatin structure (Dorsett et al., 2005, Rollins et al., 2004, Rollins et al., 1999). The location of cohesin binding to chromosomes is not random and as such it is conceivable that a similar mechanism exists in humans to control the expression of specific genes. Mice lacking *PDS5B* show characteristic features of CdLS patients but do not display any chromosome segregation defects (Zhang et al., 2007) suggesting that defects associated with this disease may not be due to defects in chromosome segregation. The effect that mutations in *NIPBL*, *SMC3* and *SMCL1* have on the dynamics of cohesin binding to DNA is currently is unknown. However, assuming that the mutations in *NIPBL* and cohesin subunits that cause CdLS have general effects on cohesin localisation then a potentially huge number of genes could be affected.

In conclusion the evidence presented in this thesis suggests that the *pqn-85* and *mau-2* genes of *C. elegans* function in chromosome segregation. The proteins encoded by these genes likely from a complex that functions in the loading of cohesin onto chromosomes. The finding that the cohesin loading complex appears to be conserved in many if not all eukaryotes has wider implications in the understanding the mechanism of chromosome segregation and in the pathogenesis of complex human diseases.

References

ALBERTSON, D. G. (1984) Formation of the 1st Cleavage Spindle in Nematode Embryos. *Developmental Biology,* 101, 61-72.

ALBERTSON, D. G., SULSTON, J. E. & WHITE, J. G. (1978) Cell Cycling and DNA-Replication in a Mutant Blocked in Cell-Division in Nematode *Caenorhabditis elegans*. *Developmental Biology,* 63, 165-178.

ALTSCHUL, S. F., MADDEN, T. L., SCHAFFER, A. A., ZHANG, J. H., ZHANG, Z., MILLER, W. & LIPMAN, D. J. (1997) Gapped BLAST and PSI-BLAST: a new generation of protein database search programs. *Nucleic Acids Research,* 25, 3389-3402.

ANDERSON, D. E., LOSADA, A., ERICKSON, H. P. & HIRANO, T. (2002) Condensin and cohesin display different arm conformations with characteristic hinge angles. *Journal of Cell Biology,* 156, 419-424.

ARUMUGAM, P., GRUBER, S., TANAKA, K., HAERING, C. H., MECHTLER, K. & NASMYTH, K. (2003) ATP hydrolysis is required for cohesin's association with chromosomes. *Current Biology,* 13, 1941-1953.

BAUER, G. A. & BURGERS, P. M. J. (1990) Molecular-Cloning, Structure and Expression of the Yeast Proliferating Cell Nuclear Antigen Gene. *Nucleic Acids Research,* 18, 261-265.

BELLOWS, A., KENNA, M. A. & SKIBBENS, R. V. (2002) Characterization of a candidate CTF7/ECO1 human homolog. *Molecular Biology of the Cell,* 13, 245A-245A.

BENARD, C. Y., KEBIR, H., TAKAGI, S. & HEKIMI, S. (2004) *mau-2* acts cell-autonomously to guide axonal migrations in *Caenorhabditis elegans*. *Development,* 131, 5947-5958.

BERNARD, P., DROGAT, J., MAURE, J. F., DHEUR, S., VAUR, S., GENIER, S. & JAVERZAT, J. P. (2006) A screen for cohesion mutants uncovers *ss13*, the fission yeast counterpart of the cohesin loading factor Scc4. *Current Biology,* 16, 875-881.

BHUIYAN, Z. A., KLEIN, M., HAMMOND, P., VAN HAERINGEN, A., MANNENS, M., VAN BERCKELAER-ONNES, I. & HENNEKAM, R. C. M. (2006) Genotype-phenotype correlations of 39 patients with Cornelia De Lange syndrome: the Dutch experience. *Journal of Medical Genetics,* 43, 568-575.

BHUIYAN, Z. A., STEWART, H., REDEKER, E. J., MANNENS, M. & HENNEKAM, R. C. M. (2007) Large genomic rearrangements in *NIPBL* are infrequent in Cornelia de Lange syndrome. *European Journal of Human Genetics,* 15, 505-508.

BLAT, Y. & KLECKNER, N. (1999) Cohesins bind to preferential sites along yeast chromosome III, with differential regulation along arms versus the centric region. *Cell,* 98, 249-259.

BORCK, G., REDON, R., SANLAVILLE, D., RIO, M., PRIEUR, M., LYONNET, S., VEKEMANS, M., CARTER, N. P., MUNNICH, A., COLLEAUX, L. & CORMIER-DAIRE, V. (2004) *NIPBL* mutations and genetic heterogeneity in Cornelia de Lange syndrome. *Journal of Medical Genetics,* 41.

BORCK, G., ZARHRATE, M., CLUZEAU, C., BAL, E., BONNEFONT, J., MUNNICH, A., CORMIER-DAIRE, V. & COLLEAUX, L. (2006) Father-

to,Daughter transmission of Cornelia de Lange syndrome caused by a mutation in the 5 ' untranslated region of the *NIPBL* gene. *Human Mutation,* 27, 731-735.

BRENNER, S. (1974) The genetics of *Caenorhabditis elegans*. *Genetics,* 77, 71-94.

BRENT, R. & PTASHNE, M. (1985) A Eukaryotic Transcriptional Activator Bearing the DNA Specificity of a Prokaryotic Repressor. *Cell,* 43, 729-736.

BURGERS, P. M. J. (1988) Mammalian Cyclin Pcna (DNA Polymerase-Delta Auxiliary Protein) Stimulates Processive DNA-Synthesis by Yeast DNA Polymerase-Iii. *Nucleic Acids Research,* 16, 6297-6307.

CHAN, R. C., CHAN, A., JEON, M., WU, T. F., PASQUALONE, D., ROUGVIE, A. E. & MEYER, B. J. (2003) Chromosome cohesion is regulated by a clock gene paralogue TIM-1. *Nature,* 423, 1002-1009.

CHAN, R. C., CHAN, A., JEON, M., WU, T. F., ROUGVIE, A. & MEYER, B. J. (2002) The *C-elegans* TIMELESS homolog is an essential regulator of chromosome cohesion. *Molecular Biology of the Cell,* 13, 150A-150A.

CIOSK, R., SHIRAYAMA, M., SHEVCHENKO, A., TANAKA, T., TOTH, A. & NASMYTH, K. (2000) Cohesin's binding to chromosomes depends on a separate complex consisting of Scc2 and Scc4 proteins. *Molecular Cell,* 5, 243-254.

CIOSK, R., ZACHARIAE, W., MICHAELIS, C., SHEVCHENKO, A., MANN, M. & NASMYTH, K. (1998) An ESP1/PDS1 complex regulates loss of sister chromatid cohesion at the metaphase to anaphase transition in yeast. *Cell,* 93, 1067-1076.

CUMMINGS, W. J., MERINO, S. T., YOUNG, K. G., LI, L. B., JOHNSON, C. W., SIERRA, E. A. & ZOLAN, M. E. (2002) The *Coprinus cinereus* adherin Rad9 functions in Mre11-dependent DNA repair, meiotic sister-chromatid cohesion, and meiotic homolog pairing. *Proceedings of the National Academy of Sciences of the United States of America,* 99, 14958-14963.

DARWICHE, N., FREEMAN, L. A. & STRUNNIKOV, A. (1999) Characterization of the components of the putative mammalian sister chromatid cohesion complex. *Gene,* 233, 39-47.

DEARDORFF, M. A., KAUR, M., YAEGER, D., RAMPURIA, A., KOROLEV, S., PIE, J., GIL-RODRIGUEZ, C., ARNEDO, M., LOEYS, B., KLINE, A. D., WILSON, M., LILLQUIST, K., SIU, V., RAMOS, F. J., MUSIO, A., JACKSON, L. S., DORSETT, D. & KRANTZ, I. D. (2007) Mutations in cohesin complex members *SMC3* and *SMC1A* cause a mild variant of Cornelia de Lange syndrome with predominant mental retardation. *American Journal of Human Genetics,* 80, 485-494.

DORSETT, D. (1990) Potentiation of a Polyadenylylation Site by a Downstream Protein DNA Interaction. *Proceedings of the National Academy of Sciences of the United States of America,* 87, 4373-4377.

DORSETT, D. (1993) Distance-Independent Inactivation of an Enhancer by the Suppressor of Hairy-Wing DNA-Binding Protein of *Drosophila*. *Genetics,* 134, 1135-1144.

DORSETT, D., EISSENBERG, J. C., MISULOVIN, Z., MARTENS, A., REDDING, B. & MCKIM, K. (2005) Effects of sister chromatid cohesion proteins on *cut* gene expression during wing development in *Drosophila*. *Development,* 132, 4743-4753.

FIRE, A., XU, S., MONTGOMERY, M. K., KOSTAS, S. A., DRIVER, S. E. & MELLO, C. C. (1998) Potent and specific genetic interference by double-stranded RNA in *Caenorhabditis elegans*. *Nature,* 391, 806-811.

FUNABIKI, H., KUMADA, K. & YANAGIDA, M. (1996) Fission yeast *cut1* and *cut2* are essential for sister chromatid separation, concentrate along the metaphase spindle and form large complexes. *Embo Journal,* 15, 6617-6628.

FURUYA, K., TAKAHASHI, K. & YANAGIDA, M. (1998) Faithful anaphase is ensured by Mis4, a sister chromatid cohesion molecule required in S phase and not destroyed in G1 phase. *Genes & Development,* 12, 3408-3418.

GARBER, P. M., VIDANES, G. M. & TOCZYSKI, D. P. (2005) Damage in transition. *Trends in Biochemical Sciences,* 30, 63-66.

GECK, P., SZELEI, J., JIMENEZ, J., SONNENSCHEIN, C. & SOTO, A. M. (1999) Early gene expression during androgen-induced inhibition of proliferation of prostate cancer cells: a new suppressor candidate on chromosome 13, in the *BRCA2-Rb1* locus. *Journal of Steroid Biochemistry and Molecular Biology,* 68, 41-50.

GILLESPIE, P. J. & HIRANO, T. (2004) Scc2 Couples Replication Licensing to Sister Chromatid Cohesion in *Xenopus* Extracts. *Current Biology,* 14, 1598-1603.

GILLIS, L. A., MCCALLUM, J., KAUR, M., DESCIPIO, C., YAEGER, D., MARIANI, A., KLINE, A. D., LI, H. H., DEVOTO, M., JACKSON, L. G. & KRANTZ, I. D. (2004) *NIPBL* mutational analysis in 120 individuals with Cornelia de Lange syndrome and evaluation of genotype-phenotype correlations. *American Journal of Human Genetics,* 75, 610-623.

GIMENEZ-ABIAN, J. F., SUMARA, I., HIROTA, T., HAUF, S., GERLICH, D., DE LA TORRE, C., ELLENBERG, J. & PETERS, J. (2004) Regulation of sister chromatid cohesion between chromosome arms. *Current Biology,* 14, 1187-1193.

GINIGER, E., VARNUM, S. M. & PTASHNE, M. (1985) Specific DNA-Binding of Gal4, a Positive Regulatory Protein of Yeast. *Cell,* 40, 767-774.

GIOT, L., BADER, J. S., BROUWER, C., CHAUDHURI, A., KUANG, B., LI, Y., HAO, Y. L., OOI, C. E., GODWIN, B., VITOLS, E., VIJAYADAMODAR, G., POCHART, P., MACHINENI, H., WELSH, M., KONG, Y., ZERHUSEN, B., MALCOLM, R., VARRONE, Z., COLLIS, A., MINTO, M., BURGESS, S., MCDANIEL, L., STIMPSON, E., SPRIGGS, F., WILLIAMS, J., NEURATH, K., IOIME, N., AGEE, M., VOSS, E., FURTAK, K., RENZULLI, R., AANENSEN, N., CARROLLA, S., BICKELHAUPT, E., LAZOVATSKY, Y., DASILVA, A., ZHONG, J., STANYON, C. A., FINLEY, R. L., WHITE, K. P., BRAVERMAN, M., JARVIE, T., GOLD, S., LEACH, M., KNIGHT, J., SHIMKETS, R. A., MCKENNA, M. P., CHANT, J. & ROTHBERG, J. M. (2003) A protein interaction map of Drosophila melanogaster. *Science,* 302, 1727-1736.

GLYNN, E. F., MEGEE, P. C., YU, H. G., MISTROT, C., UNAL, E., KOSHLAND, D. E., DERISI, J. L. & GERTON, J. L. (2004) Genome-wide mapping of the cohesin complex in the yeast *Saccharomyces cerevisiae*. *Plos Biology,* 2.

GRUBER, S., HAERING, C. H. & NASMYTH, K. (2003) Chromosomal cohesin forms a ring. *Cell,* 112, 765-777.

GUACCI, V., KOSHLAND, D. & STRUNNIKOV, A. (1997) A direct link between sister chromatid cohesion and chromosome condensation revealed through the analysis of *MCD1* in *S. cerevisiae*. *Cell,* 91, 47-57.

HAERING, C. H., LOWE, J., HOCHWAGEN, A. & NASMYTH, K. (2002) Molecular architecture of SMC proteins and the yeast cohesin complex. *Molecular Cell,* 9, 773-788.

HAERING, C. H. & NASMYTH, K. (2003) Building and breaking bridges between sister chromatids. *Bioessays,* 25, 1178-1191.

HAGSTROM, K. A. & MEYER, B. J. (2003) Condensin and cohesin: More than chromosome compactor and glue. *Nature Reviews Genetics,* 4, 520-534.

HARTMAN, T., STEAD, K., KOSHLAND, D. & GUACCI, V. (2000) Pds5p is an essential chromosomal protein required for both sister chromatid cohesion and condensation in *Saccharomyces cerevisiae*. *Journal of Cell Biology,* 151, 613-626.

HAUF, S., ROITINGER, E., KOCH, B., DITTRICH, C. M., MECHTLER, K. & PETERS, J. M. (2005) Dissociation of cohesin from chromosome arms and loss of arm cohesion during early mitosis depends on phosphorylation of SA2. *Plos Biology,* 3, 419-432.

HAYASHI, M., SAKAMOTO, K., KURATA, K., NAGATA, J., SATOH, J. & MORIMATSU, Y. (1996) Septo-optic dysplasia with cerebellar hypoplasia in Cornelia de Lange syndrome. *Acta Neuropathologica,* 92, 625-630.

HEKIMI, S., BOUTIS, P. & LAKOWSKI, B. (1995) Viable Maternal-Effect Mutations That Affect the Development of the Nematode *Caenorhabditis elegans*. *Genetics,* 141, 1351-1364.

HOU, F. J. & ZOU, H. (2005) Two human orthologues of Eco1/Ctf7 acetyltransferases are both required for proper sister-chromatid cohesion. *Molecular Biology of the Cell,* 16, 3908-3918.

IRELAND, M., DONNAI, D. & BURN, J. (1993) Brachmann-de Lange syndrome. Delineation of the clinical phenotype. *American Journal of Medical Genetics,* 47, 959-964.

IVANOV, D. & NASMYTH, K. (2005) A topological interaction between cohesin rings and a circular minichromosome. *Cell,* 122, 849-860.

IVANOV, D., SCHLEIFFER, A., EISENHABER, F., MECHTLER, K., HAERING, C. H. & NASMYTH, K. (2002) Eco1 is a novel acetyltransferase that can acetylate proteins involved in cohesion. *Current Biology,* 12, 323-328.

JACK, J., DORSETT, D., DELOTTO, Y. & LIU, S. (1991) Expression of the Cut Locus in the *Drosophila* Wing Margin Is Required for Cell Type Specification and Is Regulated by a Distant Enhancer. *Development,* 113, 735-747.

KAMATH, R. S., FRASER, A. G., DONG, Y., POULIN, G., DURBIN, R., GOTTA, M., KANAPIN, A., LE BOT, N., MORENO, S., SOHRMANN, M., WELCHMAN, D. P., ZIPPERLEN, P. & AHRINGER, J. (2003) Systematic functional analysis of the *Caenorhabditis elegans* genome using RNAi. *Nature,* 421, 231-237.

KAUR, M., DESCIPIO, C., MCCALLUM, J., YAEGER, D., DEVOTO, M., JACKSON, L. G., SPINNER, N. B. & KRANTZ, I. D. (2005) Precocious sister chromatid separation (PSCS) in Cornelia de Lange syndrome. *American Journal of Medical Genetics Part A,* 138A, 27-31.

KEEGAN, L., GILL, G. & PTASHNE, M. (1986) Separation of DNA-Binding from the Transcription-Activating Function of a Eukaryotic Regulatory Protein. *Science,* 231, 699-704.

KELLUM, R. & ALBERTS, B. M. (1995) Heterochromatin protein 1 is required for correct chromosome segregation in *Drosophila* embryos. *Journal of Cell Science,* 108, 1419-1431.

KELLY, W. G., XU, S. Q., MONTGOMERY, M. K. & FIRE, A. (1997) Distinct requirements for somatic and germline expression of a genera expressed *Caernorhabditis elegans* gene. *Genetics,* 146, 227-238.

KIM, J. S., KRASIEVA, T. B., LAMORTE, V., MALCOLM, A., TAYLOR, R. & YOKOMORI, K. (2002) Specific recruitment of human cohesin to laser-induced DNA damage. *Journal of Biological Chemistry,* 277, 45149-45153.

KLINE, A. D., STANLEY, C., BELEVICH, J., BRODSKY, K., BARR, M. & JACKSON, L. G. (1993) Developmental data on individuals with the Brachmann-de Lange syndrome. *American Journal of Medical Genetics,* 47, 1053-1058.

KRAMER, J. M., FRENCH, R. P., PARK, E. C. & JOHNSON, J. J. (1990) The *Caenorhabditis elegans Rol-6* Gene, Which Interacts with the *Sqt-1* Collagen Gene to Determine Organismal Morphology, Encodes a Collagen. *Molecular and Cellular Biology,* 10, 2081-2089.

KRANTZ, I. D., MCCALLUM, J., DESCIPIO, C., KAUR, M., GILLIS, L. A., YAEGER, D., JUKOFSKY, L., WASSERMAN, N., BOTTANI, A., MORRIS, C. A., NOWACZYK, M. J. M., TORIELLO, H., BAMSHAD, M. J., CAREY, J. C., RAPPAPORT, E., KAWAUCHI, S., LANDER, A. D., CALOF, A. L., LI, H. H., DEVOTO, M. & JACKSON, L. G. (2004) Cornelia de Lange syndrome is caused by mutations in *NIPBL*, the human homolog of Drosophila melanogaster *Nipped-B*. *Nature Genetics,* 36, 631-635.

LALORAYA, S., GUACCI, V. & KOSHLAND, D. (2000) Chromosomal addresses of the cohesin component Mcd1p. *Journal of Cell Biology,* 151, 1047-1056.

LECHNER, M. S., SCHULTZ, D. C., NEGOREV, D., MAUL, G. G. & RAUSCHER, I. F. (2005) The mammalian heterochromatin protein 1 binds diverse nuclear proteins through a common motif that targets the chromoshadow domain. *Biochemical & Biophysical Research Communications,* 331, 929-937.

LENGRONNE, A., KATOU, Y., MORI, S., YOKABAYASHI, S., KELLY, G. P., ITO, T., WATANABE, Y., SHIRAHIGE, K. & UHLMANN, F. (2004) Cohesin relocation from sites of chromosomal loading to places of convergent transcription. *Nature,* 430, 573-578.

LOSADA, A., HIRANO, M. & HIRANO, T. (1998) Identification of Xenopus SMC protein complexes required for sister chromatid cohesion. *Genes & Development,* 12, 1986-1997.

LOSADA, A., YOKOCHI, T. & HIRANO, T. (2005) Functional contribution of Pds5 to cohesin-mediated cohesion in human cells and *Xenopus* egg extracts. *Journal of Cell Science,* 118, 2133-2141.

LOSADA, A., YOKOCHI, T., KOBAYASHI, R. & HIRANO, T. (2000) Identification and characterization of SA/Scc3p subunits in the *Xenopus* and human cohesin complexes. *Journal of Cell Biology,* 150, 405-416.

MADDOX, P. S., OEGEMA, K., DESAI, A. & CHEESEMAN, I. M. (2004) "Holo"er than thou: Chromosome segregation and kinetochore function in *C. elegans*. *Chromosome Research,* 12, 641-653.

MC INTYRE, J., MULLER, E. G. D., WEITZER, S., SNYDSMAN, B. E., DAVIS, T. N. & UHLMANN, F. (2007) In vivo analysis of cohesin architecture using FRET in the budding yeast *Saccharomyces cerevisiae*. *EMBO,* 26, 3783-3798.

MEGEE, P. C. & KOSHLAND, D. (1999) A functional assay for centromere-associated sister chromatid cohesion. *Science, 285, 254-257.*

MELBY, T. E., CIAMPAGLIO, C. N., BRISCOE, G. & ERICKSON, H. P. (1998) The symmetrical structure of structural maintenance of chromosomes (SMC) and MukB proteins: Long, antiparallel coiled coils, folded at a flexible hinge. *Journal of Cell Biology,* 142, 1595-1604.

MELLO, C. C., KRAMER, J. M., STINCHCOMB, D. & AMBROS, V. (1991) Efficient Gene-Transfer in *C. elegans* - Extrachromosomal Maintenance and Integration of Transforming Sequences. *Embo Journal,* 10, 3959-3970.

MICHAELIS, C., CIOSK, R. & NASMYTH, K. (1997) Cohesins: Chromosomal proteins that prevent premature separation of sister chromatids. *Cell,* 91, 35-45.

MILUTINOVICH, M. & KOSHLAND, D. E. (2003) SMC complexes - Wrapped up in controversy. *Science,* 300, 1101-1102.

MINC, E., ALLORY, V., WORMAN, H. J., COURVALIN, J. C. & BUENDIA, B. (1999) Localization and phosphorylation of HP1 proteins during the cell cycle in mammalian cells. *Chromosoma,* 108, 220-234.

MINC, E., COURVALIN, J. C. & BUENDIA, B. (2000) HP1 gamma associates with euchromatin and heterochromatin in mammalian nuclei and chromosomes. *Cytogenetics and Cell Genetics,* 90, 279-284.

MITO, Y., SUGIMOTO, A. & YAMAMOTO, M. (2003) Distinct developmental function of two *Caenorhabditis elegans* homologs of the cohesin subunit Scc1/Rad21. *Molecular Biology of the Cell,* 14, 2399-2409.

MURZINA, N., VERREAULT, A., LAUE, E. & STILLMAN, B. (1999) Heterochromatin dynamics in mouse cells: Interaction between chromatin assembly factor 1 and HP1 proteins. *Molecular Cell,* 4, 529-540.

MUSIO, A., SELICORNI, A., FOCARELLI, M. L., GERVASINI, C., MILANI, D., RUSSO, S., VEZZONI, P. & LARIZZA, L. (2006) X-linked Cornelia de Lange syndrome owing to *SMC1L1* mutations. *Nature Genetics,* 38, 528-530.

NASMYTH, K. (2005) How might cohesin hold sister chromatids together? *Philosophical Transactions of the Royal Society B-Biological Sciences,* 360, 483-496.

NASMYTH, K. & HAERING, C. H. (2005) The structure and function of SMC and Kleisin complexes. *Annual Review of Biochemistry,* 74, 595-648.

NEUWALD, A. F. & HIRANO, T. (2000) HEAT repeats associated with condensins, cohesins, and other complexes involved in chromosome-related functions. *Genome Research,* 10, 1445-1452.

NOBLE, D., KENNA, M. A., DIX, M., SKIBBENS, R. V., UNAL, E. & GUACCI, V. (2006) Intersection between the regulators of sister chromatid cohesion establishment and maintenance in budding yeast indicates a multi-step mechanism. *Cell Cycle,* 5, 2528-2536.

NONAKA, N., KITAJIMA, T., YOKOBAYASHI, S., XIAO, G., YAMAMOTO, M., GREWAL, S. I. S. & WATANABE, Y. (2002) Recruitment of cohesin to heterochromatic regions by Swi6/HP1 in fission yeast. *Nature Cell Biology,* 4, 89-93.

PANIZZA, S., TANAKA, T. U., HOCHWAGEN, A., EISENHABER, F. & NASMYTH, K. (2000) Pds5 cooperates with cohesin in maintaining sister chromatid cohesion. *Current Biology,* 10, 1557-1564.

PASIERBEK, P., FODERMAYR, M., JANTSCH, V., JANTSCH, M., SCHWEIZER, D. & LOIDL, J. (2003) The *Caenorhabditis elegans* SCC-3 homologue is required for meiotic synapsis and for proper chromosome disjunction in mitosis and meiosis. *Experimental Cell Research,* 289, 245-255.

POCOCK, R., AHRINGER, J., MITSCH, M., MAXWELL, S. & WOOLLARD, A. (2004) A regulatory network of T-box genes and the even-skipped homologue *vab-7* controls patterning and morphogenesis in *C. elegans*. *Development,* 131, 2373-2385.

PRAITIS, V., CASEY, E., COLLAR, D. & AUSTIN, J. (2001) Creation of low-copy integrated transgenic lines in *Caenorhabditis elegans*. *Genetics,* 157, 1217-1226.

RAO, H., UHLMANN, F., NASMYTH, K. & VARSHAVSKY, A. (2001) Degradation of a cohesin subunit by the N-end rule pathway is essential for chromosome stability. *Nature,* 410, 955-959.

RIEDER, C. L. & PALAZZO, R. E. (1992) Colcemid and the Mitotic-Cycle. *Journal of Cell Science,* 102, 387-392.

ROBBINS, J., DILWORTH, S. M., LASKEY, R. A. & DINGWALL, C. (1991) 2 Interdependent Basic Domains in Nucleoplasmin Nuclear Targeting Sequence - Identification of a Class of Bipartite Nuclear Targeting Sequence. *Cell,* 64, 615-623.

ROLLINS, R. A., KOROM, M., AULNER, N., MARTENS, A. & DORSETT, D. (2004) Drosophila *Nipped-B* Protein Supports Sister Chromatid Cohesion and Opposes the Stromalin/Scc3 Cohesion Factor to Facilitate Long-Range Activation of the cut Gene. *Molecular & Cellular Biology,* 24, 3100-3111.

ROLLINS, R. A., MORCILLO, P. & DORSETT, D. (1999) Nipped-B, a Drosophila homologue of chromosomal adherins, participates in activation by remote enhancers in the *cut* and *Ultrabithorax* genes. *Genetics,* 152, 577-593.

RUSSELL, K. L., MING, J. E., PATEL, K., JUKOFSKY, L., MAGNUSSON, M. & KRANTZ, I. D. (2001) Dominant paternal transmission of Cornelia de Lange syndrome: A new case and review of 25 previously reported familial recurrences. *American Journal of Medical Genetics,* 104, 267-276.

SCHOUMANS, J., WINCENT, J., BARBARO, M., DJUREINOVIC, T., MAGUIRE, P., FORSBERG, L., STAAF, J., THURESSON, A. C., BORG, A., NORDGREN, A., MALM, G. & ANDERLID, B. M. (2007) Comprehensive mutational analysis of a cohort of Swedish Cornelia de Lange syndrome patients. *European Journal of Human Genetics,* 15, 143-149.

SCHULE, B., OVIEDO, A., JOHNSTON, K., PAI, S. & FRANCKE, U. (2005) Inactivating mutations in *ESCO2* cause SC phocomelia and Roberts syndrome: No phenotype-genotype correlation. *American Journal of Human Genetics,* 77, 1117-1128.

SEITAN, V. C., BANKS, P., LAVAL, S., MAJID, N. A., DORSETT, D., RANA, A., SMITH, J., BATEMAN, A., KRPIC, S., HOSTERT, A., ROLLINS, R. A., ERDJUMENT-BROMAGE, H., TEMPST, P., BENARD, C. Y., HEKIMI, S., NEWBURY, S. F. & STRACHAN, T. (2006) Metazoan Scc4 homologs link sister chromatid cohesion to cell and axon migration guidance. *Plos Biology,* 4, 1411-1425.

SIOMOS, M. F., BADRINATH, A., PASIERBEK, P., LIVINGSTONE, D., WHITE, J., GLOTZER, M. & NASMYTH, K. (2001) Separase is required for chromosome segregation during meiosis I in *Caenorhabditis elegans*. *Current Biology,* 11, 1825-1835.

SKIBBENS, R. V., CORSON, L. B., KOSHLAND, D. & HIETER, P. (1999) Ctf7p is essential for sister chromatid cohesion and links mitotic chromosome structure to the DNA replication machinery. *Genes & Development,* 13, 307-319.

SONODA, E., MATSUSAKA, T., MORRISON, C., VAGNARELLI, P., HOSHI, O., USHIKI, T., NOJIMA, K., FUKAGAWA, T., WAIZENEGGER, I. C., PETERS, J. M., EARNSHAW, W. C. & TAKEDA, S. (2001) Scc1/Rad21/Mcd1 is required for sister chromatid cohesion and kinetochore function in vertebrate cells. *Developmental Cell,* 1, 759-770.

STEAD, K., AGUILAR, C., HARTMAN, T., DREXEL, M., MELUH, P. & GUACCI, V. (2003) Pds5p regulates the maintenance of sister chromatid cohesion and is sumoylated to promote the dissolution of cohesion. *Journal of Cell Biology,* 163, 729-741.

STINCHCOMB, D. T., SHAW, J. E., CARR, S. H. & HIRSH, D. (1985) Extrachromosomal DNA Transformation of *Caenorhabditis elegans. Molecular and Cellular Biology,* 5, 3484-3496.

STRACHAN, T. (2005) Cornelia de Lange Syndrome and the link between chromosomal function, DNA repair and developmental gene regulation. *Current Opinion in Genetics & Development,* 15, 258-264.

STROM, L., LINDROOS, H. B., SHIRAHIGE, K. & SJOGREN, C. (2003) Postreplicative recruitment of cohesin to double-strand breaks is required for DNA repair. *Molecular Cell,* 16, 1003-1015.

STROME, S., POWERS, J., DUNN, M., REESE, K., MALONE, C. J., WHITE, J., SEYDOUX, G. & SAXTON, W. (2001) Spindle dynamics and the role of gamma-tubulin in early *Caenorhabditis elegans* embryos. *Molecular Biology of the Cell,* 12, 1751-1764.

SULSTON, J. E. & HORVITZ, H. R. (1977) Post-Embryonic Cell Lineages of Nematode, *Caenorhabditis elegans. Developmental Biology,* 56, 110-156.

SULSTON, J. E. & HORVITZ, H. R. (1981) Abnormal-Cell Lineages in Mutants of the Nematode *Caenorhabditis elegans. Developmental Biology,* 82, 41-55.

SULSTON, J. E., SCHIERENBERG, E., WHITE, J. G. & THOMSON, J. N. (1983) The Embryonic-Cell Lineage of the Nematode *Caenorhabditis elegans. Developmental Biology,* 100, 64-119.

SUMARA, I., VORLAUFER, E., GIEFFERS, C., PETERS, B. H. & PETERS, J. M. (2000) Characterization of vertebrate cohesin complexes and their regulation in prophase. *Journal of Cell Biology,* 151, 749-761.

TAKAGI, S., BENARD, C., PAK, J., LIVINGSTONE, D. & HEKIMI, S. (1997) Cellular and axonal migrations are misguided along both body axes in the maternal-effect *mau-2* mutants of *Caenorhabditis elegans. Development,* 124, 5115-5126.

TAKAHASHI, T. S., YIU, P., CHOU, M. F., GYGI, S. & WALTER, J. C. (2004) Recruitment of *Xenopus* Scc2 and cohesin to chromatin requires the pre-replication complex. *Nature Cell Biology,* 6, 991-996.

TANAKA, K., HAO, Z. L., KAI, M. & OKAYAMA, H. (2001) Establishment and maintenance of sister chromatid cohesion in fission yeast by a unique mechanism. *Embo Journal,* 20, 5779-5790.

TANAKA, K., YONEKAWA, T., KAWASAKI, Y., KAI, M., FURUYA, K., IWASAKI, M., MURAKAMI, H., YANAGIDA, M. & OKAYAMA, H. (2000a) Fission yeast Eso1p is required for establishing sister chromatid cohesion during S phase. *Molecular and Cellular Biology,* 20, 3459-3469.

TANAKA, T. U., COSMA, M. P., WIRTH, K. & NASMYTH, K. (1999) Identification of cohesin association sites at centromeres and along chromosome arms. *Cell,* 98, 847-858.

TANAKA, T. U., FUCHS, J., LOIDL, J. & NASMYTH, K. (2000b) Cohesin ensures bipolar attachment of microtubules to sister centromeres and resists their precocious separation. *Nature Cell Biology,* 2, 492-499.

TIMMONS, L., COURT, D. L. & FIRE, A. (2001) Ingestion of bacterially expressed dsRNAs can produce specific and potent genetic interference in *Caenorhabditis elegans*. *Gene,* 263, 103-112.

TOMONAGA, T., NAGAO, K., KAWASAKI, Y., FURUYA, K., MURAKAMI, A., MORISHITA, J., YUASA, T., SUTANI, T., KEARSEY, S. E., UHLMANN, F., NASMYTH, K. & YANAGIDA, M. (2000) Characterization of fission yeast cohesin: essential anaphase proteolysis of Rad21 phosphorylated in the S phase. *Genes & Development,* 14, 2757-2770.

TONKIN, E. T., WANG, T. J., LISGO, S., BAMSHAD, M. J. & STRACHAN, T. (2004) *NIPBL*, encoding a homolog of fungal Scc2-type sister chromatid cohesion proteins and fly Nipped-B, is mutated in Cornelia de Lange syndrome. *Nature Genetics,* 36, 636-641.

TOTH, A., CIOSK, R., UHLMANN, F., GALOVA, M., SCHLEIFFER, A. & NASMYTH, K. (1999) Yeast cohesin complex requires a conserved protein, Eco1p(Ctf7), to establish cohesion between sister chromatids during DNA replication. *Genes & Development,* 13, 320-333.

UHLMANN, F., LOTTSPEICH, F. & NASMYTH, K. (1999) Sister-chromatid separation at anaphase onset is promoted by cleavage of the cohesin subunit Scc1. *Nature,* 400, 37-42.

UHLMANN, F., WERNIC, D., POUPART, M., KOONIN, E. V. & NASMYTH, K. (2000) Cleavage of cohesin by the CD clan protease separin triggers anaphase in yeast. *Cell,* 103, 375-386.

UNAL, E., ARBEL-EDEN, A., SATTLER, U., SHROFF, R., LICHTEN, M., HABER, J. E. & KOSHLAND, D. (2002) DNA damage response pathway uses histone modification to assemble a double-strand break-specific cohesin domain. *Molecular Cell,* 16, 991-1002.

UNAL, E., ARBEL-EDEN, A., SATTLER, U., SHROFF, R., LICHTEN, M., HABER, J. E. & KOSHLAND, D. (2004) DNA damage response pathway uses histone modification to assemble a double-strand break-specific cohesin domain. *Molecular Cell,* 16, 991-1002.

VANDENBERG, D. J. & FRANCKE, U. (1993) Roberts-Syndrome - a Review of 100 Cases and a New Rating System for Severity. *American Journal of Medical Genetics,* 47, 1104-1123.

VASS, S., COTTERILL, S., VALDEOLMILLOS, A. M., BARBERO, J. L., LIN, E., WARREN, W. D. & HECK, M. M. S. (2003) Depletion of Drad21/Scc1 in *Drosophila* cells leads to instability of the and disruption of mitotic cohesin complex progression. *Current Biology,* 13, 208-218.

VEGA, H., WAISFISZ, Q., GORDILLO, M., SAKAI, N., YANAGIHARA, I., YAMADA, M., VAN GOSLIGA, D., KAYSERILI, H., XU, C., OZONO, K., JABS, E. W., INUI, K. & JOENJE, H. (2005) Roberts syndrome is caused by mutations in *ESCO2*, a human homolog of yeast *ECO1* that is essential for the establishment of sister chromatid cohesion. *Nature Genetics,* 37, 468-470.

WALTER, J., SUN, L. & NEWPORT, J. (1998) Regulated chromosomal DNA replication in the absence of a nucleus. *Molecular Cell,* 1, 519-529.

WANG, F., YODER, J., ANTOSHECHKIN, I. & HAN, M. (2003) *Caenorhabditis elegans* EVL-14/PDS-5 and SCC-3 are essential for sister chromatid cohesion in meiosis and mitosis. *Molecular and Cellular Biology,* 23, 7698-7707.

WANG, S. W., READ, R. L. & NORBURY, C. J. (2002) Fission yeast Pds5 is required for accurate chromosome segregation and for survival after DNA damage or metaphase arrest. *Journal of Cell Science,* 115, 587-598.

WARREN, W. D., STEFFENSEN, S., LIN, E., COELHO, P., LOUPART, M. L., COBBE, N., LEE, J. Y., MCKAY, M. J., ORR-WEAVER, T., HECK, M. M. S. & SUNKEL, C. E. (2000) The *Drosophila* RAD21 cohesin persists at the centromere region in mitosis. *Current Biology,* 10, 1463-1466.

WATRIN, E., SCHLEIFFER, A., TANAKA, K., EISENHABER, F., NASMYTH, K. & PETERS, J. M. (2006) Human Scc4 is required for cohesin binding to chromatin, sister-chromatid cohesion, and mitotic progression. *Current Biology,* 16, 863-874.

WAZENEGGER, I. C., HAUF, S., MEINKE, A. & PETERS, J. (2000) Two distinct pathways remove mammalian cohesin from chromosome arms in prophase and from centromeres in anaphase. *Cell,* 103, 399-410.

WEITZER, S., LEHANE, C. & UHLMANN, F. (2003) A model for ATP hydrolysis-dependent binding of cohesin to DNA. *Current Biology,* 13, 1930-1940.

WILLIAMS, B. C., GARRETT-ENGELE, C. M., LI, Z. X., WILLIAMS, E. V., ROSENMAN, E. D. & GOLDBERG, M. L. (2003) Two putative acetyltransferases, San and deco, are required for establishing sister chromatid cohesion in *drosophila*. *Current Biology,* 13, 2025-2036.

WORMBASE www.wormbase.org.

YAN, J., SAIFI, G. M., WIERZBA, T. H., WITHERS, M., BIEN-WILLNER, G. A., LIMON, J., STANKIEWICZ, P., LUPSKI, J. R. & WIERZBA, J. (2006) Mutational and genotype-phenotype correlation analyses in 28 Polish patients with Cornelia de Lange syndrome. *American Journal of Medical Genetics Part A,* 140A, 1531-1541.

ZHANG, B., JAIN, S., SONG, H., FU, M., HEUCKEROTH, R. O., ERLICH, J. M., JAY, P. Y. & MILBRANDT, J. (2007) Mice lacking sister chromatid cohesion protein PDS5B exhibit developmental abnormalities reminiscent of Cornelia de Lange syndrome. *Development,* 134, 3191-3201.

ZHANG, Z. J., REN, Q., YANG, H., CONRAD, M. N., GUACCI, V., KATENEVA, A. & DRESSER, M. E. (2005) Budding yeast PDS5 plays an important role in meiosis and is required for sister chromatid cohesion. *Molecular Microbiology,* 56, 670-680.